

Spring 2007

Biomedical applications of polypeptide multilayer nanofilms and microcapsules

Jai Simha S. Rudra
Louisiana Tech University

Follow this and additional works at: <https://digitalcommons.latech.edu/dissertations>



Part of the [Biomedical Engineering and Bioengineering Commons](#)

Recommended Citation

Rudra, Jai Simha S., "" (2007). *Dissertation*. 555.
<https://digitalcommons.latech.edu/dissertations/555>

This Dissertation is brought to you for free and open access by the Graduate School at Louisiana Tech Digital Commons. It has been accepted for inclusion in Doctoral Dissertations by an authorized administrator of Louisiana Tech Digital Commons. For more information, please contact digitalcommons@latech.edu.

BIOMEDICAL APPLICATIONS OF POLYPEPTIDE MULTILAYER
NANOFILMS AND MICROCAPSULES

by

Jai Simha S. Rudra, B.Tech

A Dissertation Presented in Partial Fulfillment
of the Requirements for the Degree
Doctor of Philosophy

COLLEGE OF ENGINEERING AND SCIENCE
LOUISIANA TECH UNIVERSITY

May 2007

UMI Number: 3268114

INFORMATION TO USERS

The quality of this reproduction is dependent upon the quality of the copy submitted. Broken or indistinct print, colored or poor quality illustrations and photographs, print bleed-through, substandard margins, and improper alignment can adversely affect reproduction.

In the unlikely event that the author did not send a complete manuscript and there are missing pages, these will be noted. Also, if unauthorized copyright material had to be removed, a note will indicate the deletion.

UMI[®]

UMI Microform 3268114

Copyright 2007 by ProQuest Information and Learning Company.

All rights reserved. This microform edition is protected against unauthorized copying under Title 17, United States Code.

ProQuest Information and Learning Company
300 North Zeeb Road
P.O. Box 1346
Ann Arbor, MI 48106-1346

LOUISIANA TECH UNIVERSITY

THE GRADUATE SCHOOL

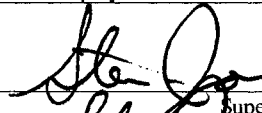
05/01/2007

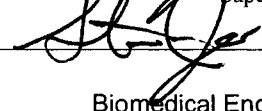
Date

We hereby recommend that the dissertation prepared under our supervision by Jai Simha S. Rudra

entitled Biomedical Applications of Polypeptide Multilayer Nanofilms and Microcapsules

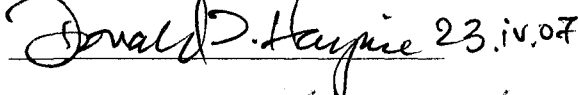
be accepted in partial fulfillment of the requirements for the Degree of Doctor of Philosophy





Supervisor of Dissertation Research


Head of Department
Biomedical Engineering
Department


Recommendation concurred in:


Donald D. Haynie 23.iv.07
04/12/07

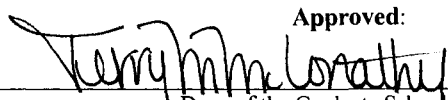


Yufei Li



Pats Ganeshandran
Advisory Committee

Approved: 

Director of Graduate Studies

Approved: 

Dean of the Graduate School



Dean of the College

ABSTRACT

The past few years have witnessed considerable growth in synthetic polymer chemistry and physics, biomaterials science, and nano-scale engineering. Research on polypeptide multilayer films, coatings, and microcapsules is located at the intersection of these areas and are promising materials for applications in medicine, biotechnology, environmental science. Most envisioned applications of polypeptide multilayers have a biomedical bent. This dissertation on polypeptide multilayer film applications covers key points of polypeptides as materials, means of polymer production, film preparation, film characterization methods, and key points of current research in basic science. Both commercial and designed peptides have been used to fabricate films for in-vitro applications such as antimicrobial coatings and cell culture coatings and also microcapsules for drug delivery applications. Other areas of product development include artificial red blood cells, anisotropic coatings, enantioselective membranes, and artificial viruses.

APPROVAL FOR SCHOLARLY DISSEMINATION

The author grants to the Prescott Memorial Library of Louisiana Tech University the right to reproduce, by appropriate methods, upon request, any or all portions of this Dissertation. It is understood that "proper request" consists of the agreement, on the part of the requesting party, that said reproduction is for his personal use and that subsequent reproduction will not occur without written approval of the author of this Dissertation. Further, any portions of the Dissertation used in books, papers, and other works must be appropriately referenced to this Dissertation.

Finally, the author of this Dissertation reserves the right to publish freely, in the literature, at any time, any or all portions of this Dissertation.

Author Jaiendra
Date 25 April 07

DEDICATION

To my mother Latha S. Rudra

TABLE OF CONTENTS

ABSTRACT.....	iii
DEDICATION.....	v
LIST OF TABLES.....	ix
LIST OF FIGURES	x
ACKNOWLEDGEMENTS.....	xiii
CHAPTER ONE INTRODUCTION.....	1
1.1 There's Plenty of Room at the Bottom.....	1
1.1.1 Biotechnology to Bionanotechnology	2
1.1.2 Proteins and Polypeptides.....	3
1.2 Designed Polypeptides.....	6
1.3 Electrostatic Layer-by-layer Assembly (LBL)	9
1.4 Advantages of LBL.....	11
1.5 Weak Polyelectrolytes	12
1.6 Polypeptide Multilayer Film Fabrication by LBL	14
1.7 Conclusions.....	18
CHAPTER TWO POLYPEPTIDE MULTILAYER FILMS.....	19
2.1 Introduction.....	19
2.2 Polypeptide Synthesis Purification and Characterization.....	20
2.2.1 Solid Phase Peptide Synthesis (SPPS).....	21
2.2.2 High Performance Liquid Chromatography (HPLC)	25
2.2.3 Capillary Electrophoresis (CE).....	27
2.2.4 Nuclear Magnetic Resonance (NMR).....	30
2.2.5 Mass Spectrometry (MS).....	31
2.3 Film Characterization Techniques.....	31
2.3.1 Quartz Crystal Microbalance (QCM)	32
2.3.2 UV-vis Spectroscopy (UV-vis).....	33
2.3.3 Circular Dichroism Spectroscopy (CD).....	34
2.3.4 Ellipsometry.....	35
2.3.5 Atomic Force Microscopy (AFM).....	36
2.4 Computational Approaches.....	37

CHAPTER THREE ANTIMICROBIAL POLYPEPTIDE MULTILAYER NANOFILMS	39
3.1 Introduction.....	39
3.2 Materials and Methods.....	42
3.2.1 LBL.....	43
3.2.2 Quartz Crystal Microbalance (QCM)	43
3.2.3 UV Spectroscopy	44
3.2.4 Bacterial Culture	44
3.2.5 Activity of HEWL Released from Films	45
3.2.6 Activity of HEWL Retained in Films	46
3.2.7 Stability of Bioactive Films	46
3.3 Results and Discussion	47
3.4 Conclusions.....	57
CHAPTER FOUR CELL CULTURE POLYPEPTIDE MULTILAYER FILMS	59
4.1 Introduction.....	59
4.2 RGD Motifs and Cell Adhesion.....	60
4.3 Cell Attachment to LBL Films	64
4.4 Peptide Design Rationale.....	64
4.5 Film Fabrication and Characterization.....	66
4.5.1 UV Spectroscopy	67
4.5.2 Circular Dichroism Spectroscopy	67
4.5.3 Atomic Force Microscopy	68
4.5.4 Ellipsometry	68
4.6 Cell Culture Studies	69
4.6.1 Cell Culture.....	70
4.6.2 Cell Proliferation.....	70
4.7 Results and Discussion	71
4.8 Conclusions.....	85
CHAPTER FIVE <i>IN VIVO</i> STUDIES OF DESIGNED POLYPEPTIDE MICROCAPSULES FOR DRUG DELIVERY APPLICATIONS	86
5.1 Introduction.....	86
5.2 Materials and Methods.....	88
5.2.1 Microcapsule Fabrication.....	88
5.2.2 Animals and Husbandry.....	88
5.2.3 Animal Grouping and Coding.....	89
5.2.4 Saphenous Vein Blood Collection	90
5.2.5 Tail Vein Injections and Monitoring.....	92
5.2.6 Blood Chemistry Analysis	93
5.2.7 Euthanasia and Preservation	93
5.3 Results and Discussion	94
5.4 Conclusions.....	98

CHAPTER SIX CONCLUSIONS.....	99
APPENDIX A.....	101
APPENDIX B.....	107
REFERENCES.....	114

LIST OF TABLES

Table 1.1.	Advantages of LBL.....	12
Table 1.2.	Properties of polypeptide multilayer films	15
Table 1.3.	Variables in polypeptide multilayer film/coating/capsules fabrication	16
Table 1.4.	Why study polypeptide multilayer films?.....	17
Table 4.1.	Designed peptides for cell culture films	65
Table 4.2.	Films formed from various peptide combinations.....	71
Table 4.3.	Secondary structure content of designed peptide multilayer films.....	76
Table 4.4.	Surface roughness of designed peptide multilayer films	79
Table 4.5.	Film thickness of peptide multilayer films at various RI values	80
Table A.1.	UV absorbance data of designed peptide films.....	102
Table A.2.	Thickness of designed peptide multilayer films	102
Table A.3.	Surface roughness values of designed peptide multilayer films.....	103
Table B.1.	Blood chemistry data for control mice before injections	108
Table B.2.	Blood chemistry data for control mice after formulation injections	109
Table B.3.	Blood chemistry data for F1 group mice before injections.....	110
Table B.4.	Blood chemistry data for F1 group mice after formulation injections.....	111
Table B.5.	Blood chemistry data for F2 group mice before injections.....	112
Table B.6.	Blood chemistry data for F2 group mice after formulation injections.....	113

LIST OF FIGURES

Figure 1.1.	Peptide bond formation [11].....	6
Figure 1.2.	Molecular models of designed peptides	8
Figure 1.3.	Schematic of Layer-by-Layer (LBL) technique.....	10
Figure 2.1.	Schematic diagram of solid phase peptide synthesis [85].....	22
Figure 2.2.	Flowchart for selecting cocktail solution	24
Figure 2.3.	Schematic of a HPLC system [89]	26
Figure 2.4.	Schematic of a CE system [95]	28
Figure 2.5.	Quartz crystal resonator.....	32
Figure 2.6.	UV-vis spectrophotometer.....	33
Figure 2.7.	Signature spectra of different secondary structures [126].....	34
Figure 2.8.	Schematic of a nulling ellipsometer	36
Figure 2.9.	Schematic of an AFM.....	37
Figure 3.1.	Schematic of HEWL and PLGA assembly by LBL.....	43
Figure 3.2.	Standard curve for HEWL activity assays.....	46
Figure 3.3.	PLGA/HEWL multilayer film assembly monitored by QCM	47
Figure 3.4.	PLGA/HEWL multilayer film assembly monitored by QCM (bilayer).....	48
Figure 3.5.	PLGA/HEWL film assembly monitored by UV spectroscopy	49
Figure 3.6.	Activity of PLGA/HEWL films against <i>M. luteus</i>	50
Figure 3.7.	Relative antimicrobial activity of PLGA/HEWL films under different conditions.....	51

Figure 3.8. Anti-microbial activity of PLGA/HEWL multilayer films of different thickness after 14 h of immersion in phosphate buffer at 30°C with continuous stirring at 200 rpm	52
Figure 3.9. Effect of PLGA/HEWL films on <i>M. luteus</i> culture.....	53
Figure 3.10. Amount of HEWL released from film-coated slides into the surrounding buffer.....	54
Figure 4.1. Opposite effects of integrin ligands. Immobilized ligands act as agonists of the ECM, leading to cell adhesion and cell survival, while non-immobilized ligands act as antagonists, leading to cell detachment, a round cell shape, and apoptosis [199].....	61
Figure 4.2. Estimated peptide net charge versus pH.....	72
Figure 4.3. Peptide multilayer film assembly monitored by UV spectroscopy	73
Figure 4.4. CD spectra of designed peptide multilayer films	75
Figure 4.5. AFM image of peptide P2 on a silicon surface	77
Figure 4.6. AFM images of designed polypeptide films	78
Figure 4.7. Ellipsometric thickness of designed polypeptide multilayer films.....	80
Figure 4.8. Variation of film thickness with RI. Film P3N3 was taken as an example due to its low surface roughness and full coverage	81
Figure 4.9. Mouse 3T3 fibroblasts on PLL/PLGA multilayer film	82
Figure 4.10. Number of cells growing on polypeptide multilayer films as determined by MTT assay.....	83
Figure 4.11. Number of cells growing on (PLL/PLGA)-polypeptide multilayer films as determined by MTT assay	83
Figure 5.1. Schematic showing the grouping of mice	90
Figure 5.2. Saphenous vein blood collection	91
Figure 5.3. Tail vein injection of formulations	92
Figure 5.4. Mice bring prepared for preservation	94
Figure 5.5. Albumin levels in mice before and after formulation injections.....	95

Figure 5.6. Total bilirubin levels in test mice before and after formulation injection.....	96
Figure 5.7. Level of blood sodium in the test mice (a) level of blood potassium in test mice (b) before and after formulation injections.....	97
Figure A.1. AFM images of designed polypeptide multilayer films (i)	104
Figure A.2. AFM images of designed polypeptide multilayer films (ii)	105
Figure A.3. AFM images of designed polypeptide multilayer films (iii).....	106

ACKNOWLEDGEMENTS

This dissertation would not have been possible without the love and support of my mother Latha Rudra, and the guidance of my advisor Dr. Don Haynie. Many thanks as well for the collaborative process with Dr. David Ash and Carol Stevens at Central Michigan University, Dr. Guangzhao Mao at Wayne State University, Tom and Laura Malone at Artificial Cell Technologies, for allowing me to take my work to new horizons. I joyfully thank Nature, God, and the Universe (all of which are One to me) for life, creativity, and movement.

CHAPTER 1

INTRODUCTION

1.1 There's Plenty of Room at the Bottom

On December 29, 1959, at the California Institute of Technology, physicist Richard Feynman gave a talk titled “There's Plenty of Room at the Bottom” [1]. The lecture's title would seem to be a pun on the title of a 1959 British film, *Room at the Top* [2]. The story is about a money- and status-seeking blue-collar worker (a lowly atom) willing to do whatever it might take to climb the ladder to success (become an essential component of the complex network of interactions that characterize a living organism). Simone Signoret won the Oscar for best actress for her role in the film [2] as the epitome of sexy, womanly vulnerability—an element of the seductive vision that motivates the sojourn of the atom from obscurity to stardom. At the time the film was current, celebrities bound for Hollywood arrived more often than not by train and disembarked not in working-class Los Angeles but in pleasant Pasadena [3]. Little imagination is needed to guess that an evening with Simone was the dream of many a science or engineering student at the then virtually all-male California Institute of Technology, and that she was the subject of a good deal of off-topic chat. Feynman's lecture is now generally taken as the genesis of nanotechnology. His thinking on the matter may have been stimulated by knowledge of or interaction with other notables at

Caltech, for instance, T. Morgan (chromosome theory of heredity), L. Pauling (genetic basis of sickle-cell anemia), and M. Delbrück (bacterial virus structure and function) (Nobel laureate, Medicine or Physiology, 1969). In his talk Feynman unveiled the possibilities available in the molecular world and his vision spawned the discipline of nanotechnology. Because ordinary matter has so many atoms, he showed that there is a remarkable amount of space in which to build.

Atoms are unbelievably small and their properties utterly foreign, which makes our intuition and knowledge of the meter-scale world useless at best and misleading at worst. When men and women first restructured matter to fit their needs, they invented a top-down approach and used tools to shape and transform existing matter. Nanotechnology takes an opposite approach in which nano-scale devices are built using a bottom-up approach atom by atom [4]. It is important to understand that atoms are not just small; they are ‘a special kind’ of small. The positioning of individual xenon atoms on nickel (110) surface at IBM is a successful example of nanotechnology [5].

1.1.1 Biotechnology to Bionanotechnology

Biotechnology grew from the use of natural enzymes to modify genetic code, which was then used to modify entire organisms. This revolution has led to myriad applications, including commercial production of hormones and drugs, elegant methods for diagnosing and curing infections and genetic diseases, and engineering of organisms for specialized tasks such as bioremediation and disease resistance. Biotechnology took several decades to gather momentum but nanoscale understanding and atomic details were not really important. Existing functionalities were combined to achieve the end goal. Bionanotechnology is a subset of nanotechnology, nanotechnology that looks to

nature for its start and requires human design and construction at the nanoscale level. Bionanotechnology has many faces, but all share a central feature: the ability to design molecular machinery to atomic specifications. It is closely married to biotechnology but adds the ability to design and modify the atomic level details of the objects created.

1.1.2 Proteins and Polypeptides

Polypeptides form one of four classes of biological macromolecules—the others being nucleic acids, polysaccharides, and phospholipids [6]. The first determination of the chemical structure of a bioactive peptide, cow insulin, was achieved by F. Sanger (Nobel laureate, Chemistry, 1958) in the early 1950s. A key feature of amino acid subunits of a polypeptide is their structure. An amino group, a carboxyl group, a hydrogen atom, and a variable side chain, R, constitute the substituents of the central carbon. There are 20 usual side chains in nature. The number of possible non-natural side chains is practically unlimited, and scores of novel ones are available from commercial sources for abiotic peptide synthesis. Amino acids are chiral: each of the natural ones has a right-handed form (d isomer) and a left-handed form (l isomer) with the exception glycine, which has just a hydrogen atom for its R side chain. All amino acids in all proteins in all known organisms are l isomers.

There are four hierarchical levels of peptide-based structures, and they were first defined by K. Linderstrøm-Lang in the 1950s [7]. Primary structure denotes the sequence of amino acid residues in a polypeptide chain. The most common types of secondary structure, α -helices and β -sheets, were predicted by L. Pauling (Nobel laureate, Chemistry, 1954) and R. Corey in the early 1950s and visualized in atomic-resolution protein structures shortly thereafter. Helices and sheets are characterized in part by

having distinctive patterns of hydrogen bonds (relatively weak electrostatic interactions) formed between chemical groups in the polypeptide backbone. Nearly all known protein structures comprise at least one α -helix or β -sheet [8]; secondary structures can also form in peptides that do not fold into proteins [9]. Tertiary structure refers to the relative spatial orientation of secondary structure elements and the noncovalent contacts between amino acids, as in the small muscle protein myoglobin. Quaternary structure is the relationship between polypeptide chains when more than one is involved in forming the overall protein structure, as in the blood protein hemoglobin, a structural relative of myoglobin.

When properly folded and biologically functional, a protein is said to be in its native state. Folded protein structure was first visualized at atomic resolution in the late 1950s and early 1960s: sperm whale myoglobin and horse heart hemoglobin by J. Kendrew and M. Perutz (Nobel laureates, Chemistry, 1962), respectively, at Cambridge University, and hen egg white lysozyme by D.C. Phillips at Oxford University. Since then, the number of protein structures determined at or near atomic resolution has risen exponentially with each passing year. A disulfide bond is a natural type of covalent cross-link that can form between cysteine side chains. Disulfide bonds stabilize protein structure by reducing the entropy of the polymer chain, particularly in a denatured state (for example, [10]). Ribonuclease A is a small protein with four native disulfide bonds. In the early 1960s C. Anfinsen (Nobel laureate, Chemistry, 1972) showed that all the instructions required for the ribonuclease polypeptide to go from a denatured state in which no disulfide bonds were intact to native protein structure in water were encoded in the amino acid sequence. In some cases, at least, acquisition of biologically functional

protein structure from a disordered conformation is driven by a minimizing the Gibbs free energy of the protein–solvent system. Genome-sequencing efforts have revealed that the myriad of DNA-encoded polypeptide chains in the different living organisms on Earth fold into a comparatively tiny number of qualitatively different structures [8].

Several broad structural classes of proteins have been identified. In globular proteins (for example, myoglobin), the polypeptide folds into a highly compact, ball-like shape. Fibrous proteins found in hair, tendons, and spider silk tend to be elongated. Elastin, for example, found in skin and lung, can be stretched without tearing. Formed of loose and unstructured polypeptide chains, this protein provides the elasticity needed to fulfill its biological role. Membrane proteins (such as the insulin receptor) are embedded in the plasma membrane of a cell. Proteins can also be classified according to function [8]. Enzymes, such as lysozyme, catalyze covalent bond formation or rupture in specific chemical reactions. Structural proteins provide mechanical support for cells and tissues. Transport proteins, such as hemoglobin, carry small molecules and ions. Motor proteins generate force, causing muscle contraction and allowing movement in the case of skeletal muscle myosin. Signaling proteins and peptides, such as insulin, are chemical signals that control physiological function, often by binding non-covalently to receptor proteins embedded in the plasma membrane which transmit the signal inside or outside the cell. Storage proteins bind ions or metabolites and store them. Gene-regulatory proteins switch gene expression on and off in response to environmental cues. Antibodies bind specific antigens and stimulate the immune system to protect the body from an invading pathogen. Proteins are nanometer-scale machines of remarkable functional variety.

Details of protein structure and function, revealed by decades of study, form a library of motifs for the design of polypeptides for multilayer film assembly.

1.2 Designed Polypeptides

Amino acids can be joined together to form a peptide or polypeptide. They are called peptides because following a condensation reaction, the carboxyl group of one amino acid joins to the amino group of another, and a covalent bond is formed. Chemically this is an amide bond but when it occurs in proteins it is given the name peptide bond. The peptide bond has an unusual property that has a marked effect on the rigidity and structure of a polypeptide chain. It has a partial double-bond character, caused by the resonance of electrons rapidly moving between the oxygen and nitrogen to make the C-N bond a partial double bond. The consequence of this arrangement is that the peptide bond is very rigid because C=N is much less flexible than a C-N bond [11]. The 19 α -amino acids in peptides and proteins (proline is an imino acid) consist of a carboxylic acid (-COOH) and an amino (-NH₂) functional group attached to the same tetrahedral carbon atom, the α -carbon. The R-groups, which distinguish one amino acid from another, are attached to the alpha-carbon (except for glycine, for which the R-group is hydrogen). The fourth substituent of the tetrahedral α -carbon of amino acids is hydrogen. The two broad classes of amino acids are based upon whether the R-group is hydrophobic or hydrophilic. Figure 1.1 shows peptide bond formation.



Figure 1.1. Peptide bond formation [11].

Hydrophobic amino acids tend to repel the aqueous environment and, therefore, reside predominantly in the interior of proteins. This class of amino acids does not ionize nor participate in the formation of H-bonds. Non-polar side chains consist mainly of hydrocarbon. Any functional groups they contain are uncharged at physiological pH and are incapable of participating in hydrogen bonding. The non-polar amino acids include alanine, cysteine, glycine, isoleucine, leucine, methionine, phenylalanine, proline, tryptophan, tyrosine and valine. The hydrophilic amino acids tend to interact with the aqueous environment, are often involved in the formation of H-bonds and are found predominantly on the exterior surfaces proteins or in the reactive centers of enzymes. The polar amino acids include arginine, asparagine, aspartic acid (or aspartate), glutamine, glutamic acid (or glutamate), histidine, lysine, serine, and threonine. Polar side chains contain groups that are either charged at physiological pH or groups that can participate in hydrogen bonding [6].

Polymers of amino acids form one of the four major classes of biomacromolecules and constitute about half of the dry mass of a living organism [12]. Polypeptides are the structural building blocks of materials ranging from hair and tendons in mammals to the silk produced by insects and spiders. The enormous range of possible amino acid side chains, of which the 20 usual ones are but a small subset, makes polypeptides particularly promising molecules for controlled design features. Degree of polymerization, degree of dispersity, and chemical modification of chain termini or side chains can be controlled, depending on the method of synthesis or purification protocol. Considering the 20 usual amino acids alone, $\sim 10^{41}$ distinct chemical structures of unmodified 32-mer polypeptides can be synthesized. Modern methods of synthesis

enable realization in the laboratory of a large proportion of this vast range of possibilities. Important design elements are amino acid side chains that are charged at neutral pH, hydrophilic side chains that are polar but uncharged at neutral pH, hydrophobic side chains, side chains capable of hydrogen bonding, and side chains that are uncharged.

A unique feature of polypeptides is their ability to form secondary structure. It is known from protein research that various sequences of amino acid show a preference to adopt a type of secondary structure, α -helix or β -sheet [13]. Both types are stabilized by hydrogen bonds which form between chemical groups in the polymer backbone. The ability of a peptide to fold into a specific structure, the control one can have over peptide sequence, and the range of possible ways of integrating polyelectrolytes with other materials, for example colloidal particles, together provide a remarkable range of opportunities for the design of nanoscale materials. To summarize, hydrophobicity, linear charge density, propensity to form secondary structure at neutral pH, and ability to form chemical crosslinks can be varied according to purpose by design of sequence. Shown in Figure 1.2, are molecular models of two designed polypeptides.

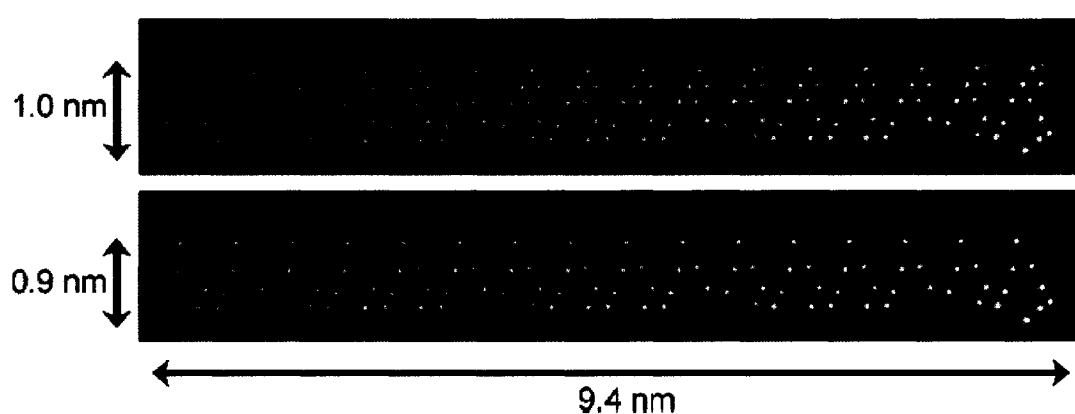


Figure 1.2. Molecular models of designed peptides.

1.3 Electrostatic Layer-by-Layer Assembly (LBL)

Layer-by-layer assembly (LBL) is a method of making a multilayer thin film from oppositely charged species [14-18] deposited in succession on a solid support. The method has attracted interest because it is simple and considerably more versatile than other techniques of thin film preparation, for example Langmuir-Blodgett deposition. The basic principle of assembly, coulombic attraction and repulsion, is far more general than the type of adsorbing species or surface area or shape of support [17]. Film assembly can be described as the kinetic trapping of charged polymers from solution on a surface. Multilayer film formation is possible because of charge reversal on the film surface after each polyion adsorption step [19-34]. Surface charge thus depends on the last adsorbed layer, permitting a degree of control over surface and interface properties. A high density of charge in the adsorbing species will result not only in strong attraction between particles in neighboring layers, but also in strong repulsion between like-charged particles in the same layer. That is, electrostatics both drives film assembly and limits it. Several layers of material applied in succession create a solid, multilayer coating. Each layer of can have a thickness on the order of nanometers, enabling the design and engineering of surfaces and interfaces at the molecular level. Subtle changes in organization and composition can influence film structure and functionality. The layering process is repetitive and can be automated, important for control over the process and commercialization prospects. Constituents of a film could be bioactive or bioresponsive materials. Since the early 1990s there has been considerable interest in making multilayer films from linear ionic polymers [14, 35]. Such films are being developed for of a variety of applications: for example, contact lens coatings, sustained-release drug delivery

systems, biosensors, and functionally advanced materials with various electrical, magnetic, optical, and antimicrobial properties [14-18, 36-42, 43]. Figure 1.3 shows a schematic of the LBL process

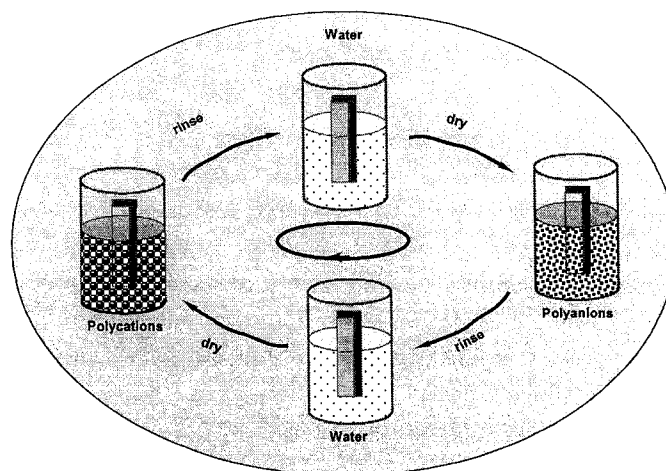


Figure 1.3. Schematic of Layer-by-Layer (LBL) technique.

Many different polyelectrolytes have been studied in this context. Examples are poly(styrene sulfonate) (PSS), poly(allylamine hydrochloride) (PAH), poly(acrylic acid) (PAA), and poly (diallyldimethylammonium chloride) (PDADMAC). These polymers are called “common” or “conventional” in view of their ready availability from commercial sources and their having been studied extensively. Polyelectrolyte structure, however, would appear to have little effect on whether LBL is possible if the ionic groups are accessible. The polymer chains, once assembled into a multilayer film, tend to become highly interpenetrated whether strong polyelectrolytes or weak ones [44, 45]. Besides synthetic polymers, “natural” polyelectrolytes such as nucleic acids, proteins, polysaccharides, and charged nano-objects such as virus particles and membrane fragments have been assembled into multilayer films [46, 47].

1.4 Advantages of LBL

A multilayer film or coating of nanometer-thick layers can be fabricated by sequential adsorption of oppositely-charged polyelectrolytes on a solid support by a method known as layer-by-layer assembly (LBL). No special apparatus is required for LBL, and the film can be made under mild, physiological conditions. LBL is a simple and benign fabrication process. The material production is relatively straightforward, and the process is amenable to automation, and scalable, and it enables exquisite control over structure and function at the nanometer scale. A diverse range of materials and surfaces are suitable for deposition as the only criteria is the net charge on the adsorbing species at the assembly pH and the process is independent of the size, shape, and composition of the surface. The process also allows for numerous control variables during the deposition process, for example concentration, ionic strength, adsorption time, pH, and temperature. Furthermore, post-fabrication processing potential is also broad. An astronomical number of possible layer architectures can be incorporated into the final film, and the process is environmentally friendly and involves no hazardous chemicals. The only cost incurred in this process would be the cost of the materials involved. Recently, alternatives to the repetitive assembly of layers by dipping [14] have been developed for the fabrication of ionic polymer films. An iterative spraying method of film assembly has been introduced by Schlenoff et al [48]. The use of spin-coaters has been demonstrated by Hong et al. [49, 50] and Wang et al. [51]. More recently, the Strasbourg polyelectrolyte film group [52, 53] has shown that continuous and simultaneous spraying of polyanion and polycation solutions [54, 55] onto a vertically-oriented charged surface can create a uniform film that grows continuously

with spraying time. The advantages of LBL fabrication process for multilayer film production are summarized in Table 1.1.

Table 1.1. Advantages of LBL.

General advantage	Further applications
Diverse materials available	Non-polyelectrolytes, Polyelectrolytes
Independent of surface shape and size, Astronomical number of possible layer architectures, Environmentally-friendly process, Low-cost production process	Non-biological surfaces (e.g. plates, stents, contact lenses), Colloids (e.g. latex or calcium carbonate micro particles), Biological 'cells' (e.g. viruses or red blood cells)
Numerous control variables for deposition	Concentration, Adsorption time, Ionic strength, Temperature, Solvent composition
Broad pre- and post-fabrication processing potential	pH, Ionic strength, Temperature

1.5 Weak Polyelectrolytes

In a water-soluble polyelectrolyte with a fixed fraction of equally charged monomers, if the net charge arises from strong dissociating groups, they will remain charged throughout a pH range. This is the case of a *quenched* or *strong polyelectrolyte*. If the net charge arises from reversible proton transfer with the solvent and is therefore pH dependent, it is called an *annealed* or *weak polyelectrolyte*. If the net charge consists of both positive and negative contributions, the polymer is a *polyampholyte*. A polypeptide is a weak polyelectrolyte. Depending on sequence and pH, a polypeptide might be a polyampholyte.

The linear charge density of a weak polyelectrolyte is "tunable" by simple adjustment of pH. Many such polymers are essentially fully charged at neutral pH. The pKa of ionizable groups in a weak polyelectrolyte, however, will be sensitive to the local electronic environment, and the net charge can shift significantly from the solution value

on formation of a polyelectrolyte complex or film [56-63]. Extensive study by Rubner and colleagues has revealed key aspects of the LBL assembly behavior of “conventional” weak polyelectrolytes [44], e.g., PAA and PAH. Fabrication of films from these polymers represents a type of molecular-level blending process. Control of the type and extent of blending enables manipulation of the bulk and surface properties of the resulting film. Weak polyelectrolytes thus afford great latitude for controlling internal and surface material composition, thickness, molecular organization, ionic “crosslink” density, molecular conformation, wettability, swelling behavior, surface properties, and reactive functional groups. Possible molecular conformations in polypeptide films will include not only the “flat” and “loopy” structures of conventional polyelectrolyte adsorption [64] but also α -helices and β -sheets. The pH sensitivity of weak polyelectrolytes enables changes in film morphology after film preparation. Such changes can be reversible or irreversible.

Control of internal and surface composition of weak polyelectrolyte films is achieved by control of amount of polyelectrolyte adsorbed [65]. Another approach is to alter the charge density of the adsorbed polyelectrolyte by changing the pH of solution of the other polyion. This alters the surface charge while keeping the internal structure similar, enabling creation of designer films using the same polyions. Assembly of polyelectrolytes of different charge density allows non-stoichiometric pairing of polyions. The result in the case of PAA and PAH is a swellable film. Such films can bind metal cations from aqueous solution by ion exchange with the protons of the PAA carboxylic acid groups [66].

A final point about weak polyelectrolyte films is pH-driven reorganization of morphology. Under certain circumstances, notably when the internal film structure is

characterized by fully charged, “loopy,” randomly-arranged chains, reorganization can result in the formation of micropores. For example, exposing a pH 3.5 PAA/pH 7.5 PAH film to pH 2.4 for 15 s and then rinsing with water leads to phase separation and micropore formation [58]. The phenomenon has been exploited to “load” polyelectrolyte microcapsules with various soluble molecules, including enzymes. Membrane fragments have been assembled into multilayer films [47].

1.6 Polypeptide Multilayer Film Fabrication by LBL

A polypeptide multilayer film is defined as a multilayer film made of polypeptides. In some instances another type of polymer is involved in the fabrication process, for instance a chemically-modified polypeptide, [67] a non-biological organic polyelectrolyte, [68] or a polysaccharide, [69]. A polypeptide film might be deposited to confer specific biofunctionality on a surface that was otherwise bioinert, or to convert a bioactive surface into one not adhesive to cells [70-74]. Study of polypeptide multilayer films constitutes a confluence of two more mature streams of inquiry: peptide structure and function, a significant area of basic research since about 1905, and polyelectrolyte multilayer films, developed since the early 1990s. Multilayer films are promising for the development of applications which encompass some of the following desirable features: anti-fouling, biocompatibility, biodegradability, specific biomolecular sensitivity, edibility, environmental benignity, thermal responsiveness, stickiness or non-stickiness. Polypeptides are ideally suited for such applications by virtue of their biochemical nature- the control one can have over chemical structure in various approaches to polymer synthesis, the ability to control formation of secondary structure, or the

availability of genomic data. The properties of polypeptides and multilayer films are summarized in Table 1.2.

Table 1.2. Properties of polypeptides and multilayer films.

Polypeptides	LbL multilayer films
“Designable”	Nano-meter scale control over thickness
Can be produced en masse in bacteria	Engineered architecture
Susceptible to proteolysis	Arbitrary surface area
Biodegradable	Arbitrary surface shape
Edible	Simple methodology
Environmentally benign	Environmentally-friendly methodology
Sequence-specific immunogenicity	Low-cost methodology
Predictable α -helix/ β -sheet propensity	Can be used to make capsules
Fold into proteins in some cases	Suitable for a broad range of particles
Specific bioactivity in some cases	Interesting material properties

Control over structure and synthesis could also be important for using designed polypeptides to gain insight on the nature of polyelectrolyte multilayer film assembly and stability. The important point here is that one can have control over this range of variables even when polypeptides are selected for more specific reasons, for example the extent of control over polymer synthesis, biocompatibility, or environmental benignity. Given a peptide design, synthesis is accomplished by a chemical method or a biological method. The approach to synthesis will depend on sequence, degree of polymerization, required fidelity with respect to sequence or length, cost, and production time. Common fabrication concerns in preparing polypeptide multilayer films, coatings, or capsules are summarized in Table 1.3.

Table 1.3. Variables in polypeptide multilayer film/coating/capsule fabrication.

General area	More specific considerations
Peptide synthesis	Sequence
	Length
	Fidelity
Crosslinking	Yes
	No
Internal properties	Active
	Inactive
External properties	Bioactive
	Non-bioactive
Transport	Small molecules
	Macromolecules
Half-life	<i>Ex-vitro</i>
	<i>In-vivo</i>

If “natural” crosslinking of the film is required, for example to stabilize film structure, at least one of the peptides must feature the amino acid cysteine. The thiol group of cysteine provides an “inherent” means of crosslinking polypeptides under mild reaction conditions. A polypeptide multilayer film or capsule will have surface (“external”) properties which make it bioactive or non-bioactive. Examples of bioactive properties are anti-microbial activity, immunogenicity, and cytophilicity. Although some antibiotics are small molecules, and some non-protein polyelectrolytes are non-immunogenic or cytophilic, use of polypeptides enables a great degree of control over bioactive properties in defined and “natural” ways. Non-bioactive properties include hydrophobicity, hydrophilicity, and physical protein adsorption. Quite apart from any biofunctionality a polypeptide might exhibit, the polymer is a mere chemical on some level. In general, then, bioactive materials will encompass features of non-bioactive

materials. The film or capsule will be “inactive” or “active” with regard to “internal” properties. For example, an active film might feature an entrapped functional enzyme or some other type of chemically reactive agent. Transport and release properties of the film or capsule will depend on the choice of peptides and method of fabrication. The film preparation process could be optimized for the transport of small molecules which may or may not be soluble in water or some other solvent, or release of macromolecules, for example nucleic acids and peptides. Other recent advances in polypeptide science outside the area of multilayer films are peptides that self-assemble into various types of nanostructure, [75-78] diblock copolypeptides that self-assemble into spherical vesicular assemblies, [79] or peptide block copolymers that self-assemble into fibrils [80]. The application areas of polypeptide multilayer films are shown in Table 1.4.

Table 1.4. Why study polypeptide multilayer films?

Science	Technology
Physics	Engineering
“Unusual” backbone role of entropy in adsorption	Coatings
Primary structure, role of interactions	Capsules
Secondary structure and nano-scale organization	Self assembly
Chemistry	Bio-based materials production
“Inherent” covalent crosslinking	Medicine
Similarity to protein folding and stability	Tissue engineering
Biochemical properties	Artificial cells
Biology	Immunogenicity
“Inherent” bioactivity	Edibility
Environmental benignity	Implant Coatings
Biodegradation	Drug delivery vehicles

1.7 Conclusions

Polypeptides are weak polyelectrolytes these biomacromolecules are of fundamental importance to life as we know it. One cannot assume that what has been learned about multilayer film fabrication from extensive study of non-polypeptide polyelectrolytes, including weak polyelectrolytes, will form a sufficient basis for predicting the physical, chemical and, most important, biological properties of polypeptide multilayer films. One gathers from what has been said thus far that polypeptide multilayer film development combines knowledge of physics, chemistry, biology, medicine, biotechnology, and engineering. There is great promise for the development of useful films and multifunctional coatings. Developments in synthetic chemistry and biotechnology are likely to prove crucial to commercialization efforts, many of them likely to be aimed toward applications in medicine and biotechnology.

CHAPTER 2

POLYPEPTIDE MULTILAYER FILMS

2.1 Introduction

Polypeptides are weak polyelectrolytes. Much is known about peptide structure and function, and about conventional weak polyelectrolytes in LBL. It does not follow, however, that physical properties of polypeptide films can easily be predicted from knowledge of amino acid sequence and weak polyelectrolyte LBL alone. Polyelectrolyte self assembly is very complex. Bulk film properties will arise from details of interactions between constituent molecules, and predictions of chemical and biological properties of a polypeptide film will be all the more speculative, at least in general terms, even if environmental benignity can generally be assumed. Considering the 20 usual amino acids alone, simple combinatorics says there are 32^{20} ($\sim 10^{41}$) chemically distinct polypeptides 32 residues long. Important for commercial prospects of polypeptide multilayer films, a large proportion of the possible peptide structures can be realized; moreover, large quantities of material can be prepared by solid-phase synthesis or genetic engineering of bacteria. The physical, chemical and biological properties of polypeptide multilayer films can be studied using various techniques that have been applied to other polyelectrolyte multilayer films. The choice of technique, however, will depend on the intended application of the multilayer film.

2.2 Polypeptide Synthesis Purification and Characterization

There are two basic approaches to designed polypeptide production: abiotic synthesis and biotic synthesis. Abiotic synthesis, whether solution phase or solid phase, the preferred approach for most laboratory studies of film assembly, stability, and functionality, and biotic synthesis the logical option for large-scale preparation of short peptides or production of long ones. The abiotic approach also permits the study of polypeptides containing non-natural amino acids. Nowadays it is possible to prepare kg quantities of short peptides by chemical synthesis. Solution-phase synthesis is practically useful for preparation of homopolypeptides or peptides of defined composition but indefinite sequence only [81, 82]. Degree of polymerization in the solution-phase approach will be determined by the synthesis conditions, for example duration of reaction and temperature, and they must be worked out by empirical study. Solid-phase synthesis, by contrast, starts with an $N\alpha$ -derivatized amino acid attached to an insoluble resin via a suitable linker molecule [83]. The $N\alpha$ protecting group is removed in a deprotection step, and the next amino acid in the chain (also $N\alpha$ -protected) becomes coupled. This process is imperfect, but certain methods, for instance double coupling, give good overall efficiency. The deprotection/coupling cycle is repeated until the desired sequence of amino acids is generated. The peptide-linker support is cleaved, yielding the peptide and side chain protecting groups. And finally the protecting groups are removed. Solid-phase synthesis has made it possible to obtain useful amounts of a specific peptide on a routine basis.

2.2.1 Solid Phase Peptide Synthesis (SPPS)

Solid-phase peptide synthesis was pioneered by Merrifield [84], resulting in a paradigm shift within the peptide synthesis community. The concept of SPPS is to retain chemistry proven in solution, but to add a covalent attachment step (anchoring) that links the nascent peptide chain to an insoluble polymeric support. An appropriate polymeric support (resin) must be chosen that has adequate mechanical stability, as well as the desired physiochemical properties that facilitate solid phase synthesis. The synthesis beads will retain strong bondage to the peptides until cleaved by a reagent such as trifluoroacetic acid. The anchored peptide is extended by a series of deprotection/coupling cycles, which are required to proceed with exquisitely high yields and fidelities. It is the essence of solid-phase approach that reactions are driven to completion by the use of excess soluble reagents, which can be removed by simple filtration and washing without manipulative losses. Because of the speed and simplicity of the repetitive steps, carried out in a single reaction vessel at ambient temperature, the major portion of the solid-phase approach is readily amenable to automation. Due to amino acid excesses used to ensure complete coupling during each synthesis step, polymerization of amino acids is common in reactions where each amino acid is not protected. To prevent this polymerization, protective groups are used. The Fmoc (9-fluorenylmethyl carbamate) is currently a widely used protective group that is generally removed from the N terminus of a peptide in the iterative synthesis of a peptide from amino acid units. Once the desired linear sequence has been assembled satisfactorily on the polymeric support, the anchoring linkage must be cleaved. Depending on the chemistry of the original handle and on cleavage reagent selected, the product from this

step can be a C-terminal peptide acid, amide, or other functionality. The advantage of Fmoc is that the peptide is cleaved under very mild basic conditions. This adds additional deprotection phases to the synthesis reaction, creating a repeating design as shown in Figure 2.1.

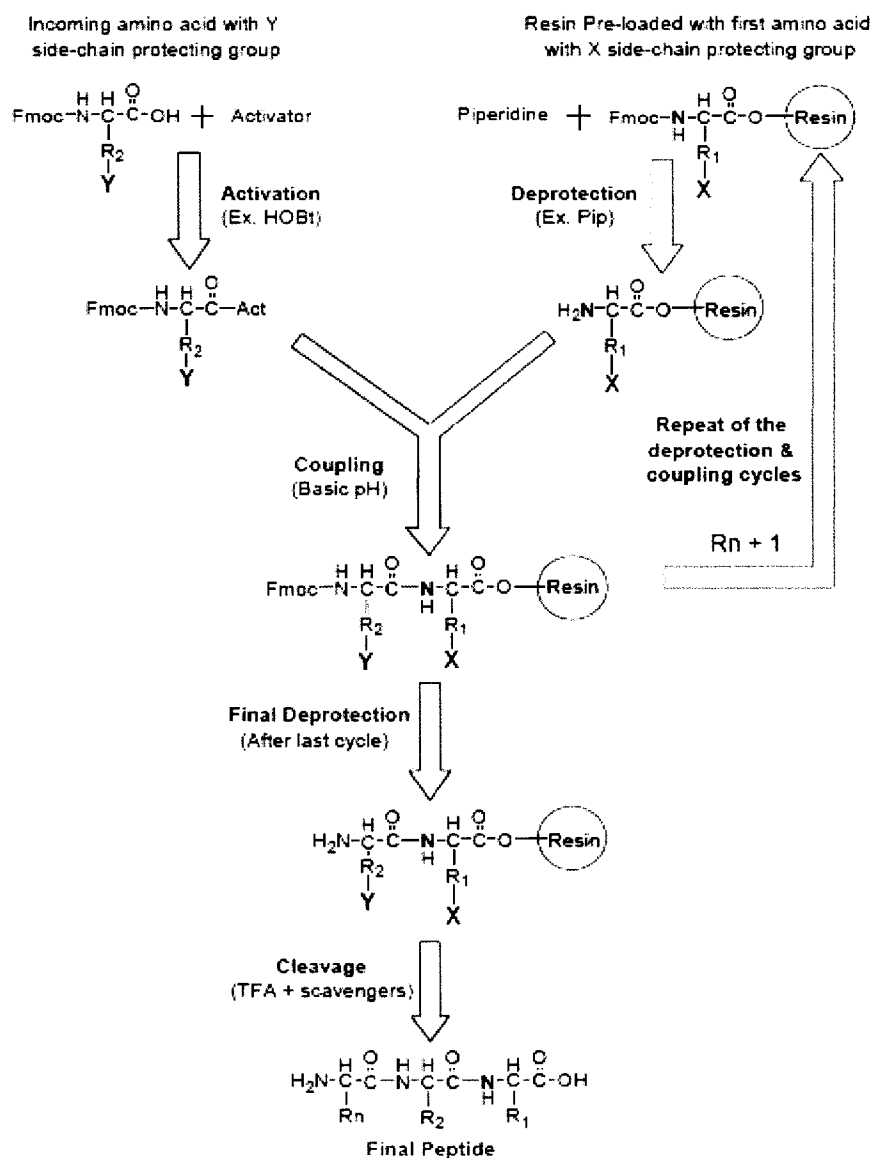


Figure 2.1. Schematic diagram of solid phase peptide synthesis [85].

The peptide synthesis in our laboratory was conducted on a Protein Technologies Inc. SYMPHONY which uses Fmoc chemistry to synthesize up to 12 peptides simultaneously. The synthesis scale is 5-100 μmol , and peptide-resin cleavage is performed on the instrument. The software allows us to enter the desired sequences and scale of synthesis and the amounts of reagents required are calculated. The instrument is programmed according to the desired sequences and the amounts of reagents required are calculated. Clean reaction vessels are used and resin is added in the required amount depending on the scale of synthesis. The resin is first swelled for a few minutes in DMF and drained the resin is also washed with DMF after each amino acid coupling. Fmoc deprotection after each amino acid coupling is accomplished using 20% piperidine in DMF, with mixing using nitrogen gas for a given time after each step. The resin is then washed with DMF. The first amino acid is coupled to the Fmoc-deprotected N-terminal amine of the resin, or a previously coupled amino acid, using a solution of amino acid dissolved in HBTU and 0.4 M N-methylmorpholine in DMF while mixing using nitrogen gas. Once the coupling of an amino acid is complete, the resin is washed, the Fmoc group deprotected with piperidine, and the resin is washed again to prepare it for the next coupling. This process is repeated until all the amino acids are coupled. The resin is allowed to dry and treated with an appropriate cocktail solution to cleave the peptide from the resin. The resin is then filtered away and the cocktail solution is added to cold ether to precipitate the dissolved peptides. The peptide suspension is then centrifuged and the ether decanted. This process is repeated a number of times to remove the scavengers and traces of trifluoroacetic acid followed by evaporation and lyophilization of the

peptide. The choice of the cocktail solution depends on the peptide sequence as shown in Figure 2.2.

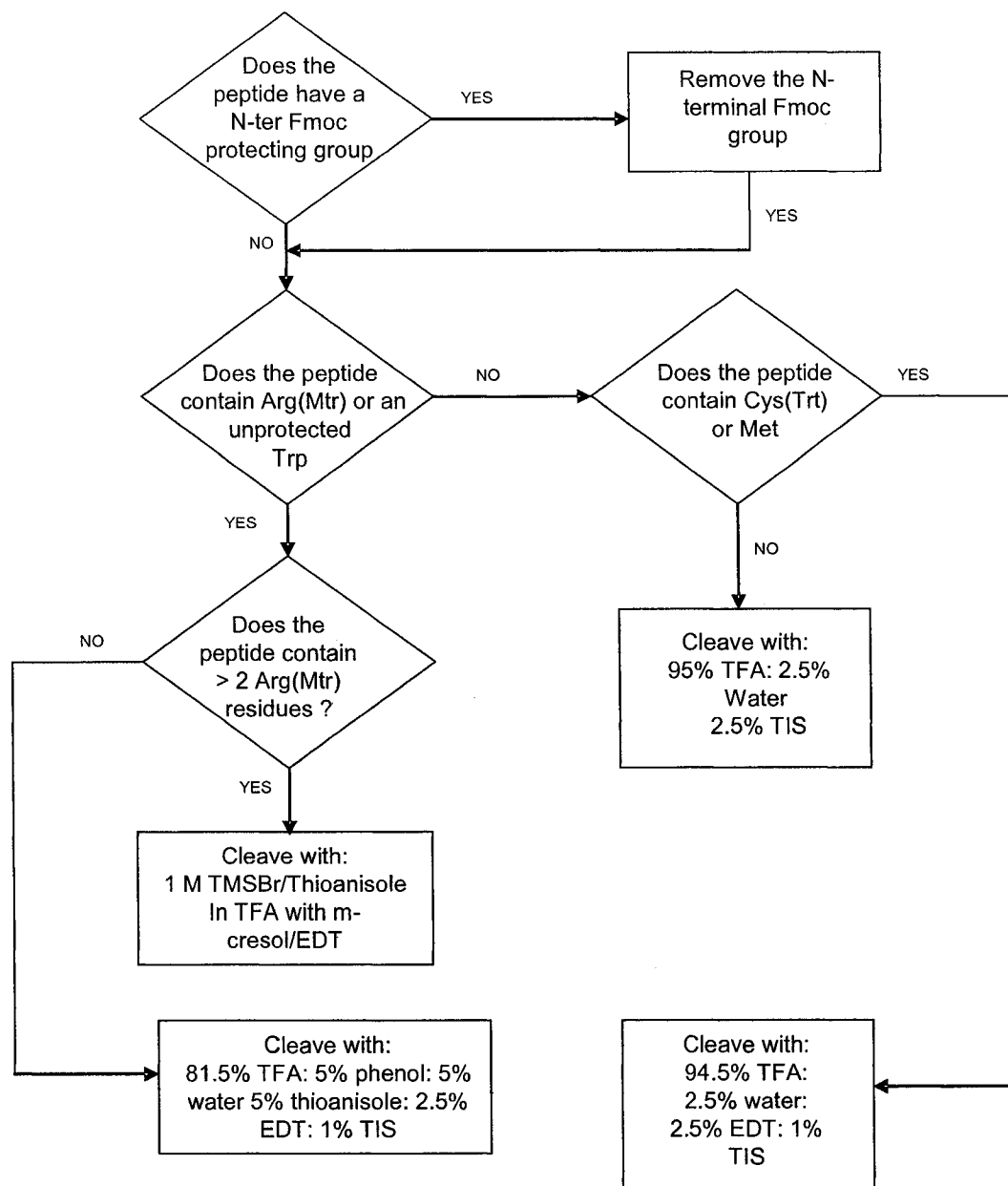


Figure 2.2. Flowchart for selecting cocktail solution.

2.2.2 High Performance Liquid Chromatography (HPLC)

High-performance liquid chromatography (HPLC) is an essential tool for the identification, purification and characterization of biomacromolecules. It is used mostly in biotechnology and pharmaceutical industries in all stages of a process from research and development to quality assurance and validation. The aim of the research and the molecular nature of the investigated molecules determine the choice of the chromatographic method and the type of high-performance equipment. Currently, most classes of biomacromolecules, including amino acids, peptides, proteins, carbohydrates, nucleic acids and lipids are analyzed primarily by HPLC. Several basic modes of HPLC are currently in use for peptide and protein analysis and purification, which include size-exclusion, ion-exchange, normal-phase, hydrophobic interaction, reversed-phase and hydrophilic interaction chromatography.

Reversed-phase High-performance liquid chromatography (RP-HPLC) techniques are very versatile and flexible, and they dominate the application world with peptides and proteins at the analytical- and laboratory-scale preparative levels. Unique aspects of peptide and protein structure, unexploited by methods other than hydrophobicity, drive the highly selective binding to (and elution from) the reversed-phase matrix, through multiple weak vander waals-type interactions. The resolving power of this technique is remarkable, permitting, in many cases, total separation of nearly identical molecules. Generally in all types of HPLC, division of the analyte molecules is involved between two phases within the column, *viz* the mobile phase and the stationary phase. The mobile phase is typically a liquid which is passed through a column containing an organic stationary phase that is chemically bonded to the surface of the support particles making

up the column packing. In RP-HPLC, the stationary phase is non-polar and the mobile phase is polar. As such, a differential migration of species takes place as the sample is eluted through the column based upon the relative polarity of the individual analytes themselves. A non-polar analyte will have greater affinity for the non-polar stationary phase than it will for the relatively polar mobile phase and will be more tightly bound to the column and vice-versa. In this mode of separation, the most polar analyte is the first to be eluted from the column [86-88]. Figure 2.3, shows the schematic of a HPLC

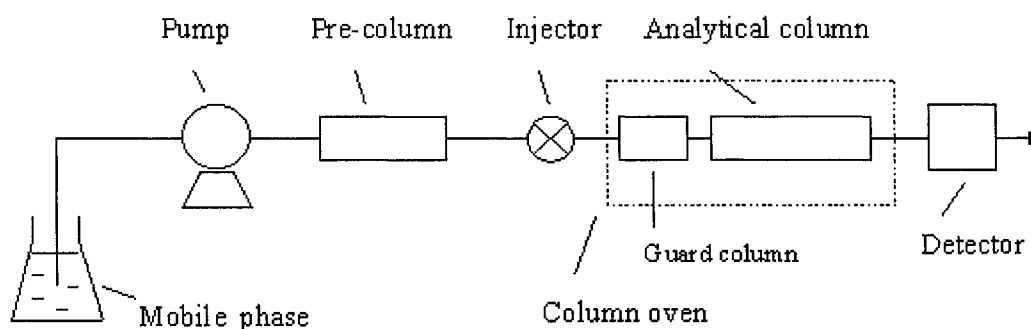


Figure 2.3. Schematic of a HPLC system [89].

Gradient elution is usually preferred for RP-HPLC polypeptide separations. Effectively separation of similar polypeptides can be achieved when shallow gradients are used and where isocratic separation would be problematic. Correlation between side-chain hydrophobicity and retention time in a peptide can be problematic due to limited interactions imposed by tertiary structures in most peptides. Peptide separations are also sensitive to the pH of the elution buffer due to the protonation and de-protonation of the acidic and basic side-chains. Polypeptide separation and resolution is not affected much by the flow-rate. RP-HPLC is used for the separation of peptide fragments from

enzymatic digests and for purification of natural and synthetic peptides. Preparative RP-HPLC is frequently used to purify synthetic peptides in milligram and gram quantities [90, 91] and used to purify micro-quantities of peptides for sequencing and purify milligram to kilogram quantities of biotechnology-derived polypeptides for therapeutic use [92, 93]. The hydrophobic part of a polypeptide, responsible for the separation, is very sensitive to molecular conformation. This sensitivity of RP-HPLC to protein conformation results in the separation of polypeptides that differ not only in the hydrophobic part but also oxidized amino acids or in single amino acid substitutions. Scalability of any HPLC procedure involves changing from existing columns to either larger or smaller columns. It is often desirable to retain the same resolution and retention. To achieve the same retention times and performance on the columns with different geometries, flow velocities must remain constant by adjusting flow rates accordingly. The use of different elution solvents, ion-pairing agents, buffers and gradient conditions may also be involved.

2.2.3 Capillary Electrophoresis (CE)

The need for high-resolution separation of biopharmaceuticals and concerns about toxic compounds in the environment paved the way for the development of capillary electrophoresis. Michaelis separated proteins on the basis of their isoelectric point in 1909 and coined the term “electrophoresis”. The pioneering work of Hjerten [94] laid the ground work for modern day CE analysis of various analytes. Over the last few years CE has proved a rapid and versatile analytical technique that combines simplicity with high reproducibility. CE can be used for the separation of a variety of analytes of different size

and charge: simple molecules, organic and inorganic ions, peptides, proteins, carbohydrates and nucleic acids.

The basic instrumentation consists of four parts. A narrow diameter capillary is required for the separation, a high voltage power supply is required to drive the separation, a detector is required to detect the presence and amount of analyte and a safety interlock-equipped enclosure is used to protect the operator from high voltage. Either pressure or vacuum is applied to the sample and 10 - 100 nL is injected, or an electrical current is applied through the sample and only the charged molecules enter the capillary. Figure 2.4, shows the schematic of a CE system

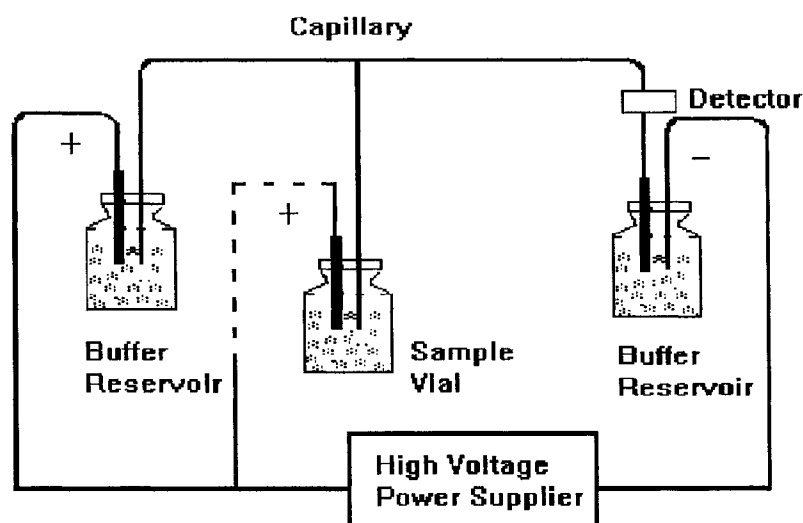


Figure 2.4. Schematic of a CE system [95].

The resulting migration of a charged particle in CE is a sum of the electrophoretic flow, determined by the size and charge on the molecule, and the electroosmotic flow, determined by the charge on the inner surface of the capillary. The plot of detector response with time is generated and called an electropherogram. The flow of electrolyte,

known as electroosmotic flow, EOF, results in the flow of the solution along the capillary towards the detector.

Numerous peptide applications using CE have been explored in the last decade. Peptides, because of their fairly simple structure, show little interaction with the capillary and show high separation efficiencies. Due to the presence of limited number of ionizable groups in their structure, peptides are often separated at extremes of pH where all the side chains are either protonated or deprotonated. These extremes in pH are used to separate peptides of different length that will differ by their charge to mass ratios. The greatest selectivity difference for acidic residues can be found in the range of pH 2 to 7, while, for basic residues it is usually pH 8 to 10. Various studies have been done towards achieving optimal separations [96-101] however, understanding the relationship between structure and charge is the most direct way of optimization. Additives like organic solvents, surfactants, and chiral selectors are used when the compounds are closely related and pH optimization does not lead to desired resolution.

CE is a powerful analytical tool that replaces methodologies that are inherently slow and labor intensive. Low injection volumes and rapid analysis times enable the analysis of a large number of samples over a short period of time. The process can be scaled up by advances in instrumentation and detection systems. As is the case with any pharmaceutical, an antibiotic must be characterized in terms of its potency and the presence and quantity of impurities. Additionally, any residue or metabolite that may be present as a result of its use must be monitored. Many CE techniques have been used in the analysis of antibiotics, addressing the various aspects of quantifying, profiling, and monitoring. The auto-sampler tray, through which samples and buffers are injected into

the capillary facilitates automated analysis of more than one sample one after the other. Also, recently multiple capillary instruments have been reported which have five capillaries, enabling the analysis of as many samples at any given time. In view of the increasing sample complexity and the requirement for obtaining structural information from extremely limited amounts of material, coupling CE instrumentation with mass spectral detection offers unparalleled advantages over single parameter detection systems.

2.2.4 Nuclear Magnetic Resonance (NMR)

Nuclear magnetic resonance is a phenomenon which occurs when the nuclei of certain atoms are immersed in a static magnetic field and exposed to a second oscillating magnetic field. Some nuclei experience this phenomenon, and others do not, depending upon whether they have a property called spin. An NMR structure is an atomic model based on the interpretation of a set of interatomic distances. NMR measurements provide crucial evidence regarding behavior in solution and can provide structural information on rapid time scales. Multidimensional NMR spectroscopy gained substantial power with the advent of multi-isotope and heteronuclear techniques, which facilitate the resolution of spectra that are tightly packed and impossible to resolve in two dimensions. Using different isotopes (generally ^{14}C and ^{15}N) it is now possible to obtain a sufficient number of constraints to define structures of peptides and proteins [102]. Kinetic behavior on a wide variety of time scales can be studied by NMR relaxation spectra [103-106]. Solid-state NMR spectroscopy has been used to monitor the layer-by-layer (LBL) growth of polyelectrolyte multilayers on colloidal silica. The dynamics and conformation of polyelectrolyte multilayers comprised of the weak polycation, poly(allylamine) hydrochloride, and the strong polyanion, poly(sodium-4-styrene sulfonate), assembled at

pH 7 and pH 10 were studied by a combination of ^1H and ^{13}C NMR measurements and the effect of adsorbed water has also been investigated [107-110]. Extension of these studies to polypeptide multilayer films would provide us with a greater insight into the physics of interaction of designed polypeptides in the film and would lay the foundation of designing peptides for highly specific applications.

2.2.5 Mass Spectrometry (MS)

Ionization methods suitable for peptides include secondary ionization mass spectrometry (SIMS) [111], electrospray ionization (ESI) [112], and matrix-assisted laser desorption ionization (MALDI) [113]. Each of the techniques has its own advantages. Peptide signals may be suppressed by the presence of salts, detergents, or other peptides. In most cases, salts are removed during peptide mapping by reversed phase HPLC where TFA is used as an ion-pairing agent. It should be remembered that all peptides from a map must be collected and stored in polyethylene or polypropylene tubes. To get a good signal, the peptide must be soluble and be able to migrate to the surface of the liquid matrix where the ionization takes place. Small polar peptides tend to give poor signals, perhaps due to surface phenomenon, and must be derivatized by esterification to overcome this problem [114].

2.3 Film Characterization Techniques

Various tools are used to characterize polyelectrolyte multilayer films. The emphasis here is on physical techniques. One might be also interested in chemical properties or biofunctionality in the case of polypeptide films. Examples of such properties include redox potential and immunogenicity more specifically related to target applications than basic film properties. The polyelectrolyte LBL literature is too large to

provide a comprehensive account of references however, references to papers in which the indicated methods have been used to study polypeptide multilayer films have been provided.

2.3.1 Quartz Crystal Microbalance (QCM)

The Quartz Crystal Microbalance (QCM) is an extremely sensitive mass sensor, capable of measuring mass changes in the nanogram range. QCMs are piezoelectric devices fabricated of a thin plate of quartz with electrodes affixed to each side of the plate. QCM crystals are used as sensors to determine mass changes as a result of frequency changes. Frequency shift is converted to mass increment by the relation $\Delta f \approx -\Delta m (1.83 \times 10^8)/A$, where f is the resonant frequency in Hz, m is the deposited mass in g, and A is the surface area of the resonator [115]. QCM provides information on mass change and kinetics of polyelectrolyte adsorption by way of change in resonant frequency [116-122]. The streaming potential method is used to characterize electrical properties of a film surface. The basic principle is to measure pressure and potential difference on both sides of a capillary [67, 71, 73, 123, 124]. Figure 2.5 shows a quartz crystal resonator

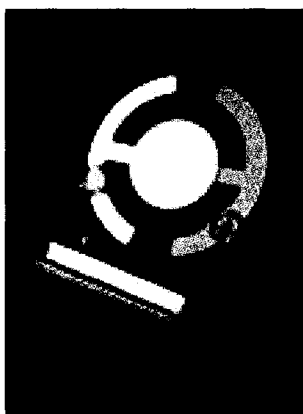


Figure 2.5. Quartz crystal resonator.

2.3.2 UV-vis Spectroscopy

UV-vis spectroscopy is a relatively cheap way to measure the optical mass of assembled polypeptides in terms of absorbance increase per layer, or disassembled material in terms of absorbance decrease [118,120]. For just visible spectroscopy, ordinary glass cuvettes may be used, but ultraviolet spectroscopy requires special cuvettes made of a ultraviolet-transparent material such as quartz. The polypeptides are assembled from solution onto a quartz substrate for a given time. The substrate is then rinsed, dried and placed in the path of a light beam that scans from 190-300 nm. Molecules which absorb photons of energy corresponding to wavelengths in the range 190 nm to about 300 nm exhibit UV-vis absorption spectra. The peak maxima occur at 214 nm corresponding to the peptide bond absorbance and absorbance from aromatic amino acids (tyrosine, tryptophan, and phenylalanine) can be observed at 280 nm. In some cases UV spectroscopy can provide useful information on structure in terms of position of absorbance peak maximum. Figure 2.6 shows a Jasco V-530 UV-vis spectrophotometer.

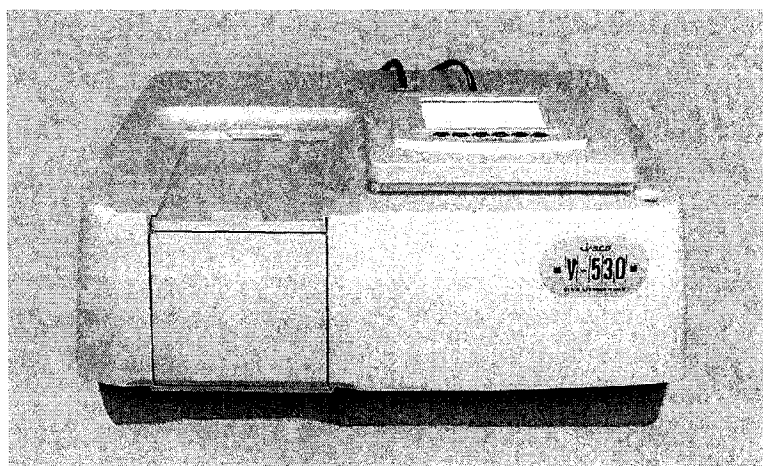


Figure 2.6. UV-vis spectrophotometer.

2.3.3 Circular Dichroism Spectroscopy (CD)

Circular dichroism is the observed elliptical polarization of right and left circularly polarized light produced by an optically active medium in the vicinity of its absorption bands. Circular dichroism spectrometry (CD) enables a moderately accurate determination of film secondary structure content, important when polypeptides are involved [116, 118, 120-122, 125]. The far-UV CD signal is particularly sensitive to conformation of the polypeptide backbone; different secondary structures have more distinctive spectral signatures in CD [126]. CD can provide extensive information on secondary structures in peptides [13, 127-130] and it measures the differential absorption of right- and left circularly polarized light. In the far-UV region of the spectrum, 180-260 nm, the signal is very sensitive to the average conformation of the polypeptide backbone whether the peptide is in solution or in a film [131]. Figure 2.7 shows signature spectra for various secondary structures in proteins.

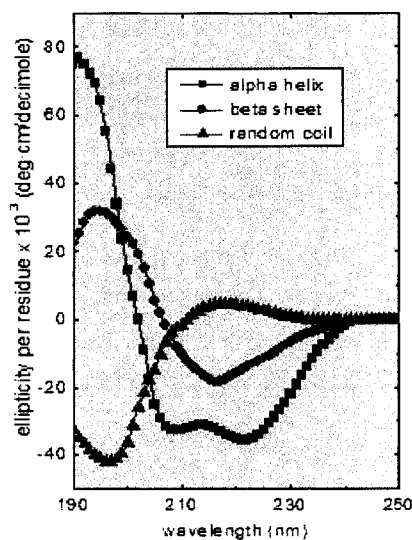


Figure 2.7. Signature spectra of different secondary structures [126].

A set of reference spectra and some assumptions underlie spectral analysis [132]. The reference spectra generally are proteins or peptides for which the secondary structure content is known by an independent means, for example X-ray crystallography. The basic principle of analysis is that a CD spectrum can be regarded as a linear combination of spectra of distinct secondary structures. By this approach one can estimate the fractional content of α helix, β sheet, β turn, and random coil with considerable accuracy. Comparison of the various physical methods would suggest that CD is the most informative one for obtaining information on the conformation of polymers in a polyelectrolyte thin film. CD analysis of polypeptide films [118,121,122,133] has yielded the most detailed experiment-based view to date of polymer structure in a polyelectrolyte multilayer film than FTIR.

2.3.4 Ellipsometry

Ellipsometry is an optical technique that relies on the optical physics of the stratified media. Excellent treatments of the subject exist and ellipsometry is one of the few techniques that can accurately monitor thin-film processes while they occur, yielding both fundamental properties and process information about the system under measurement. In addition it is possible to use feedback to affect control of thickness, composition, and temperature, for example, which are process related parameters. If linearly polarized light of a known orientation is reflected at oblique incidence from a surface then the reflected light is elliptically polarized.

An ellipsometer measures the changes in the polarization state of light when it is reflected from a sample. If the sample undergoes a change, for example a thin film on the surface changes its thickness, then its reflection properties will also change. Measuring

these changes in the reflection properties can allow us to deduce the actual change in the film's thickness [72,118,125,134,135]. The amount of material adsorbed can be calculated from the thickness and refractive index. Figure 2.8 shows a schematic of an ellipsometer

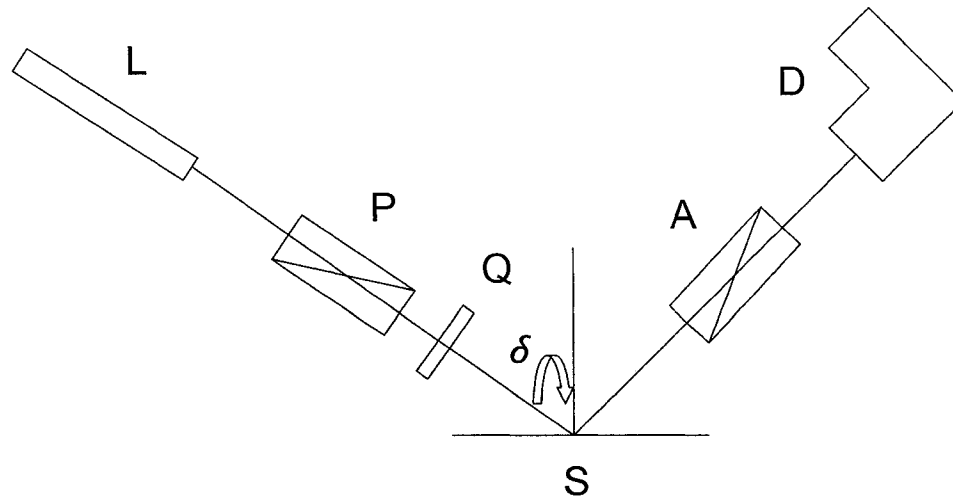


Figure 2.8. Schematic diagram of a nulling ellipsometer.

2.3.5 Atomic Force Microscopy (AFM)

The atomic force microscope (AFM) is a very high-resolution type of scanning probe microscope. The AFM was invented by Binnig, Quate and Gerber in 1985, and is one of the foremost tools for the manipulation of matter at the nanoscale. A cantilever scans the solid surface and the deflection of the cantilever is detected by the reflection of a laser beam. The primary modes of operation are contact mode, non-contact mode, and dynamic contact mode. In the contact mode operation, the force between the tip and the surface is kept constant during scanning by maintaining a constant deflection. In the non-contact mode, the cantilever is externally oscillated at or close to its resonance frequency. The oscillation is modified by the tip-sample interaction forces; these changes in oscillation with respect to the external reference oscillation provide information about the

sample's characteristics [136]. In simple terms, AFM is similar in principle to early record players, where the movement of the sharp needle in the groove reproduced the sound. Because the AFM relies on actual contact to sense the nature of the sample surface, it can be used to non-conducting materials like biological molecules, organic material, biopolymers, and living cells. Figure 2.9 shows a schematic of an AFM

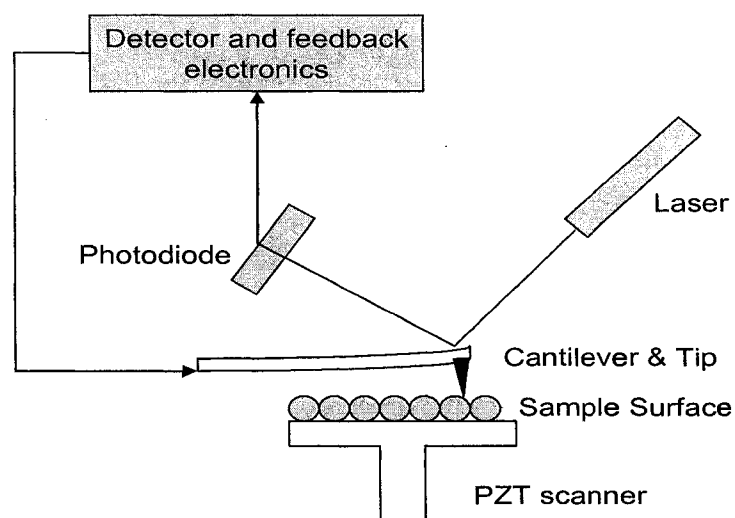


Figure 2.9. Schematic of AFM

The biggest advantage of AFM is that most samples can be investigated in their natural state including aqueous environments. AFM has thus become a well established and valuable tool in three-dimensional topographical imaging of biopolymers [137-142] and has been used to characterize film surface morphology, roughness, and thickness of polypeptide multilayer films [73,118,120,123-125,143,144].

2.4 Computational Approach

Computer-based approaches for the development of polyelectrolyte multilayer thin film technology have already appeared in the scientific literature [145-152]. Important for commercialization of polypeptide multilayer films, MD simulations can also be used to study some aspects of the peptide design process. Such analysis will provide insight on polyelectrolyte complexation and the relationship between electrostatic interactions, hydrophobic interactions, hydrogen bond formation, secondary structure, and film stability. Simulations could also help to understand the internal structure of an LBL film. A series of MD simulations on designed peptides have been done to test the role of differences in amino acid sequence on aspects of peptide interaction [133]. The initial structure in each case was a parallel or anti-parallel β sheet with standard bond angles, selected on the basis of the known secondary structure content of polypeptide films. The results show that primary structure can have a major impact on the interaction energy in general and the number of hydrogen bonds between strands in particular, especially when the charge density is high and the electrostatic interactions between side chains extensive. These conclusions are consistent with corresponding experimental studies [133].

CHAPTER 3

ANTI-MICROBIAL POLYPEPTIDE MULTILAYER FILMS 2

3.1 Introduction

A multilayer coating (or film) of nanometer-thick layers with antimicrobial properties can be made by sequential adsorption of oppositely charged polyelectrolytes on a solid support. The method is known as layer-by-layer assembly (LBL). No special apparatus is required for LBL and nanofilms can be prepared under mild, physiological conditions. formed by the nano-scale fabrication process known as electrostatic LBL [15, 152]. The method involves the sequential adsorption of oppositely-charged species onto a solid support. Polyelectrolyte multilayer film layers have a thickness on the order of 1 nm per layer, the precise value depending on the linear charge density and molecular weight of the adsorbing polymers, extent of film hydration, and ionic strength. The basic character of LBL, however, depends neither on the surface area of the support nor its shape, just the charge properties of the surface and the assembling species. Polyelectrolyte multilayer films and coatings can feature a variety of useful properties, for example, biofunctionality, as when a macromolecule with specific biochemical properties is incorporated [47]. The layering process in LBL is repetitive and has been automated, important for commercial prospects of applications of the technology.

Films and coatings with antimicrobial properties are being developed for a variety of purposes. For example, ductwork coatings are used to improve indoor air quality [153]. Colonization of bacteria is inhibited by the incorporation of anti-bactericidal agents in the coatings and the release of the bactericides over time. Antimicrobial films have been investigated in medical research as a means of accelerating wound and scar healing and lowering infections due to implanted devices [154-156]. Antimicrobials have been incorporated into textiles [157]. Coating a food with an edible antimicrobial material could serve a variety of purposes, such as preventing physical, chemical, or biological degradation of food items while preserving moisture, flavor, and quality [158-161].

Edible and biodegradable food coatings are attractive because they can reduce packaging costs and municipal waste [162]. Numerous chemicals that could be incorporated into a thin film to inhibit microbial biofouling, however, will also abrogate edibility. A need exists therefore to develop coatings that both inhibit microbial contamination and maintain edibility [163]. Incorporation of antibacterial enzymes into biodegradable films seems more advantageous than incorporation of antimicrobials into plastic wrappers, because most biodegradable films are edible and they can be formed under mild conditions [164]. The antimicrobial enzyme incorporated into the polypeptide thin films studied here is HEWL. This enzyme is edible and widely used for food preservation.

The natural biopolymers known as peptides and proteins constitute roughly half of the dry mass of an organism. Peptides and proteins can be purified from a plant or animal source for use as a raw material for the production of biocompatible films,

coatings, and microcapsules [165]. Structural and functional properties of proteins have been exploited in the development of thin films for diverse applications, for example, biomedical implants, biosensors, chromatographic membrane separations, and food coatings [166]. Edible films prepared from various proteins have attracted much attention for use in food protection and preservation as they present a number of advantages over synthetic films, including favorable degradability and environmental characteristics [167]. The thin films studied here are polypeptide multilayer films [142] consisting of PLGA, a readily available synthetic homopolypeptide, and HEWL, a readily available enzyme that is straightforward to purify by virtue of its high net charge at mildly acidic pH. Given the generality of LBL, the method is appropriate for all antibacterial compounds which have a suitable surface charge at the pH of film assembly. The incorporation of antibacterial proteins or polypeptides in multilayer films represents a promising area for development in biomaterials and biotechnology. In this chapter a multilayer nanofilm in which one of the constituent species is an antimicrobial protein have been fabricated and studied for activity and sustained release. The basic approach was to fabricate the films using LBL and study the release of the antimicrobial protein over time and under various conditions. An attempt has also been made to quantify the amount of protein released over time and all methods were developed empirically for further work.

Earlier work has shown that antimicrobial peptides [168] or silver nanoparticles [169] can be incorporated into a multilayer film, conferring antimicrobial functionality. It seemed to us that antimicrobial proteins or peptides could be combined with polypeptide LBL to explore the development of novel biodegradable and edible food

coatings or packaging techniques, or a new generation of coatings for implant devices. Here, we show that multilayer films in which HEWL is incorporated by simple electrostatic attraction will inhibit *M. luteus* proliferation in the surrounding medium. The results indicate that HEWL molecules are released from films over time and that a proportion of the HEWL molecules incorporated into the films retain functionality. The results suggest that similar films could be developed for various practical applications where microbial biofouling is a concern.

3.2 Materials and Methods

PLGA (13 kDa), HEWL, Luria-Bertani (LB) broth, *M. luteus* (lyophilized), 4-methylumbelliferyl N-acetyl-chitotrioside ((GlcNAc)₃-MeU), monobasic and dibasic sodium phosphate, sodium acetate, ethylenediaminetetraacetic acid (EDTA), sodium chloride and sodium azide were from Sigma-Aldrich (USA). Glycerol was from Pfaltz and Bauer (USA). Tris(hydroxymethyl)aminomethane (Tris) and glycine were from ICN Biomedicals (USA). All other chemicals were from Sigma-Aldrich. 18.2 M_Ω-cm water (SIMS60000 water purifier, Millipore, USA) was used in all experiments. In addition, all buffers were filtered at 0.45 μm before use, limiting bacterial contamination. LB broth was prepared by dissolving 20.6 g of broth mix in 1 l water and then autoclaving. Solutions for film assembly were prepared by dissolving PLGA in 10 mM Tris, 75 mM NaCl, pH 7.4 to a final concentration of 1 mg/ml, and HEWL to 2 mg/ml in the same buffer.

3.2.1 LBL

Films were fabricated by repetitive alternate adsorption of PLGA and of HEWL from aqueous solution with an intermediate rinsing step in water. Figure 1 presents a schematic illustration of LBL. Each cycle of the assembly procedure consisted of immersing the substrate in HEWL solution for 15 min, rinsing with water, immersing the substrate in PLGA solution and rinsing with water. The process was repeated until 3, 7, 11, 15, or 21 layers were adsorbed; in all cases HEWL was deposited in the final layer. Where indicated, films were dried with nitrogen gas prior to adsorption of the oppositely charged species. Figure 3.1 shows the schematic assembly of HEWL (spheres) and PLGA (irregularly structured polymers)

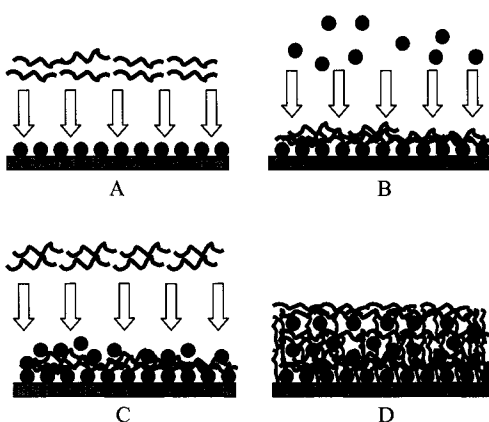


Figure 3.1. Schematic of HEWL and PLGA assembly by LBL.

3.2.2 Quartz Crystal Microbalance (QCM)

PLGA/HEWL films were assembled at room temperature on silver-coated resonators of 9 MHz nominal resonant frequency (Sanwa Tsusho, Japan). Resonator surfaces were cleaned with a solution of equal parts of water, 1 M NaOH and 70% ethanol. Resonant frequency was determined with an Agilent 53131A 225 MHz universal

counter (USA) after deposition of each layer of PLGA or HEWL. The film was always dried before measurement, enabling frequency shift to be converted to mass increment [115] by the relation $\Delta f \approx -\Delta m (1.83 \times 10^8)/A$, where f is the resonant frequency in Hz, m is the deposited mass in g and A is the surface area of the resonator (0.16 cm² per side). Five sets of 2-ml assembly solutions of PLGA and HEWL were prepared as described above. The first set had 0.1% azide in each, the second 2 mM EDTA in each, and the others 5, 15, or 25% (w/v) glycerol in each. Azide and EDTA are known antimicrobials. Glycerol, a plasticizer, reduces film brittleness.

3.2.3 UV Spectroscopy

Quartz cover slips (ElectronMicroscopy Sciences, USA), 7.5 cm×2.5 cm×0.1 mm in size, were cut into rectangular pieces of 1.25 cm × 2.5 cm, cleaned for 30 min in 1% sodium dodecylsulfate at 80°C with agitation and washed for 2 h with 1 M NaOH/C₂H₅OH (60:40, v/v) and overnight with H₂SO₄/H₂O₂ (75:25, v/v). The slides were then rinsed extensively and stored in ultra-pure water until film assembly. The substrate was glass instead of quartz in cases not requiring UV analysis. In all cases the films were dried with nitrogen gas before spectral characterization.

3.2.4 Bacterial Culture

The well-studied model microbe *M. luteus* was cultured in LB broth overnight at 30°C and stirring at 200 rpm after sterilization of the medium by autoclaving. In a typical HEWL activity experiment, log phase culture was diluted to an initial optical density (OD) at 600 nm of 0.005. All OD measurements were taken with a Jasco V-530 spectrophotometer (Japan) outfitted with a constant temperature cell holder. A decrease in concentration of bacteria in the liquid culture surrounding each film was measured as a

decrease in OD at 600 nm. The OD of *M. luteus* suspension decreases in the presence of active HEWL due to decreased strength of the cell wall, lysis and the reduced ability of cell membranes and cellular debris to scatter light at 600 nm relative to intact cells.

3.2.5 Activity of HEWL Released from Films

The activity of HEWL in the liquid medium surrounding PLGA/HEWL films of 0, 3, 7, 11, 15, or 21 layers was quantified by *M. luteus* assays or by hydrolysis the HEWL of 4-methylumbelliferyl N-acetyl-chitotrioside ((GlcNAc)₃-MeU), a fluorescent substrate analog [170]. In the bactericidal assays, the relative activity of HEWL released by PLGA/HEWL films into the surrounding liquid medium was determined by change of OD. Each assay was done by mixing 0.25 ml of the buffer in which the PLGA/HEWL film was immersed with 2.75 ml *M. luteus* cell suspension (0.25 mg/ml in 50 mM sodium phosphate, pH 7.0). There was continuous stirring at 200 rpm and, and the temperature was held at 30°C. Change in OD 600 nm was determined after 10 min.

In (GlcNAc)₃-MeU assays, labeled saccharide was dissolved to a known concentration in 0.1 M sodium acetate, 0.5 M NaCl (pH 3.8). The anionic form of MeU is fluorescent, and equilibrium disfavors anion formation at the pH of the assay. In each case the reaction mixture consisted of 100 μ l liquid medium in which the film was immersed, 100 μ l saccharide solution and 300 μ l water. The pH of the mixture was 4.5. The enzymatic reaction mixtures were incubated at 42°C for 1 h. Then the reactions were stopped, and released MeU was converted to the anionic form by addition of an equal volume of glycine buffer at pH 12. MeU concentration was quantified by measurement of fluorescence intensity at 465 nm. The excitation wavelength was 360 nm. A standard curve shown in Figure 3.2 was prepared to quantify the amount of released HEWL.

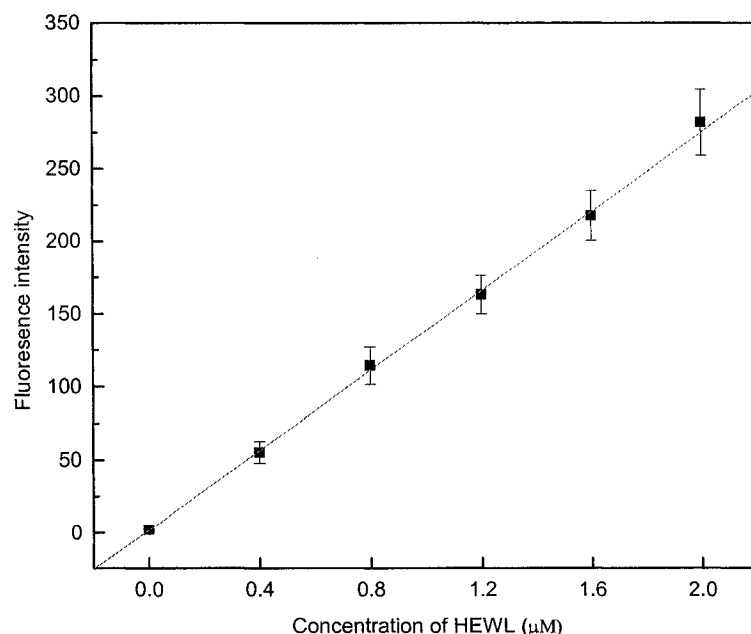


Figure 3.2. Standard curve for HEWL activity assays.

3.2.6 Activity of HEWL Retained in Films

The activity of PLGA/HEWL films was determined after immersing film-coated slides in Petri dishes containing 4 ml 0.25 mg/ml *M. luteus* suspension in 50 mM sodium phosphate (pH 7.0), incubating at 30°C and stirring at 200 rpm. Relative activity was measured as change in OD at 600 nm.

3.2.7 Stability of Bioactive Films

The longevity of anti-*Micrococcus* activity of PLGA/HEWL films was tested after immersion of the films in 50 mM phosphate (pH 7.0) at 4°C for 1 month or lyophilization and storage at 4°C for 1 month. The liquid medium surrounding the films was assayed for HEWL activity after 14 h incubation at 30°C and 200 rpm continuous stirring as described above. 0.01 mg/ml HEWL solution was kept in 50 mM phosphate (pH 7.0) at 4°C for 1 month as a control on loss of activity due to spontaneous inactivation of enzyme molecules by any mechanism.

3.3 Results and Discussion

15-layer films were fabricated on QCM resonators to study mass deposition in PLGA/HEWL film assembly. Film mass increment, however, was positive for HEWL deposition and negative for PLGA as shown in Figure 3.3.

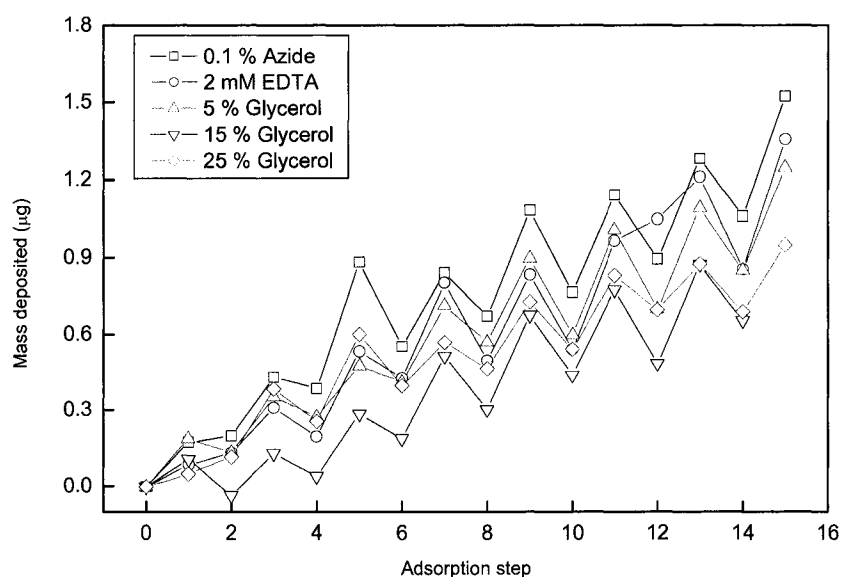


Figure 3.3. PLGA/HEWL multilayer film assembly monitored by QCM.

The data suggest that a portion of film material returned to solution during PLGA adsorption steps, possibly by formation of a soluble complex between PLGA molecules and previously adsorbed HEWL molecules. The loss of HEWL on adsorption of PLGA suggests that HEWL is unlikely to be uniformly oriented on the film surface: some molecules will be more strongly adsorbed than others, owing to the non-uniformity of substrate surface charge density, the complex nature of the molecular surface of HEWL and deformation of HEWL structure on adsorption. Highly-charged and disordered polypeptides tend to adsorb on a surface more effectively than HEWL and, probably, proteins in general [120]. The results show an overall linear increase in film mass with

number of layers deposited because frequency shift is proportional to mass increment for dry films [115] (Figure 3.4).

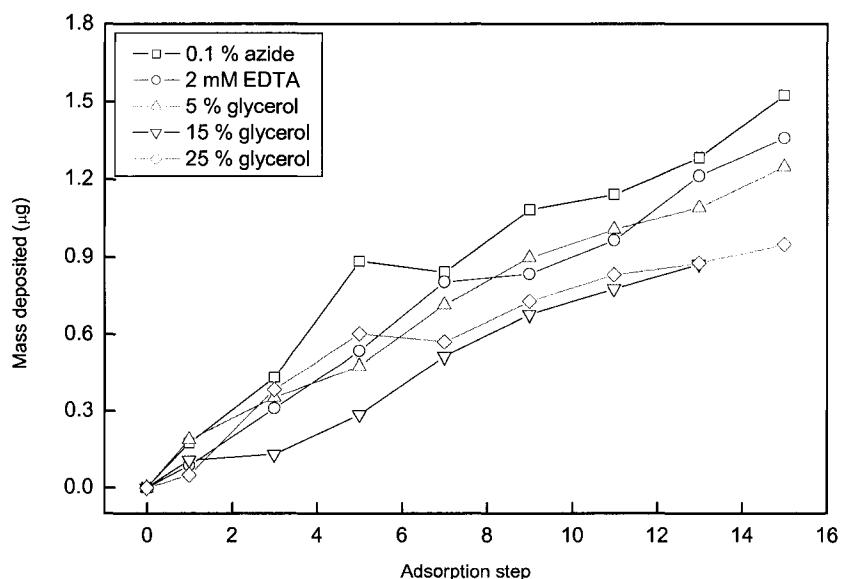


Figure 3.4. PLGA/HEWL multilayer film assembly monitored by QCM (bilayer).

Nevertheless, the data show that enough of the adsorbed HEWL molecules remain bound to the film surface during PLGA deposition for peptide adsorption to occur and be sufficient for the subsequent adsorption of another layer of HEWL. The conditions under which the frequency shift measurements were made, i.e., dry films, enable quantitative statements to be made with regard to mass deposited on and mass lost during the assembly process. The total mass of HEWL deposited in 15 layers was about 1.3 μg . This is the difference between the cumulative mass gained during deposition steps and the cumulative mass lost during PLGA deposition steps. The surface density of HEWL was about 4.1 $\mu\text{g}/\text{cm}^2$. This result suggests that approximately 22 μg of HEWL were deposited in 15-layer films on a quartz or glass slide of surface area approx. 7 cm^2 .

Glycerol is a plasticizer in edible films and food coatings [171], and it stabilizes the folded protein structure in aqueous solution [172]. EDTA, a chelating agent that

enhances the antimicrobial activity of bacteriocins, and is useful for broadening the spectrum of other antimicrobials [173]. As shown in Figure 3.4 neither glycerol nor EDTA substantially altered multilayer film assembly under the conditions studied here; film assembly occurred in both cases and the additives had no practical effect on the general character of film assembly.

Data on PLGA/HEWL film assembly have also been obtained by UV absorbance. The films were prepared on quartz slides; glass is largely opaque to UV. The data show that the amount of material deposited is not a strictly linear function of the number of layers as seen in Figure 3.5. The consistency of film preparation on different surfaces is relevant to the scope of applicability of the basic methodology outlined here. The amount of material adsorbed onto the surface depended to some extent on whether the film was dried between assembly steps, albeit little. The data suggest that intermediate drying steps are unnecessary for film fabrication, potentially important for manufacturing.

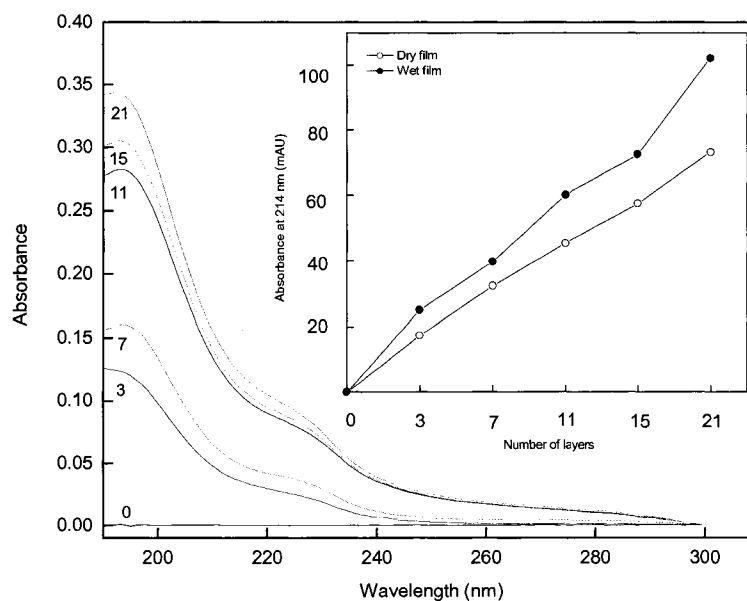


Figure 3.5. PLGA/HEWL film assembly monitored by UV spectroscopy.

In any case, multilayer film assembly of a protein and peptide is a more complex process than assembly of two disordered polypeptides, given the complex structure and charge properties of the folded state of a protein and the more flexible nature of a largely unstructured and uniformly charged peptide [119]. Nevertheless, in general the assembly behavior obtained by UV absorbance corroborates that by QCM.

Enzyme is released from PLGA/HEWL films over time into the surrounding aqueous environment. Some of the enzyme retained in the film is active. Both regions of HEWL activity have been characterized in this work. The results indicate that the greater the amount of HEWL deposited, the greater the amount of HEWL released in a given interval of time. Lysis of *M. luteus* cells increased as the number of film layers increased. This implies that the amount of HEWL that leaches out of a film depends on the number of layers of HEWL and, therefore, on the amount of HEWL in the film. The antimicrobial activity of PLGA/HEWL films in liquid culture medium is illustrated in Figure 3.6.

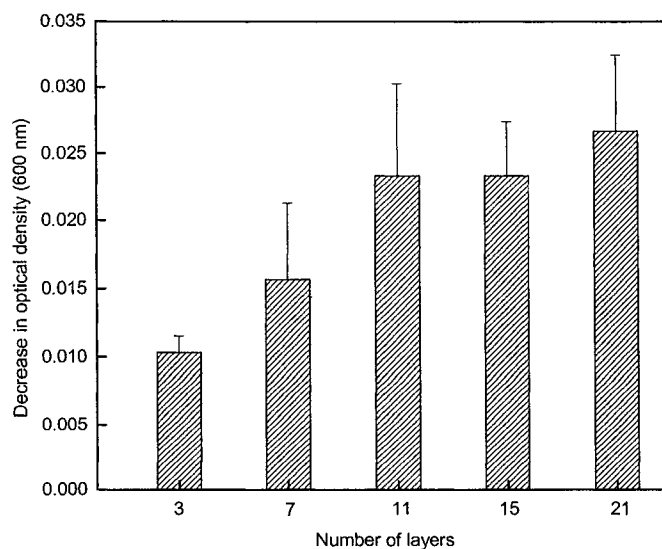


Figure 3.6. Activity of PLGA/HEWL films against *M. luteus*.

A higher concentration of active HEWL in solution will result in a greater decrease in OD at 600 nm in a given time interval, because a greater proportion of cells are ruptured and fewer particles are available to scatter light effectively at 600 nm [174]. HEWL activity in the aqueous medium surrounding PLGA/HEWL-coated slides of a certain number of layers was studied by fabricating fresh films and freeze drying, or by fabricating and incubating in buffer for 1 month. In films immersed in buffer, a large percentage of adsorbed HEWL is released into the surrounding buffer during 1 month at 4 °C. Antibacterial activity increased with an increase in the number of layers. In lyophilized films, HEWL remained active and was released on immersion in an aqueous medium. The activity of lyophilized films was comparable to that of freshly prepared ones. The total activity of HEWL in films after immersion in an aqueous medium will probably be lower than that of a lyophilized film or a freshly prepared film as shown in Figure 3.7.

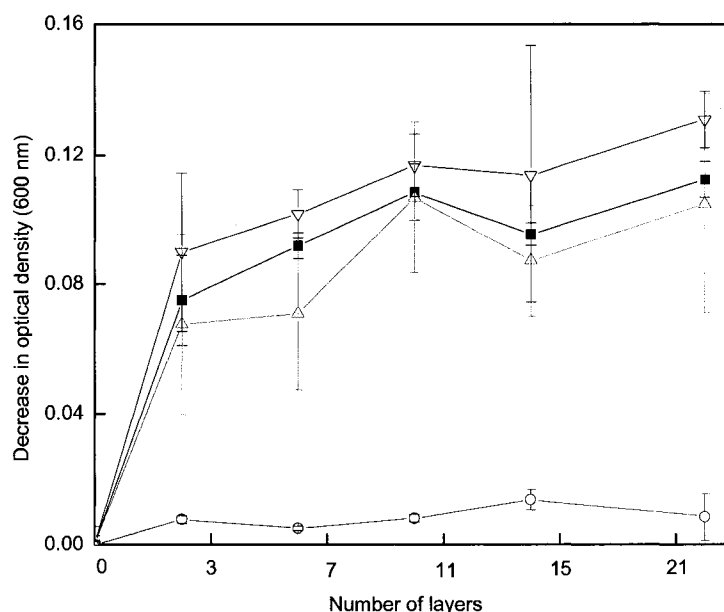


Figure 3.7. Relative antimicrobial activity of PLGA/HEWL films under different conditions.

About 20% activity in control samples consisting of HEWL in aqueous solution was lost in the course of 1 month. There is relatively little difference in the ability of the films to kill *M. luteus* after the initial leaching period. This suggests that the bacteria are killed either by a similar quantity of HEWL immobilized on the film surface, or by an approximately constant rate of release of HEWL from the film. In any case, it is somewhat surprising that the 3-layer film is about has about the same bactericidal effectiveness as the 21-layer film under the conditions studied here. The activity of the films (due to immobilized HEWL) in bacterial culture medium after a 14-h period of leaching of HEWL into buffer is shown in Figure 3.8. There is little difference in the bactericidal effectiveness of fresh and lyophilized films, whereas films stored in buffer for clearly do lose activity over the course of a month.

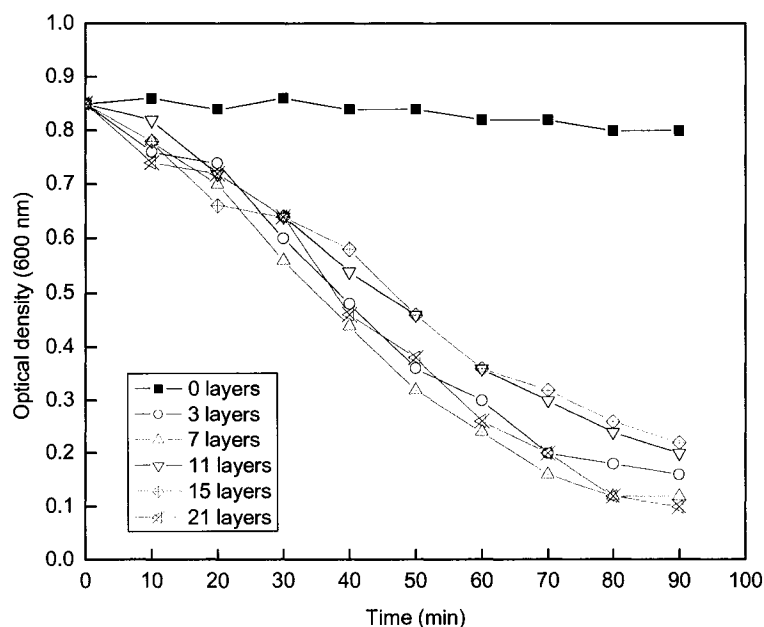


Figure 3.8. Anti-microbial activity of PLGA/HEWL multilayer films of different thickness after 14 h of immersion in phosphate buffer at 30°C with continuous stirring at 200 rpm.

The OD at 600 nm after 100 min incubation with *M. luteus* suspension of freshly prepared films, films stored for 1 month in buffer, and lyophilized films is shown in Figure 3.9.

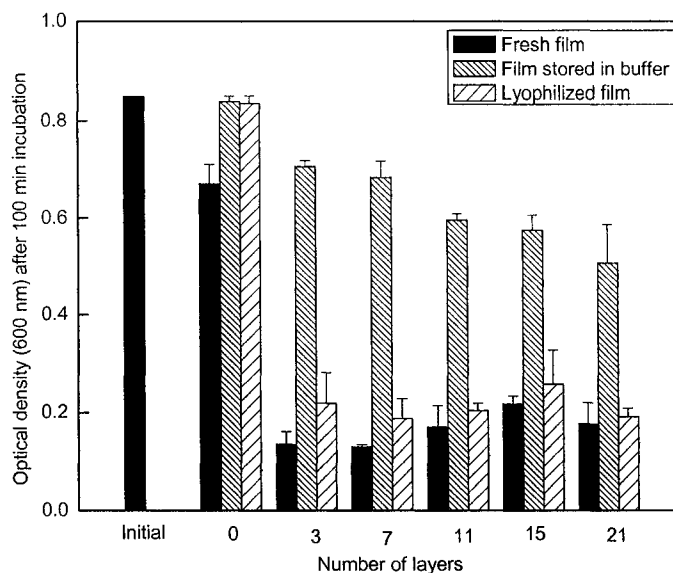


Figure 3.9. Effect of PLGA/HEWL films on *M. luteus* culture.

Taken together, these experiments show that the polypeptide multilayer films both release HEWL into the surrounding medium and retain HEWL activity over an extended period of time. HEWL activity is approximately independent of the number of layers and also independent of whether the films are fresh or lyophilized. HEWL either becomes inactivated over time in films stored in buffer or it leaches out of the films. The amount of HEWL released is a roughly linear function of the number of film layers. The data indicate that the amount of HEWL in the surrounding medium of a 15-layer film was approx. $9 \mu\text{g}$, or about $2/5$ of the amount originally adsorbed on the slide. The quantity of HEWL released from PLGA/HEWL films is shown in Fig. 6. The HEWL concentration ranged from 0 to $0.4 \mu\text{M}$, as determined by comparison of the fluorescence of samples

taken from surrounding aqueous environment as shown in Figure. 3.10 with a standard curve (Figure. 3.2).

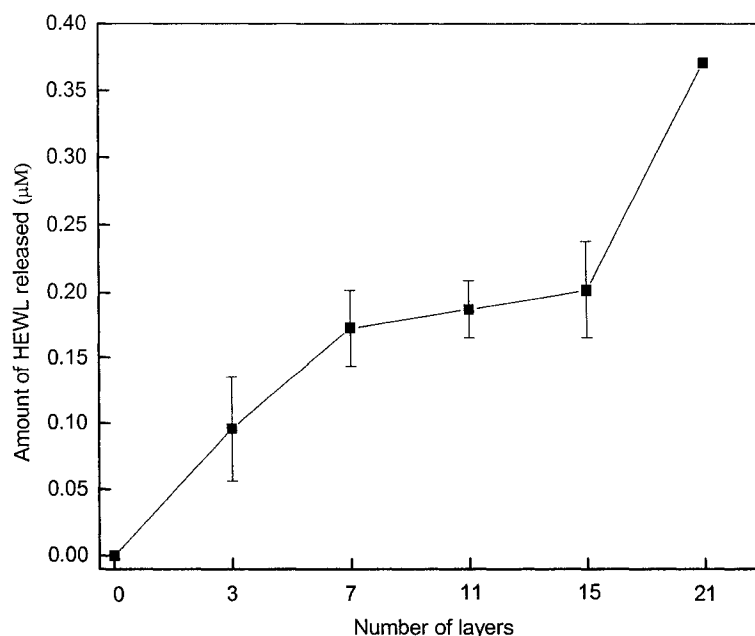


Figure 3.10. Amount of HEWL released from film-coated slides into the surrounding buffer.

Notable natural antimicrobial peptides and proteins, known collectively as bacteriocins, are colicin, nisin, pediocin, reutrin and lysozyme. As an enzyme that is widely distributed in animals, including humans [175], lysozyme hydrolyzes preferentially the β -1,4 glycosidic linkage between N-acetylmuramic acid and N-acetylglucosamine. This sugar occurs in the mucopeptide cell wall structure of certain microorganisms, for example, *M. luteus* [176], the model organism chosen for the present work. HEWL is known to be active against various microbes of concern in food safety, notably, *Listeria monocytogenes* and certain strains of *Clostridium botulinum* [177]. When added to EDTA, HEWL has an antimicrobial spectrum that extends to Gram-negative bacteria [173]. HEWL-EDTA is a common combination of antimicrobial agents

in packaging applications [178]. HEWL has been efficiently incorporated into zein films as a preservative; in concert with EDTA, HEWL inhibits growth of *Escherichia coli* in such films [179].

Retention or slow release of an antimicrobial is essential for extending antimicrobial activity over time and protecting against microbial colonization. Some of the experiments on PLGA/HEWL films described here were done after an initial release of material during a given time interval. The measured activity of the films is not a reflection of their HEWL content *per se*, but of the activity of HEWL released from the film and, in some cases, of HEWL present at the film–liquid interface. PLGA/HEWL films that had been pre-conditioned by immersion in buffer for 14 h showed no pattern of increase or decrease of bacterial growth with respect to number of film layers (Fig. 5, bottom); antimicrobial activity was about the same in each case. The net decrease of intact bacteria in solution due to retained HEWL in the films also did not depend significantly on the number of layers (Fig. 5, continued). This suggests that about the same amount of active HEWL was present on the film surface or was released from the film per unit time in each case. It would appear that the amount of HEWL on a film surface or lost from the film to the surrounding liquid medium reaches a plateau for a given surface area, irrespective of the number of final layers in the film. The film longevity experiments show that the PLGA/HEWL films are stable and active after lyophilization. Storing the films in an aqueous medium, by contrast, results in the slow release of enzyme into the surrounding environment.

The net charge of a multilayer film must be zero by the condition of electroneutrality. The charge of one polyelectrolyte is compensated by the charge of the

other and small counter-ions. The release of HEWL from the film, therefore, can be attributed to soluble complex formation with PLGA and the replacement of HEWL molecules by counter-ions from the bulk solution. The concentration of HEWL in solution is in the micromolar range, whereas the concentration of counter-ions is 1000-times greater. The QCM data are consistent with a soluble complex model. The charge per molecule of HEWL at neutral pH is around 7, whereas that on the average PLGA molecule is over 100 electronic charges. Therefore, there is a large net negative charge on a 1:1 complex of PLGA and HEWL, making it highly soluble in water. The release of HEWL from films can also be attributed to some extent to the concentration gradient of HEWL between the surrounding buffer and the film. Further research could reveal ways of achieving greater control over HEWL release or retention properties, important for commercialization of the antimicrobial polypeptide multilayer film technology.

There is considerable potential in the development of antimicrobial coatings for a broad range of purposes. Bacteriocins, including HEWL and various antimicrobial peptides, have become an increasingly important class of molecules in medicinal chemistry and physiology [82]. Multiple mechanisms for a single bacteriocin are possible, but each antimicrobial is thought to have a unique mechanism of action with respect to specific microorganism. Bacteriocin structure could be engineered to optimize solubility, stability to proteolysis, and suitability for polypeptide multilayer film assembly.

Peptides are of considerable and growing interest in multilayer thin film fabrication, particularly in applications where biodegradability and edibility are key design concerns. The character of polypeptide assembly in a multilayer context depends

on pH and ionic strength, as linear charge density and secondary structure content depend on these variables [116]. Polypeptide multilayer film roughness and density depend on pH [125] and on polypeptide sequence [180]; this could be important for applications of the technology [152]. Polypeptide films can be reversibly stabilized by disulfide bond formation between cysteine residues [117, 121], possibly useful for controlling the release of incorporated or encapsulated material [181, 182].

3.4 Conclusions

The present work was aimed at assessing whether polypeptide multilayer nanofilms with specific antimicrobial properties could be prepared by incorporation of a known antimicrobial agent in the film structure, in this case the edible protein hen egg white lysozyme (HEWL). An advantage of LBL in this context is that the nanofilm is fabricated directly on the surface of interest, eliminating the need to incorporate the antimicrobial in other packaging materials. Here, nanofilms were made of poly(L-glutamic acid) (PLGA), which is highly negatively charged in the mildly acidic pH range, and HEWL, which has a high net positive charge at acidic pH. It has been shown that PLGA/HEWL nanofilms inhibit growth of the model microbe *Micrococcus luteus* in the surrounding liquid medium. The difference in activity of wet and dried films is a key component in selecting a particular species for assembly. The amount of HEWL released from PLGA/HEWL films depends on the number of HEWL layers and therefore on the total quantity of HEWL in the films. Potential applications of such films include strategies for food preservation and coatings for implant devices. Antimicrobial activity can be conferred not only by proteins and peptides but also other charged species like nanoparticles, and small drug molecules. The difference in the assembly behavior and

activity over time can be different depending on the type of antimicrobial agent used. Thus, one can gather from the experimental data presented here that the same behavior is not warranted while working with other compounds. This initial study provides a sketch of the scope for further development of LBL in the area of antimicrobial polypeptide multilayer films.

CHAPTER 4

CELL CULTURE POLYPEPTIDE MULTILAYER FILMS

4.1 Introduction

A large number of synthetic polymeric materials are available for various medical applications and tissue engineering matrices. However, reduced unspecific protein adsorption, enhancement of adsorption of specific proteins, and immobilization of cell recognition motives are approaches to improve biomaterials [183-191]. The extracellular matrix (ECM) consists of various proteins secreted by cells: fibronectin, laminin, vitronectin, and collagen [192] so early researchers coated materials with these proteins [193-197]. However, tedious purification, undesirable immune response, increased infection risks, stochastic orientation on the surface, and susceptibility to proteolysis degradation are some serious disadvantages. These disadvantages can be overcome by using short peptides that incorporate cell recognition motifs. The extracellular matrix (ECM) proteins normally contain many different cell recognition motives, whereas small peptides represent only one single motif. This feature enables them to address one particular type of cell adhesion receptors. Attachment of a cell to the ECM determines cell shape and maintains cell function and tissue integrity. The nature of a cell's physical contacts with its surroundings depends on the stability, organization, and composition of the ECM. Cell attachment is mediated by

transmembrane heterodimeric protein receptors called integrins. The process of integrin mediated cell adhesion has four partly overlapping events: cell attachment, cell spreading, organization of actin cytoskeleton, and formation of focal adhesions. In tissue engineering, substrate or scaffold requirements include biocompatibility, biodegradability, cell adhesion, and sufficient mechanical strength to withstand long-term cell culture *in vitro*.

4.2 RGD Motifs and Cell Adhesion

The RGD (R:Arginine, G:Glycine, D:Aspartic acid) sequence is by far the most effective and often employed peptide sequence for stimulated cell adhesion on synthetic surfaces. Since RGD peptides have been found to promote cell adhesion in 1984 [198] numerous materials have been RGD functionalized for academic or medical purposes and an excellent review of the subject exists [199]. Apart from RGD other important cell adhesion motifs have been identified. Therefore, RGD sequence is not the “universal cell recognition motif”, but it is unique with respect to its broad distribution and usage. The conformation of the RGD containing loop and its flanking amino acids in the respective proteins are mainly responsible for their different integrin affinity [200]. Formation of focal adhesions only occurs if the ligands withstand the cells contractile forces, hence stable linking of RGD peptides to a surface is essential to promote strong cell adhesion [201-203]. These forces can redistribute weakly adsorbed ligands on a surface, which leads to only weak fibrillar adhesions [204-206]. Furthermore cells can move mobile integrin ligands by internalization [207, 208]. Simple adsorption of small RGD peptides only leads to poor cell attachment [209-214]. RGD peptides can be covalently attached to the polymer, e.g. via functional groups like hydroxyl-, amino-, or carboxyl groups to

provide a stable linking. Because many polymers do not have functional groups on their surface, these have to be introduced by blending, co-polymerization, networks, chemical and physical treatment, and immobilization [199].

RGD sequence is found to be an “active modulator of cell adhesion”, and is recognized by 8 to 12 of the 20 known integrins, a class of transmembrane cell surface receptors. While peptides and proteins containing the RGD cell attachment site inhibit cell adhesion in solution, they in fact promote cell adhesion when covalently attached to a surface as shown in Figure 4.1.

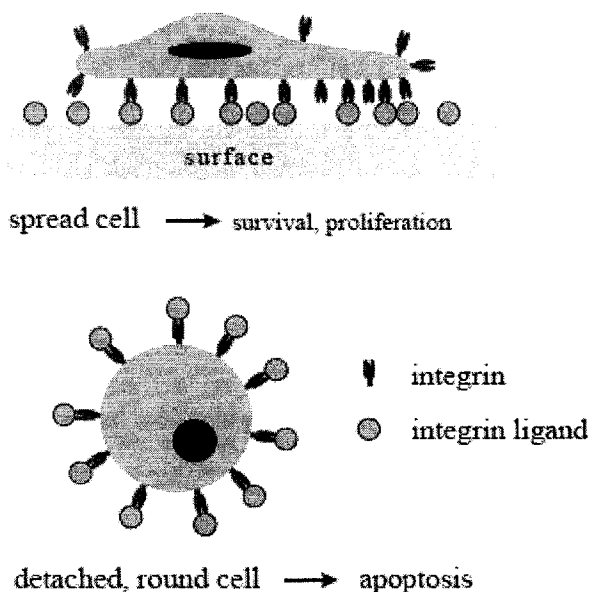


Figure 4.1. Opposite effects of integrin ligands. Immobilized ligands act as agonists of the ECM, leading to cell adhesion and cell survival, while non-immobilized ligands act as antagonists, leading to cell detachment, a round cell shape, and apoptosis [199].

Cell adhesion blocking of RGD site has potential applications in combating pathological conditions such as metastasis, thrombosis, and angiogenesis. RGD-containing peptides and proteins can initiate cell signaling and influence many diseases

such as tumors, thrombosis, osteoporosis, and cancer. This property of the RGD motif makes it a viable target in drug delivery, and makes it a “prototype adhesion signal” in “cell adhesion biology” [215]. RGD sequence is found in several proteins of the extracellular matrix (ECM), blood, and cell surfaces. Fibronectin [216-218], fibrinogen [219, 220], vitronectin [218], von Willebrand factor [220], thrombospondin, laminin [221], and some collagens, etc. – all these proteins contain RGD cell attachment sites [222, 223]. Integrins are transmembrane receptors that recognize spatially restricted extracellular ligands and play a significant role in mediating cell-cell and cell-matrix adhesion. These ligands include the RGD site in proteins and/or peptides, and bind to them selectively. Cell attachment site such as RGD motif, together with the corresponding integrin receptors, serve as a recognition system for cell adhesion. Integrins are heterodimeric proteins, i.e. they have two different subunits, α and β , each of which contains potential binding sites for the ligand contributes to ligand specificity [215]. Both α and β subunits of integrins have ligand binding sites is in close vicinity of divalent cation-binding sites [224]. RGD binding to integrin has found to cause “extrusion of divalent cations from the integrin” [225]. In most cell attachment sites including RGD, aspartic acid (or glutamic acid) appears to be the most significant contributing factor, as Asp (or Glu) is a potential contributor of divalent cation-binding.

RGD-integrin interaction is important in biological processes like morphogenesis, tissue remodeling [226], and pathological pathways. The exact sequence R-G-D is important, and replacement of any of the three amino acids with any other similar amino acids (such as lysine for arginine, glutamic acid for aspartic acid, or alanine for glycine) affects the peptide attachment activity [255]. Moreover, activity can be influenced by the

optical conformation of the amino acids; while replacement of L-arginine in RGD with D-arginine will not affect the activity, replacement of L-aspartic acid with D-aspartic acid will deactivate the RGD site's cell attachment capabilities [223]. Other factors that affect the RGD site activity include the availability of the tripeptide motif near the surface of the protein or peptide, retro-inversion [228], and the amino acid sequence in the vicinity of the RGD sequence [223]. Amino acid residues on the C-terminal of the RGD peptides seem to have more influence on the integrin affinity and binding than those on the N-terminal [243]. Affinity and effectiveness of RGD-containing peptides is also influenced by charge distribution of these peptides [229].

Structure of RGD peptides significantly influences the cell adhesion and inhibitory activities of these peptides [229, 230]. RGD peptides exist as cyclic or linear structures. In solution, short RGD peptides tend to take a secondary structure called the β -turn [231]. It has been noticed in some cases that the rigidity of RGD, or the lack of it, may increase affinity towards a particular integrin. Larger RGD peptides are more rigid than shorter ones, and the rigidity and or the size of the peptides can influence the affinity to particular integrins. Cyclic RGD peptides have restricted conformation, which can in turn enhance integrin affinity [223]. The presence of Asp residue in RGD sequence induces chemical degradation that contributes to loss of biological activity [232]. Cyclic forms are found to be more stable due to the side chain orientation of aspartic acid and arginine residues. In platelet aggregation inhibition, cyclic peptides have proved more efficient than linear peptides [229].

4.3 Cell Attachment to LBL Films

A number of studies have focused on modification of surfaces using LBL with different materials to control cell attachment behavior. Analogous to proteins, cell adhesion occurs on LBL films terminated with positively charged polyelectrolytes [71, 233]. Surfaces can be rendered cytophilic or cytophobic depending on the materials used and the intrinsic structure of the LBL film [234, 235]. Modification has been achieved by using polyelectrolytes in conjunction with other materials like polypeptides [236], polysaccharides [237], proteins [238], hyaluronic acid [239, 240], carbon nanotubes [241], and nanoparticles [242]. Some researchers have investigated the positioning of cell growth on surfaces by depositing cytophilic or cytophobic LBL films to improve or prevent cell adhesion at desired positions [243-246]. The versatility of the LBL technique also allows modification of surfaces with any geometry which has led to the development of 3D scaffolds for cell adhesion and growth [247-249]. LBL coatings have also been used to alter the cytotoxicity of certain substrates [250]. More recently, it was shown that cells can be deposited on polypeptide multilayer films fabricated from poly-(L-lysine)/poly-(L-glutamic acid) (PLL/PLGA) [71, 144] and poly-(L-lysine)/Hyaluronic acid (PLL/HA) [251, 252] and grown for several days in culture.

4.4 Peptide Design Rationale

The design of any specific peptide depends on the use for which it is intended and the synthetic considerations. The present study is aimed at quantifying cellular interactions with polypeptide multilayer films with inherent RGD motifs and other physical characteristics. Substrates coated with designed peptides using LBL will be used to study cell adhesion and proliferation. The peptide design has been varied to study

spectroscopic detection. K and E are ionized in solution at neutral pH. For all the peptides electronic charge per amino acid residue at neutral pH was ≈ 0.25 . The solubility of P2 and N2 in an aqueous medium is lower than that of other peptides owing to the relatively large nonpolar surface of the valine side chain and the peptides were found to form aggregates in solution. Peptides P4 and N4, each encode four RGD sequences in them which is a known cell adhesion motif.

4.5 Film Fabrication and Characterization

The peptides were purchased from Celtek Bioscience (Nashville, USA) at 70% purity (some sample heterogeneity, due apparently to nonideal monomer coupling, was tolerated) and all other reagents were from Sigma-Aldrich and were used without further purification. Typical nonpeptide polymer preparations in the multilayer film literature are highly polydisperse. 18.2 M Ω -cm water was used in all experiments. In addition, all buffers were filtered at 0.45 μm before use, preventing bacterial contamination. Lyophilized peptides were reconstituted in PBS buffer (10 mM phosphate buffer salts, 120 mM NaCl, and 2.7 mM KCl) pH 7.4 at 1 mg/mL. Multilayer nanofilms of all four combinations of designed peptide were fabricated on negatively charged solid supports by layer-by-layer assembly (LBL). The magnitude of the surface charge density might be different in case of different substrates and depends on the cleaning procedure employed. In the first peptide adsorption step, a positively charged peptide was deposited by immersion of the substrate in 1 mg/mL peptide solution for 15 min. Loosely bound polycations were removed by rinsing the substrate with deionized water, and the film was dried with N₂ gas. Then a negatively charged peptide was deposited on the initial layer, and loosely bound polyanions were removed as before. The resulting bilayer was dried

with N₂ gas, completing the first adsorption cycle. All films were dried for characterization *ex situ*.

4.5.1 UV Spectroscopy

Quartz cover slips (ElectronMicroscopy Sciences, USA), 7.5 cm×2.5 cm×0.1 mm in size, were cut into rectangular pieces of 1.25 cm × 2.5 cm, cleaned for 30 min in 1% sodium dodecylsulfate at 80 °C with agitation and washed for 2 h with 1 M NaOH/C₂H₅OH (60:40, v/v) and overnight with piranha solution (H₂SO₄/H₂O₂ 75:25, v/v). The slides were stored in piranha solution, and they were rinsed extensively with DI water and dried with N₂ gas before the peptide film was assembled for UV-vis (Jasco, USA) and Circular dichroism (Applied Photophysics, UK) characterization. In all cases the films were dried with nitrogen gas before spectral characterization. After the UV spectra were obtained, the films were stored in vials purged with N₂ gas and were sealed using parafilm. The slides were stored at 4 °C until further use. The films fabricated on silicon substrate were stored in a similar fashion.

4.5.2 Circular Dichroism Spectroscopy

CD enables determination of the structure of chiral molecules by detection of the differential absorption of right- and left-circularly polarized light. In the far-UV region of the spectrum, 180-260 nm, the signal is highly sensitive to the average conformation of the polypeptide backbone. The absorbance of all the peptide solutions was adjusted to 1.5 (at 195 nm). The quartz slides used for UV-vis spectroscopy were used to determine the secondary structure of the films by placing them in the path of light by securing the slide on the sample holder using a piece of adhesive tape. The temperature was 25 °C. Twenty scans of each sample were collected in a quartz cell of 0.1 cm path length, using a

Applied Photophysics, Chirascan spectropolarimeter (UK) with 100 mdeg sensitivity, 1 nm bandwidth, 0.2 s response time, 1 nm data pitch, and 100 nm·min⁻¹ scanning rate. The scans were averaged. Buffer baselines were determined with the same instrument settings and subtracted from the respective sample spectra. Raw CD data were converted to mean molar residue ellipticity.

4.5.3 Atomic Force Microscopy

Peptide films were built on Si wafers (N/Phos <100>, resistivity 1-10 ohm-cm, thickness 375-425 μm , diameter 100 ± 0.5 mm; Silicone Technology Corp., USA) for evaluation of thickness by ellipsometry (Beaglehole Instruments, New Zealand) and surface morphology by Atomic Force Microscopy (Veeco, USA). The wafers had a very thin layer of naturally grown SiO₂ (≈ 3 nm) on the Si surface. Wafers were cut into pieces in a clean room, rinsed with deionized H₂O, dried with N₂ gas, and stored in sealed dust-free vials until use. Multimode IIIa AFM (Digital Instruments/VEECO) with an E-scanner (maximum scan area = $14.2 \times 14.2 \mu\text{m}^2$) was used to image the multilayer films in air. Tapping Mode in air was conducted using silicon tips (TESP, VEECO) at different points on the film surface and the AFM images were captured over two different area sizes $5 \times 5 \mu\text{m}$ and $1 \times 1 \mu\text{m}$. Height images were plane-fit in the fast scan direction with no additional filtering operation. The root mean square roughness (Rms) and average roughness (Ra) were calculated using the Nanoscope software over $5 \times 5 \mu\text{m}$ and $1 \times 1 \mu\text{m}$ areas.

4.5.4 Ellipsometry

The film thickness measurements were performed on a silicon wafer using a phase-modulated ellipsometer (Beaglehole Instruments, (New Zealand) fixed at the angle

of incidence near the Brewster angle ($\theta_B \approx 55^\circ$). The ellipticity, $\rho = \text{Im}(r_p/r_s)|_{\theta_B}$ measured by the ellipsometer, where r_p and r_s are the complex reflection amplitudes for p and s polarizations, respectively, is readily converted to film thickness using Drude equation. The large contrast between the optical dielectric constant for the silicon wafer ($\epsilon_{\text{Si}} = 15.07$) and the organic film provides an extremely good film thickness resolution of 0.02nm averaged over the focused laser beam diameter of ≈ 0.25 mm. As the organic components in the multilayer possess only a marginal difference in their optical dielectric constants, the film has been modeled as a slab of thickness L with a fixed dielectric constant. The experiments were performed in air on three independent points substrate covered with the LBL films. The substrates had a naturally grown ≈ 3 nm SiO_2 layer on the surface. The measurements were taken at two refractive index values 1.34 and 1.6. To study the variation of thickness with the refractive index (n), the thickness of a sample film (P3N3) was measured at different 'n' values from in the range 1.35-1.6 with an increment of 0.05.

4.6 Cell Culture Studies

For cell culture studies the polypeptide multilayer films were deposited on 12 mm round glass slides (0.13-0.16 mm thick). Before assembly the glass slides were cleaned and sterilized using 70 % ethanol and later thoroughly rinsed using ultrapure water (Hydro Picopure®2 system, with a resistivity greater than 18.2 M Ω .cm). Polypeptide solutions were always freshly prepared before assembly experiments. Three different types of film coatings were prepared by depositing 15 layers of peptide and the final layer was positive. The combinations assembled were chosen based on preliminary data for various physical and biochemical characteristics. The peptide combinations used for cell culture

studies are P2N2, P3N1 and P4N4. In addition to these individual peptide combinations films were made by using precursor layers of PLL and PLGA (10 layers) and then coated with the above-mentioned peptide combinations (5 layers). The films were sterilized using 70% ethanol before seeding cells on to them.

4.6.1 Cell Culture

3T3 cells were maintained in Dulbecco's Modified Eagles Medium (DMEM, ATCC) containing 10 % calf bovine serum (CBS, ATCC) and 1 % antibiotic (Penicillin-Streptomycin, GIBCO Invitrogen). Culture medium was replaced every alternate day, and cells were allowed to grow until sufficient confluence was reached. Cells were trypsinized (Trypsin, ATCC) and collected by centrifugation at 220g for 5 min, and resuspended in complete media prior to counting and seeding. Substrates with coatings were immersed in 70 % ethanol and later rinsed with Hank's balanced salt solution (HBSS) and placed in a 24 well plate before seeding cells on them. The cells with substrates were then incubated at 37 ° C and a humidified environment of 5 % CO₂ and 95 % air.

4.6.2 Cell Proliferation

MTT (3-(4,5-Dimethylthiazol-2-yl)-2,5-diphenyltetrazolium bromide) assay was done on the cells adherent on the multilayer films to determine cell proliferation. A calibration curve correlating the absorbance with the number of cells was first obtained. The cells were seeded at cell density of 7500 cells/cm² and incubated for 72 hr with media change on alternate days. At the end of 72 hrs the medium was removed and substrates were transferred to a new well plate. The cells on coated substrates were later incubated with 10 % MTT solution (ATCC) in media for 4 hrs. Incubation detergent

(ATCC) was added and the plates were left in the dark overnight to dissolve the formazan crystals (formed due to the interaction of MTT solution with cells). Absorbance of the plate was measured at 570 nm, with background subtraction at 690 nm (Molecular Devices Spectra Max), and the number of cells was determined from the calibration curve.

4.7 Results and Discussion

The different films that were fabricated from the designed peptides are shown below in Table 4.2. However, cell attachment studies were performed only on P2N2, P3N1 and P4N4 and are the only combinations discussed here. These films were selected based on their significant difference in surface morphology and physical composition. The characterization data for all other combinations is provided in the supplementary information section.

Table 4.2. Films formed from various peptide combinations.

P1N1	P1N2	P1N3	P1N4
P2N1	P2N2	P2N3	P2N4
P3N1	P3N2	P3N3	P3N4
P4N1	P4N2	P4N3	P4N4

Polypeptides, are weak polyelectrolytes and the pKa of ionizable groups in a weak polyelectrolyte are sensitive to the local electronic environment. The net charge can shift significantly from the solution value on formation of a polyelectrolyte complex or film. The net charge on the positive and negative peptides varies considerably below pH

4 and above pH 10 which are close to the pKa's of glutamic acid and lysine respectively which are the charged amino acids in the peptide sequences. At the assembly pH around 7.4 the charge density on all the peptides is approximately the same. In peptide N1 the side chains of glutamic acid will repel those of cysteine when the latter become ionized; otherwise the side chain of cysteine is neutral. The pKa of cysteine is around 8.9. The net charge can also vary significantly in solution with the pH and its dependence on pH is shown in Figure 4.2 for the various peptides used.

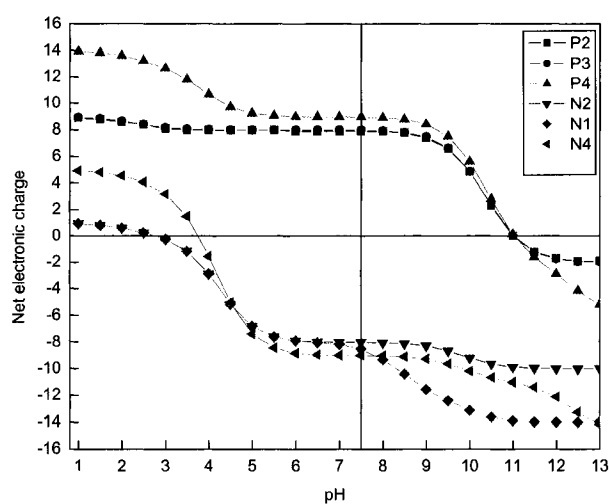


Figure 4.2. Estimated peptide net charge versus pH.

The film growth was monitored by UV spectroscopy and was confirmed in triplicate. The increase in the peptide bond absorbance indicates that material is being deposited at every step of film assembly. The variations in the magnitude of deposition from layer to layer cannot be precisely estimated by this technique and hence no conclusions can be made about the physical growth properties. Nevertheless, it provides a definite proof of film growth throughout the fabrication process. The absorbance was

collected after every 3 layers of peptide was deposited for a total of 15 layers with appropriate baseline correction. The data show that more material is deposited in case of P2N2 compared to P3N1 or P4N4. This could be due to the aggregate deposition in case of P2N2 compared to polymer deposition in the other cases. The solubility of P2 and N2 in an aqueous medium is lower than that of other peptides owing to the relatively large number of valine residues (50%) and the nonpolar surface of the valine side chain. By contrast, P3N1 shows more deposition than P4N4 due to the presence of valine and serine residues in P3 and valine and cysteine residues in N1. Peptides P4 and N4 are devoid of any hydrophobic or polar residues and the adsorption is purely electrostatic. The UV absorbance data in Figure 4.3 shows the increment in peptide deposition at different layer numbers

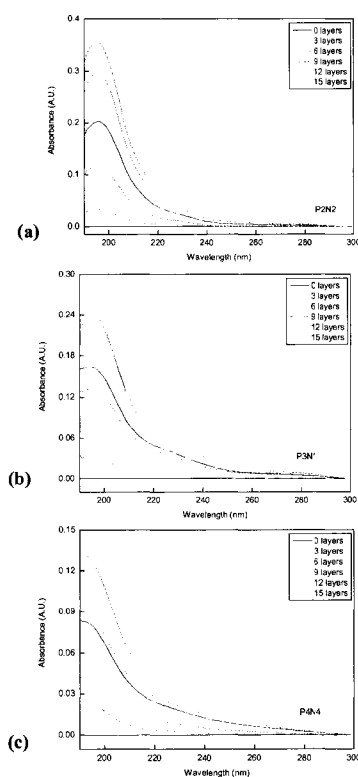


Figure 4.3. Peptide multilayer film assembly monitored by UV spectroscopy.

The adsorption of a peptide onto surface depends on its charge or more specifically its charge density. The role of molecular structure and charge on polypeptide multilayer film assembly has been studied by Haynie et. al. [116]. The adsorption process results in a substantial decrease in the number of conformations accessible to the peptide molecule. The forces that inhibit the return of the adsorbed peptide back to solution are electrostatic attraction, hydrophobic interactions, and hydrogen bonds. The weakest of the three are the hydrogen bonds which are usually broken easily and hydrophobic interactions are formed not due to the attractive forces between the nonpolar side chains but due to the repulsive forces from the surrounding polar environment. The strongest forces are the electrostatic attractions and the LBL method is based on the attractive interaction of complementary charges which drives the process. Therefore, the type and the amount of charged groups in a polymer can be satisfactory criteria to predict its usefulness for the LBL technique and the polymer must bear a minimal number of charged groups, below which the LBL procedure does not work. In particular cases, alternative interactions may be even strong enough to allow for LBL assembly without ion-ion interactions.

The designed peptides have a charge per unit length of ≈ 0.25 which is lower compared to homopolypeptides like PLL and PLGA which have a charge per unit length of 1. Designed polypeptides with a charge per unit length of 0.5 have been successfully assembled into multilayer films with interesting growth properties [253]. The design of the peptides for the cell culture films was based on the charge properties of the RGD peptide. The RGD motif has two charged residues arginine (positive) and aspartic acid (negative) making the motif uncharged at physiological pH. It is also known that RGD

mediated cell adhesion also depends on the flanking residues. In the designed peptides these flanking residues have been substituted by glycine, the simplest amino acid. This design limits the charge on the peptide to ≈ 0.25 for a 32 mer. The other peptides have been designed to have the same charge density at physiological pH. The deposition of the peptides overall is lower compared to that of highly charged peptides. The presence of glycine residues (50%) in case of P4 and N4 could also have limited the adsorption of the peptide. This is relevant because the peptide backbone is very flexible in the vicinity of glycine residues. During the assembly process the adsorption of P4 and N4 is less favored than that of others from the point of view of chain entropy.

The CD data shown in Figure 4.4 reflect the differences in the peptide deposition. CD spectra are sensitive to the secondary structure of the films, which will depend on different amino acid sequences of designed peptides. The cotton effect amplitudes vary as $P2N2 > P3N1 > P4N4$. The CD spectra show a predominant β -sheet structure in the case of P2N2 and a mix of α -helix and β -sheet in case of P3N1. The CD signal from P4N4 was very weak and could be due to the sporadic deposition of the peptide as evident from other characterization techniques.

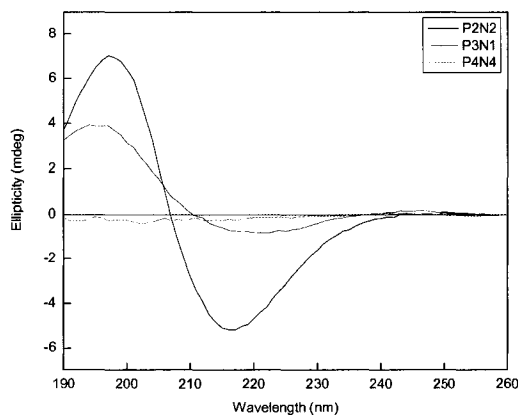


Figure 4.4. CD spectra of designed peptide multilayer films.

The CDProsoftware suite, which includes popular methods for estimating the secondary structure content of a sample from CD spectra was used to deconvolute far-UV CD spectra into contributions from α -helix, β -sheet, β -turn, and coil. A set of spectra of model polypeptides or reference proteins of known three dimensional structures is used to determine the relative contributions of the component spectra and it is assumed that contributions from individual secondary structures are additive. The reference set consisted of the far-UV CD spectra of 43 proteins of known secondary structure content. The programs CONTIN/LL and CDSSTR were used to estimate the secondary structure. The data are shown below in Table 4.3. The secondary structure of P2N2 was predominantly β -sheet and β -turn which accounted for nearly 80% of the secondary structure content. P3N1 also approximately had 60% β -sheet and β -turn and also showed some coiled structure. The results of P4N4 cannot be interpreted in a definite way because of the poor deposition nature of P4N4 and the possibility that light might have passed through regions of incomplete coverage during measurement of the spectra.

Table 4.3. Secondary structure content of designed peptide multilayer films.

P3N1				
Structure	Helix	Sheet	Turn	Coil
CONTIN/LL	0.034	0.378	0.238	0.350
CDSSTR	0.016	0.393	0.198	0.380
P4N4				
Structure	Helix	Sheet	Turn	Coil
CONTIN/LL	0.036	0.416	0.214	0.334
CDSSTR	0.014	0.023	0.023	0.032
P2N2				
Structure	Helix	Sheet	Turn	Coil
CONTIN/LL	0.061	0.596	0.227	0.115
CDSSTR	0.166	0.401	0.191	0.251

The peptides P2 and N2 were studied using AFM to look at the physical nature of the aggregates formed. It was suspected that these peptides formed elongated fibril like structures but upon investigation showed a globular morphology. Peptide P2 or N2 was adsorbed on a silicon surface for 10 min and then rinsed with DI water and dried before imaging. It is easy to picture the deposition process of P2 and N2 as a scenario of hydrophobically driven assembly. Figure 4.5 shows the AFM image of peptide P2 compared with a bare silicon wafer.

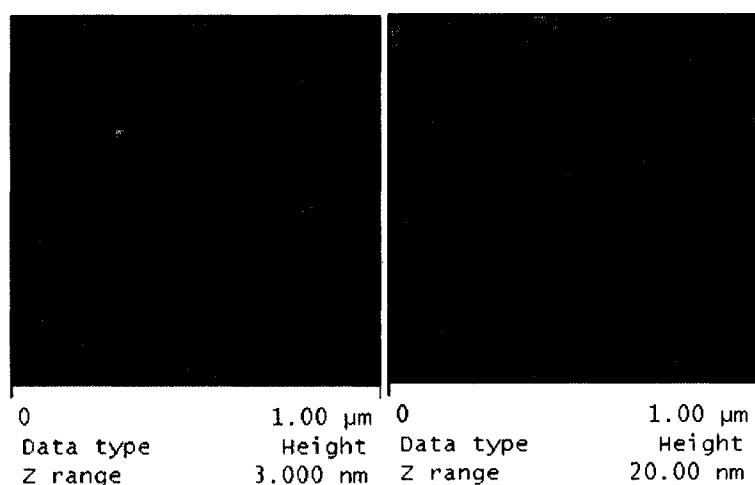


Figure 4.5. AFM image of peptide P2 on a silicon surface.

The surface morphology of the peptide films varies greatly in accordance with their amino acid composition and the magnitude of deposition. P2N2 showed a rough uneven surface with aggregation and a good coverage. P3N1 showed a fibrous morphology with evenly sized fibers covering the surface. The fiber formation can be attributed to the hydrogen bonding capability of serine residues in P3 or the disulfide bonding capability of cysteine residues in N1. P3N1 showed a fibrous morphology with evenly sized fibers covering the surface. However, after immersing in PBS buffer

overnight P4N4 showed a better coverage profile when imaged under PBS buffer. The interstitial spaces could be filled with the buffer or the film might have reorganized in hydrated conditions as shown in Figure 4.6.

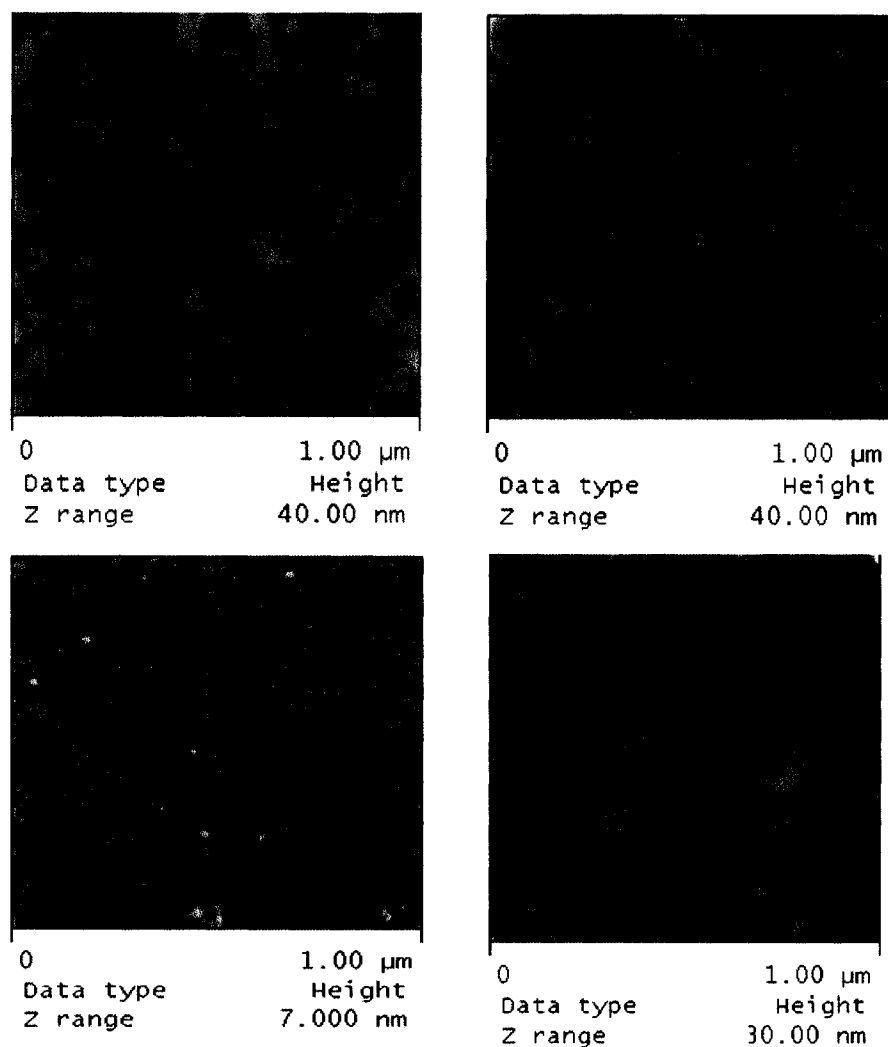


Figure 4.6. AFM images of designed polypeptide films.

Cells are impacted by various nonspecific environmental factors such as pH, ionic strength, temperature, surface chemistry, and topography. Surface topography has been documented to influence a variety of cell behavior and has a role in how a cell responds

to environmental stimuli. A number of studies have evaluated random nano-scale surface features defined in terms of surface roughness. Cellular responses reported on these surfaces vary depending on the material and cell type investigated. It is hard to determine trends in such cases. It is also difficult to compare the effect of topography based on comparing surface roughness value Ra which can be the same for two surfaces with very different features. Surface roughness measurements show that despite having completely different morphologies P2N2 and P3N1 have the about the same average roughness. The surface roughness of P4N4 is very low almost 6 times less than P2N2 and P3N1. The root mean square roughness and average roughness of the films is shown below in Table 4.6.

Table 4.4. Surface roughness of designed peptide multilayer films.

Film	Average Roughness (nm)		Rms Roughness (nm)	
	5 μm	1 μm	5 μm	1 μm
P2N2	3.65	3.17	4.83	3.93
P3N1	3.89	3.32	5.96	4.16
P4N4	0.61	0.57	0.99	0.70
Bare	0.15	0.61	0.21	0.16

Film thickness was higher in the case of P2N2 and varied as P2N2>P3N1>P4N4 as shown in Fig 4-5. The deposition of aggregates in the case of P2N2 might have contributed to higher thickness for the same number of layers as compared to the others. The thickness of P3N1 is higher than P4N4 owing to the greater deposition of mass due to the presence of valine residues. The change in RI with film thickness may need to be considered when attempting to infer structural information such as layer thickness from

optical measurements using an assumed RI. The thickness of different peptide films is shown in Figure 4.7 below.

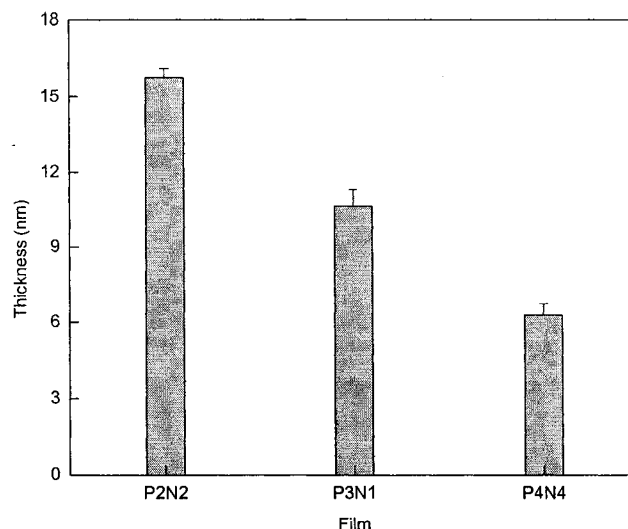


Figure 4.7. Ellipsometric thickness of designed polypeptide multilayer films.

The refractive index (RI) of adsorbed protein layers has been reported to vary from 1.34 to 1.6 [254, 255]; therefore, the thickness was measured at both the extremes of RI at three independent points on the film surface to obtain an average thickness value and the average RI was estimated to be around 1.47. The thickness values at various RI are shown in Table 4.5.

Table 4.5. Film thickness of peptide multilayer films at various RI values.

Film	RI=1.34		RI=1.6		RI=1.47	
	Avg	SD	Avg	SD	Avg	SD
P2N2	17.7	0.4	13.8	0.35	15.75	0.375
P3N1	12	0.76	9.3	0.58	10.65	0.67
P4N4	7.1	0.51	5.5	0.38	6.3	0.445

The variation of thickness with RI was also measured using a relatively smooth peptide film P3N3 which had a very good surface coverage as evident from AFM. The data show that the relationship between film thickness and RI is almost linear as shown in Figure 4.8 and the average thickness was calculated from the values obtained for the extremes.

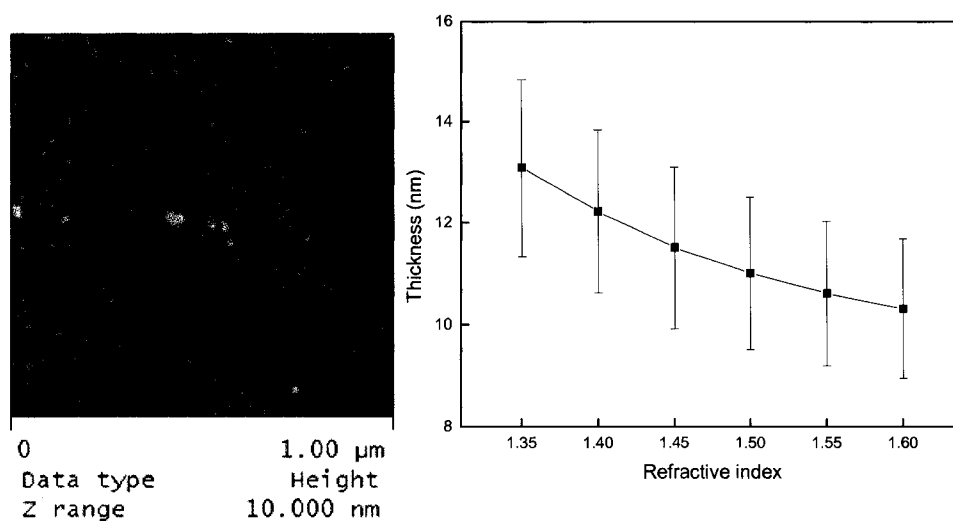


Figure 4.8. Variation of film thickness with RI. Film P3N3 was taken as a non limiting example due to its low surface roughness and full coverage.

Mouse 3T3 fibroblast cells were seeded and allowed to grow on peptide multilayer films and the confluence was monitored. An MTT assay was used to determine the number of cells growing on the films which was deduced from a standard curve. Figure 4-10 shows a light microscope image of cells growing on a PLL/PLGA film.

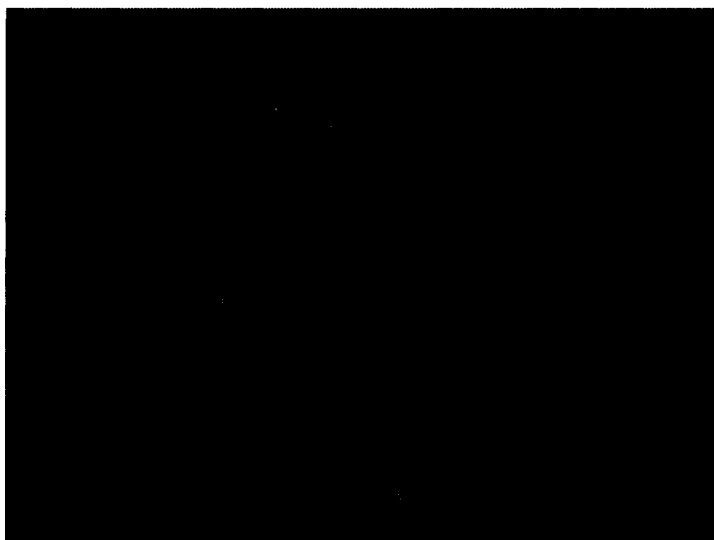


Figure 4.9. Mouse 3T3 fibroblasts on PLL/PLGA multilayer film.

Data from the MTT assay show that more number of cells were present on substrates coated with P4N4 as compared to P2N2 or P3N1. The growth varied as P4N4>P3N1>P2N2. A bare glass slide and a slide coated with poly-(L-lysine)/poly-(L-glutamic acid) (PLL/PLGA) were used as controls. Maximum proliferation occurred on the substrates coated with PLL/PLGA as compared with the designed peptides. The number of cells growing on P2N2 and the control glass slide is almost the same. Cells were also seeded on films with 10 layers of PLL/PLGA and 5 layers of designed peptide to study the effect of precursor coatings and also minimize the amount of peptide required for achieving optimal cell growth. The precursor layers were fabricated from PLL and PLGA of $\approx 1500-3000$ Da almost the same molecular weight as the designed peptides. The data show that the number of cells growing on (PLL/PLGA)-P2N2 and (PLL/PLGA)-P3N1 was almost the as in the case of P2N2 and P3N1 whereas the number of cells growing on (PLL-PLGA)-P4N4 decreased by almost 25%. All the films were fabricated in triplicate to check for reproducibility and the standard deviations in all cases

are less than 10%. MTT assay data for the different peptide films are shown in figure 4.10 and figure 4.11 below.

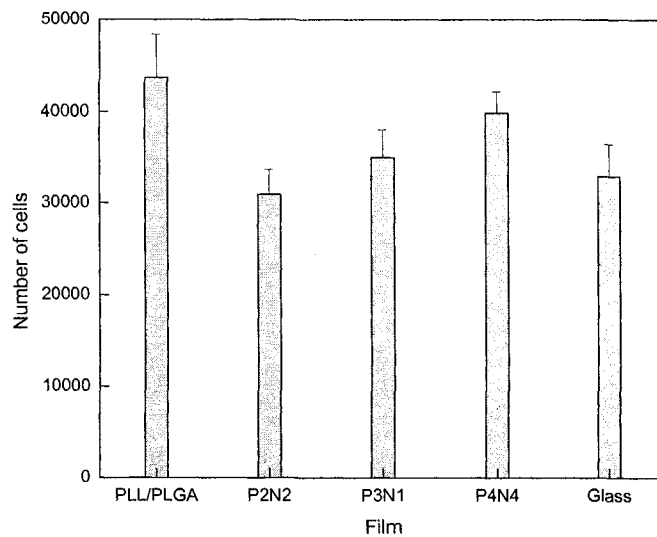


Figure 4.10. Number of cells on polypeptide multilayer films as determined by MTT assay.

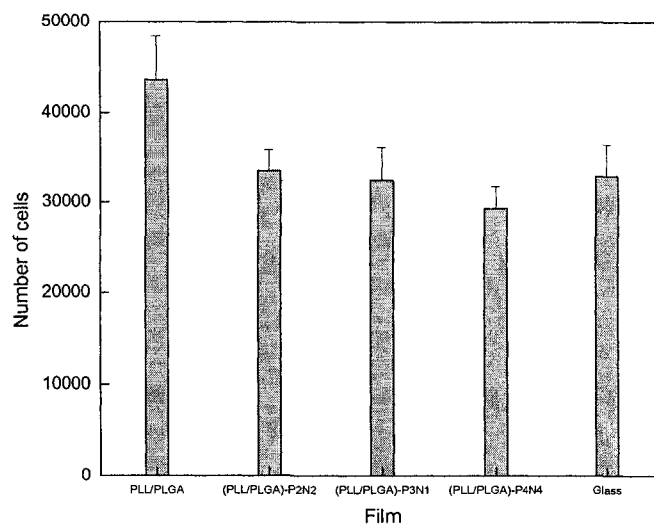


Figure 4.11. Number of cells growing on (PLL/PLGA)-polypeptide multilayer films as determined by MTT assay.

It has been shown that the polypeptide multilayer films can be used as substrates for cell culture and the properties of the substrate can be controlled by incorporating specific amino acids in the designed peptides. It is impossible to predict the trend of cell growth depending on the physical or biochemical properties of the films studied here. Cells behave differently on different substrates and different cell lines do not show identical behavior on the same substrate. However, it can be concluded that polypeptide multilayer films show substantial promise as substrates for cell attachment and growth. Solid-phase peptide synthesis techniques can be employed to synthesize RGD peptides in the laboratory. Customizability of RGD peptides enables synthesis of specially designed RGD containing peptides that can be made to bind specifically to certain integrins for specific applications.

Certain general design criteria for custom peptides [109], such as using conformation-restraining residues (Gly and Pro) at specific locations in the sequence, selectively choosing neighborhood residues of RGD sequence, choosing the locations of cysteine residues for plausible disulfide bridge formation and cyclization can help design and engineer RGD-containing peptides for various purposes. “Integrin-selective peptides” may be designed for specific purposes, in order to enhance integrin affinity, selectivity, and/or sensitivity of RGD peptides [215]. Synthesis of short RGD peptides ensures that the RGD motif is available on the surface of the peptide for integrin interaction, unlike large proteins and peptides where the RGD motifs are not necessarily available for integrin binding. The presence of inherent RGD motifs in the peptide sequence also eliminates certain chemical processes required to “RGD-modify” other polymers. The amino acid sequence and the peptide itself can be subjected to any or all of

amino acid analysis (AAA), high-performance liquid chromatography (HPLC), mass spectrometry (MS), or circular dichroism (CD) techniques to ensure the desired properties and structural features are present in the synthesized peptide.

4.8 Conclusions

Designed polypeptides with inherent RGD motifs can be used in LBL as surface coatings for cell culture applications. The relationship between film structure, roughness, thickness, biochemical composition, and the flanking residues can be investigated in great depth as RGD peptides occur in many different proteins including collagen, fibronectin, vitronectin and fibrinogen. The experiments show that RGD peptides can be used for coating surfaces to facilitate cell growth and attachment. RGD peptides can help in cell recognition, and possible applications of RGD peptide multilayer films can include enhanced wound healing, skin regeneration, etc. Layer-by-layer assembly of synthetic RGD peptides is a promising field with potential applications. The data show that low charge density on a peptide is a key factor in building a multilayer film using LBL. The fibril formation in the case of peptides P2 and N2 due to hydrophobic interactions is a result of low charge. However, careful design of peptides with a balance of physical and biochemical properties can result in well defined films which can mimic the extracellular matrix and play a key role in understanding cell growth, proliferation, and differentiation on coated surfaces.

CHAPTER 5

IN VIVO STUDIES OF DESIGNED POLYPEPTIDE

MICROCAPSULES FOR DRUG DELIVERY

APPLICATIONS

5.1 Introduction

The encapsulation of materials at the macroscopic scale has long been used to store different solids or liquids and to protect them from environmental influences. Microencapsulation of materials is of highest interest for various applications in pharmaceutical, cosmetic, food, textile, adhesive, and agricultural industries. Today, microcapsule systems have the highest potential in the pharmaceutical industry since many different requirements have to be fulfilled to deliver a drug at the right moment, in the right place, and at an adequate concentration. One of the simplest examples is the protection of orally applied drugs from the attack of acids in the stomach before they can be adsorbed in the intestine. This problem is solved in many cases by the use of gelatin microcapsules, which are insoluble at the low pH values found in the stomach allowing the desired release later in the intestinal tract.

Several approaches have been used to fabricate microcapsules. One approach is to use systems that self-assemble into capsules at given conditions, such as the aggregation of lipid molecules into spherically closed bilayer structures like vesicles or liposomes

[256, 257]. Block copolymers can also aggregate in aqueous solution to vesicular structures [258]. A second method is to use dendrimers or hyperbranched polymers for nanoencapsulation [259, 260]. However, the particle preparation requires a rather costly and tedious procedure, which clearly presents a limiting factor for possible applications.

Another method involves the use of LBL technology [261] which uses a sacrificial template core that can be dissolved. The LBL assembly process developed for macroscopic planar surfaces can be adapted to colloidal particles 0.1-10 μm in diameter for the preparation of capsules [261, 262]. Dissolution of the template particles [263] will yield empty capsules with a wall thickness of 5-50 nm, depending on the assembly procedure, materials, and cycles of polyion adsorption. In principle, a large variety of polyelectrolytes could be used as capsule components to yield a correspondingly broad range of microcapsule functionalities. Haynie et al. [181] used designed polypeptides containing cysteine residues to form microcapsules and the polypeptide layers were crosslinked by oxidation, forming disulfide-bond-“locked” capsules. This process, which is reversible, [117, 121] stabilized the capsules in “harsh” environments. High-capacity, high-activity loading of glucose oxidase into polypeptide microcapsules has been achieved by addition of polyethylene glycol 300 (PEG300) to aqueous solutions of oppositely charged polypeptides used in capsule assembly. These microcapsules have been shown semipermeable to small molecules and allowed the enzymatic breakdown of the encapsulated glucose oxidase [264]. The inherent biocompatibility of the encapsulating polypeptides presents advantages for biomedical applications over the more common non-biodegradable synthetic polyelectrolytes.

5.2 Materials and Methods

Poly (L-glutamic acid) (PLGA) (15 kDa), Poly (L-lysine) (PLL) (15 kDa) were from Sigma-Aldrich (USA). Designed peptide was from Global Peptide Analysis (USA). Phosphate buffered saline (PBS) was from Invitrogen (USA) and calcium carbonate microparticles (3 μ m dia) were from GmbH (Germany) . 18.2 M Ω -cm water was used in all experiments. In additional, all formulations were filtered through 5 μ m filter to ensure low aggregation. Solutions for film capsule assembly were prepared by dissolving the peptides in PBS to a final concentration of 1 mg/ml.

5.2.1 Microcapsule Fabrication

Two different microcapsule formulations were prepared using LBL technique on calcium carbonate microparticle templates. In one formulation (formulation 1) the microcapsules were fabricated using PLL/PLGA with the outermost layer being PLGA. In another formulation (formulation 2) the microcapsule was fabricated with layers of PLL/PLGA with the outermost layer being a designed peptide (GDAAECAD)₃-GDAAECAY. A formulation with uncoated calcium carbonate microparticles was used a control. All formulations were prepared to two strengths; a high dose and a low dose. A typical high dose had 5 \times 10⁶ microcapsules and a low dose had 1 \times 10⁶ microcapsules per 100 μ L of formulation.

5.2.2 Animals and Husbandry

BALB/cJ mice used in this study were purchased from Jackson Labs (USA) and came from a specific-pathogen-free (SPF) colony. 16 males and 16 females at 7 weeks of age were maintained in isolation rooms in 70 sq in. filter top cages with aspen wood chip bedding. Care-taking personnel entered the rooms in a specific order to avoid

contamination and had to wear different protective clothing in each room. The light cycle in the rooms was 12 hours daily, the room temperature was at 72 F and the rooms had humidity in the range of 40–70%. All mice were fed 8664 food pellets (6% fat) from Teklad (USA) and tap water. This study met the standards of the *Guide for the Care and Use of Laboratory Animals* and the study protocol was approved by Institutional Animal Care and Use (IUCAC) Committee.

5.2.3 Animal Grouping and Coding

The mice were divided into four groups containing eight mice each and all of them comprised of four females and four males. The males and females in each group were divided into two subgroups of two males and two females each. The four groups were labeled as control (C), formulation1 (F1), formulation2 (F2), and spare. A mouse from the spare group was substituted in case of accidental death under trial. Each group received its own formulation and the male and female subgroups received a high or low dose. Animals were caged according to the above schematic and were tattooed with numbers 1 and 2 in each cage. To avoid further confusion one line or two lines were drawn horizontally across the tails with tattoo ink to identify them. The cages were coded according to a standard format as Formulation # - Sex - Dose - #. For example if a male mouse #2 received a high dose of formulation 2 it was labeled as F2-M-H-2. Control formulation was coded as 'C'. In case of a substitution additional number in parenthesis was included to identify it. For example, if female mouse #1 in the control group which received a low dose was substituted it was labeled as C-F-L-1(2). The grouping schematic is shown below in Figure 5.1.

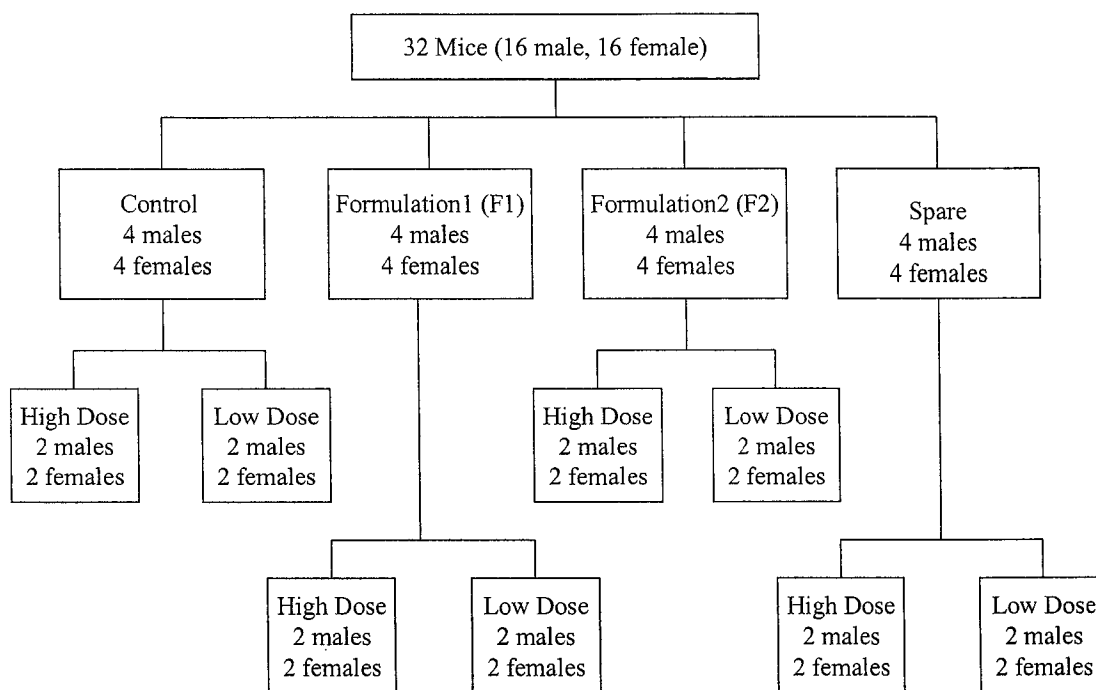


Figure 5.1. Schematic showing the grouping of mice.

5.2.4 Saphenous Vein Blood Collection

The conscious mouse was restrained in an uncapped 50 ml falcon tube that had had air holes drilled into the closed end with the mouse's nose at the closed end of the tube with the back legs, rear and tail of the animal exposed at the open end of the tube. The left hind leg was extended and fixed by firmly holding the fold of skin between the tail and thigh. The skin is held with the same hand holding the restraining tube and the hair was then removed from the outer surface of the fixed leg using an electric shaver. By pinching the skin between the tail and thigh of the mouse blood flow was restricted from the lower limb causing the saphenous vein to protrude. The skin was wiped clean with 70% ethanol and dried with a dry piece of gauze. A small amount of vaseline was wiped onto the shaved skin to reduce clotting. The saphenous vein was punctured using a 25 gauge needle which was held almost parallel to the vein. Drops of blood were collected

as they appeared on the surface of the leg in an appropriate capillary tube held on a 45° angle with one end of the tube at the edge of the drop of blood collecting on the leg surface. Approximately 300 μ l of blood was collected from each mouse using this method. A second puncture of the same vessel or use of the saphenous vein in the other leg was done if necessary to collect the desired volume of blood. When the desired volume of blood has been collected, the blood was dispensed into a 0.5 ml microtube. The tube was capped and the contents of the tube were mixed by flicking the side of the tube. The tube of blood was stored under the appropriate conditions (stored on crushed ice for biochemistry analysis or at room temperature for hematology). To reduce the flow of blood to the puncture site, the mouse's foot was flexed and slight pressure was then applied to the puncture site with a gauze compress until the bleeding stopped. The mouse was then returned to its cage. Figure 5.2 shows a saphenous vein blood draw.



Figure 5.2. Saphenous vein blood collection.

5.2.5 Tail Vein Injections and Monitoring

For administration of the formulation the mouse was sedated using anesthesia (isofluorene/oxygen) to restrain it. The tail was rotated slightly to visualize the vein and was immersed in warm water to dilate it. The tail was then disinfected and a needle containing the formulation was inserted into the vein at a slight angle. Aspiration is not possible; instead 100 μ L of formulation was injected slowly and observed for clearing of the lumen. If incorrect positioning resulted in a slight bulge in the tail the needle was removed and process was repeated proximal to previous site. Upon completion the needle was removed and the injection site was bandaged for a few minutes before returning the mouse to its cage. The animals were injected one month apart and then monitored for signs of illnesses. The animals were weighed daily and a score sheet was developed for an unbiased decision to euthanize any mouse with signs of disease. The animals were monitored from a distance to observe eating/drinking, socialization, respiration, and rough hair coat, hunched posture, tremors and movement and were also handled to observe crusty eyes, diarrhea on the fur, cool to the touch, blue extremities and other symptoms. The score sheets were filled out everyday and anything abnormal was noted down. Figure 5.3 shows a tail vein injection in progress



Figure 5.3. Tail vein injection of formulations.

5.2.6 Blood Chemistry Analysis

Blood chemistry analysis was performed on a Abaxis Vetscan (USA) machine with appropriate rotors to load the samples. The analysis was performed under an hour of collecting the samples to ensure correct readings. The blood was tested for albumin (ALB), alkaline phosphatase (ALP), alanine amino transferase (ALT), total bilirubin (TBIL), blood urea nitrogen (BUN), calcium (Ca⁺⁺), phosphorous (Phos), creatinine (CRE), glucose (GLU), sodium (Na⁺), potassium (K⁺), total protein (TP), and globulins (GLOB). The analysis was performed on a pre-bleed to act as control and subsequently blood samples were drawn and analyzed a month after injections.

5.2.7 Euthanasia and Preservation

The animals were euthanized in a humane way using isofluorene as a sedative and drawing blood from the heart. The mice succumbed due to the loss of blood and were preserved for the study for gross pathology and tissue analysis. Immediately following their termination according to the approved protocol, an incision was on the ventral side of the animals from the throat to the genitalia. The ribs were cracked open to expose the lungs and other internal organs. The lungs, which deflate over time, were inflated as follows: a thread was looped over the trachea, and formalin was introduced gently. The trachea was sutured below the needle point to prevent leakage. Larger organs, such as the lungs and liver, were cross-sectioned to ensure adequate surface area for the preservative to seep into the tissues and preserve them. The preservative was 10 % buffered formalin with a final pH of 6.8. The buffer was phosphate buffered saline. Figure 5.4 shows the preservation process.

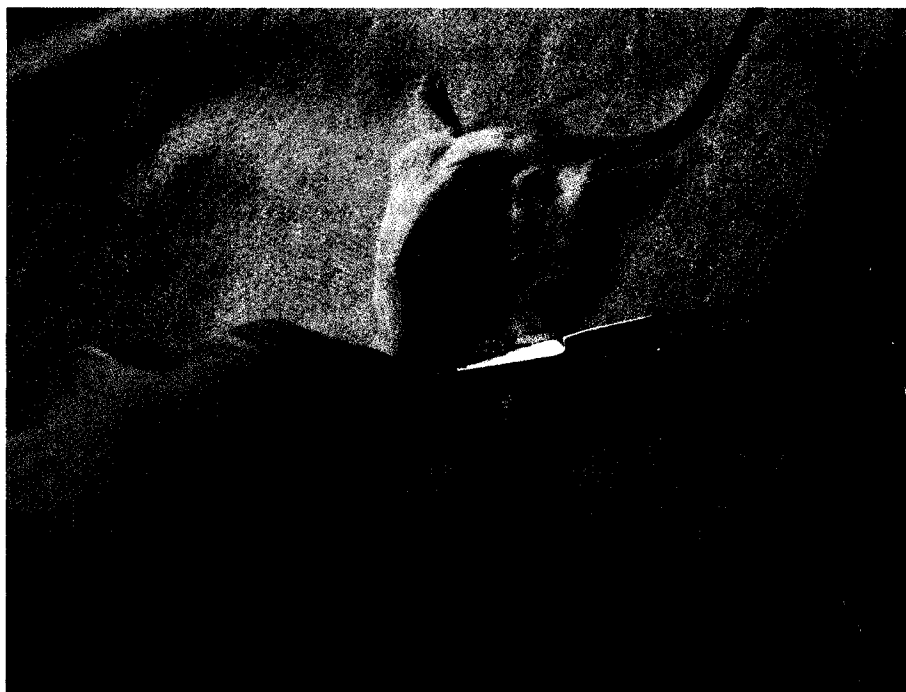


Figure 5.4 Mice being prepared for preservation.

5.3 Results and Discussion

Generally, all formulations were well tolerated by the mice. Some animals exhibited a slight ruffle coated appearance at times, but they appeared clinically normal. Mice treated with the designed polypeptide formulation tolerated the formulation very well at both levels of dosage. Changes in blood chemistry were monitored after a month to ensure that the formulations would not give rise to delayed complications. Blood contains large amounts of proteins, ions, and other metabolites maintained at appropriate levels to ensure a healthy system. The levels of these metabolites may be elevated or reduced under certain conditions like infection, inflammation, and stress. The values of these metabolites in the blood were checked after the formulation injections and were compared to a prebleed control. Some aspects of the analysis are discussed here.

The total amount of blood protein and the amounts of the two main protein groups, albumin and globulin indicate the general state of nutrition and can provide clues to help diagnose some diseases. Albumin is produced mainly in the liver. It helps transport some drugs and other substances through the blood and can be broken down to assist with tissue growth and healing. It also helps prevent blood from leaking out of blood vessels, so when albumin levels drop, edema may develop, with fluid collecting in the ankles, lungs, or abdomen. The levels of albumin in the blood before and after injections are shown below in Figure 5.5. The data show that there is a slight increase in albumin levels before and after the formulation injections, and it is within the normal value. Data is averaged for all mice within the same group and the average albumin level in BalbC mice is usually around 2.5-4.8 g/dL.

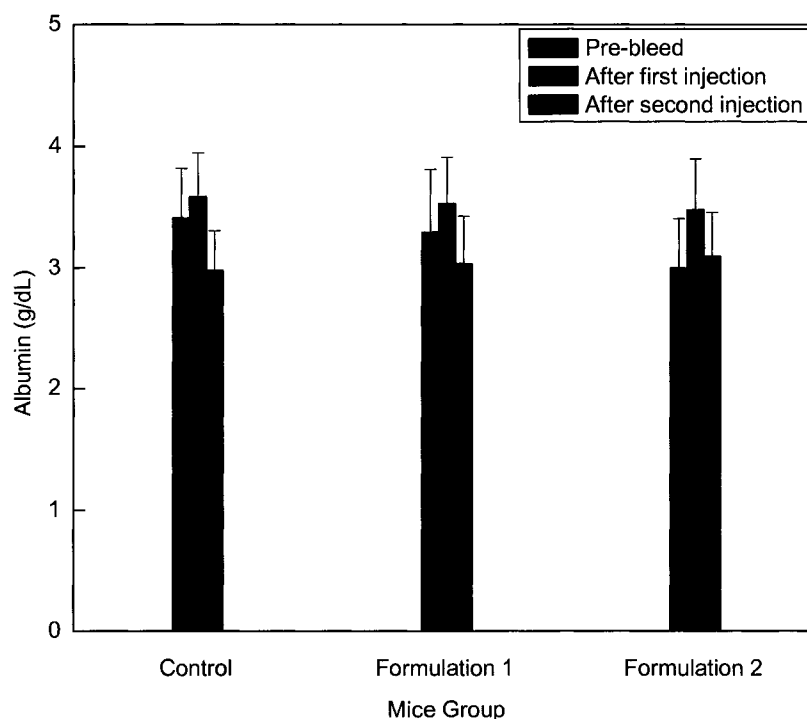


Figure 5.5. Albumin levels in mice before and after formulation injections.

Bilirubin is formed primarily from the breakdown of a substance in red blood cells called "heme." It is taken up from blood processed through the liver, and then secreted into the bile by the liver. An increase in the level of bilirubin may be caused by the decreased removal of bilirubin from the blood stream due to liver disease, or the increased destruction of red blood cells. Very high levels are usually noticeable as jaundice. The bilirubin may be elevated in many forms of liver or biliary tract disease, and thus it is also relatively nonspecific. However, serum bilirubin is generally considered a true test of liver function, and significant changes in the bilirubin levels would mean that the formulations could be interfering with the liver's ability to take up, process, and secrete bilirubin into the bile. The normal level of bilirubin in BalbC mice is usually around 0.1-0.9 mg/dL. The levels of bilirubin in both the control mice and mice injected with formulations are within the normal range as shown in Figure 5.6.

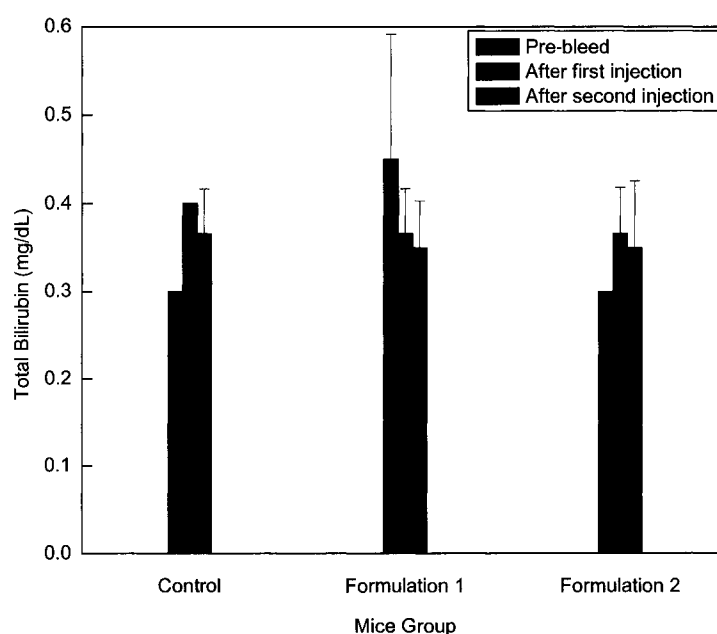


Figure 5.6. Total bilirubin levels in test mice before and after formulation injection.

Sodium and potassium are the major positive ions of body fluids. The concentration of sodium in body fluids is about thirty times the level inside body cells. The sodium ion content of the blood is a result of a balance between dietary intake and renal excretion. Only a small percentage is lost through the stool or sweat. Water and sodium are interrelated - retention of increased sodium is followed by retention of fluid and vice versa. However, the body can regulate sodium and water separately if necessary. Potassium is the major positive ion within cells and it is particularly important for maintaining the electric charge on cell membranes, necessary for neuromuscular communication, for transporting nutrients into cells and for removing waste products from cells. Small changes in the potassium levels outside cells can have substantial effects on the activity of nerves and muscles, particularly with the heart muscle. Low levels cause increased cardiac activity, which can lead to heart arrhythmia, whereas high levels decrease heart activity. In extreme circumstances either situation may lead to cardiac arrest. Figure 5.7a and 5.7b show the levels of sodium and potassium in the normal ranges of 151-165 mmol/L and 4.6-8 mmol/L respectively.

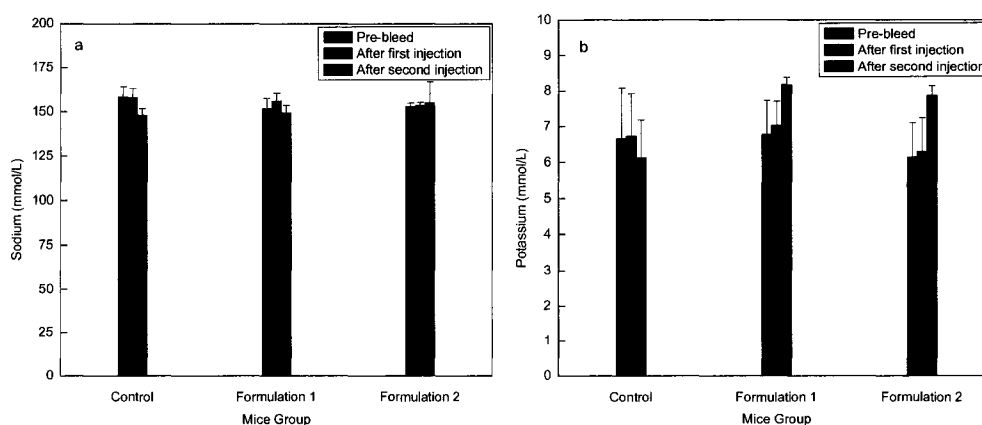


Figure 5.7. Levels of blood sodium in the test mice (a) levels of blood potassium in test mice (b) before and after formulation injections.

Alanine amino transferase (ALT) is an enzyme located in liver cells and can make its way into the bloodstream by leaking out of liver cells that are injured. ALT is a specific indicator of liver inflammation. The reasonable levels of ALT in the data suggest that the formulations do not cause liver injury. The relatively stable levels of creatinine show normal kidney function. Creatinine level checks are widely used as a test of renal (kidney) function both as a general screen, along with urine protein, for kidney disease, as a test for serial monitoring of kidney function and where there is potential or actual kidney disease. All mice exhibited normal behavior, continued to consume feed and water, and did not exhibit abnormal behavior directed at the injection sites (i.e., chewing or biting). The formulations showed excellent biocompatibility and no foreign body reaction was observed. The coatings of the capsules are biodegradable which could have been digested by the enzymes in the blood and assimilated or the capsules could aggregate in capillary beds like the lungs or the liver. Further histochemical analysis would be required to address the matter of the “fate” of these microcapsules after injection.

5.4 Conclusions

Polypeptide microcapsules coated with designed polypeptides can be used as vehicles for drug delivery and the designed peptide can be engineered to be stable in the environment into which it is introduced. The biocompatibility and immunogenicity of polypeptide microcapsules will be more favorable for biomedical applications of LBL structures than those made from more usual organic polyelectrolytes, particularly if the sequences are based on genomic information.

CHAPTER 6

CONCLUSIONS

Since the development of the LBL technique lots of materials have been used to assemble multilayer thin films towards understanding the theoretical principles underlying the technique as well as towards the development of successful patented applications. In electrostatic LBL assembly of polypeptide multilayer films, assembly is driven primarily by columbic interactions, but hydrophobic interactions and hydrogen bonds also contribute to film formation and stability, the amount depending on polypeptide design.

The field of polypeptide multilayer nanofilm research flourishes where study of protein structure and function shares a border with development of polyelectrolyte multilayers. The soil is fertile for creative input and promises a harvest of interesting results: the structure of a film can be predetermined on a layer-by-layer (LBL) basis, a huge variety of polypeptide sequences can be realized in large quantities by modern methods of synthesis, and the fabrication process is environmentally benign. However, the biomedical applications of polypeptide multilayer nanofilms are still in the early stages and many await discovery. Promising applications of the polypeptide multilayer film platform technology include coatings for medical implant devices, scaffolds for

tissue engineering, coatings for targeted drug delivery, artificial cells for oxygen therapeutics, and artificial viruses for immunization. In each case peptide structure is tailored to the application.

The development of polypeptide microcapsules requires effort in the area of synthesizing biodegradable and biocompatible cores. The tunable semi permeability, high stability, size range, monodispersity, high interior volumes, multifunctionalization, modification of physiochemical properties, and the ease and low cost of preparation opens the way for creating shells with highly specific properties. These properties are of great potential for drug delivery applications and diagnostics. The investigation of designed polypeptide multilayer films and microcapsules for biomimetic applications is almost in its initial stages and many new developments can be expected in future of this highly fascinating research field.

APPENDIX A

PHYSICAL CHARACTERIZATION DATA OF DESIGNED POLYPEPTIDE FILMS FOR CELL CULTURE APPLICATIONS

Table A.1. UV absorbance data of designed peptide films.

Film	Abs max (195 nm)
P1N1	0.2
P1N2	0.2
P1N3	0.14
P1N4	0.18
P2N1	0.09
P2N2	0.32
P2N3	0.08
P2N4	0.11
P3N1	0.28
P3N2	0.14
P3N3	0.14
P3N4	0.09
P4N1	0.15
P4N2	0.09
P4N3	0.07
P4N4	0.13

Table A.2. Thickness of designed peptide multilayer films.

Film	Refractive Index = 1.34		Refractive Index = 1.6		Refractive Index = 1.47	
	Avg	SD	Avg	SD	Avg	SD
P1N1	21.9	1.6	17	1.3	19.45	1.45
P1N2	20	1	15.6	0.8	17.8	0.9
P1N3	13.9	0.6	10.6	0.4	12.25	0.5
P1N4	13	0.86	10	0.7	11.5	0.78
P2N1	15.8	0.525	12.2	0.425	14	0.475
P2N2	17.7	0.4	13.8	0.35	15.75	0.375
P2N3	13.2	1.3	10.2	1	11.7	1.15
P2N4	16.6	1.7	12.8	1.36	14.7	1.53
P3N1	12	0.76	9.3	0.58	10.65	0.67
P3N2	13	0.85	10	0.64	11.5	0.745
P3N3	12.3	1	9.5	0.78	10.9	0.89
P3N4	11	1	8.6	0.8	9.8	0.9
P4N1	15.5	1.2	12	0.9	13.75	1.05
P4N2	10	0.62	7.7	0.47	8.85	0.545
P4N3	14.1	0.62	11	0.47	12.55	0.545
P4N4	7.1	0.51	5.5	0.38	6.3	0.445

Table A.3. Surface roughness values of designed peptide multilayer films.

Sample	Average Roughness (nm)		Rms Roughness (nm)	
	5 μm	1 μm	5 μm	1 μm
P1N1	7	6.28	9	7.82
P1N2	4.15	3.34	6.29	4.16
P1N3	2.07	1.72	2.91	2.21
P1N4	1.38	0.89	1.76	1.15
P2N1	3.76	3.45	5.42	4.36
P2N2	3.65	3.17	4.83	3.93
P2N3	2.24	1.73	3.13	2.18
P2N4	1.50	0.98	3.35	1.30
P3N1	3.89	3.32	5.96	4.16
P3N2	2.06	1.28	3.11	1.64
P3N3	0.72	0.52	1.08	0.75
P3N4	3.31	2.02	4.90	2.49
P4N1	1.44	0.61	2.33	0.79
P4N2	2.03	1.72	3.24	2.34
P4N3	1.53	0.86	2.06	1.15
P4N4	0.61	0.57	0.99	0.70
P2	2.04	1.32	2.80	1.71
N2	0.88	0.57	1.24	0.74
Bare	0.15	0.61	0.21	0.16

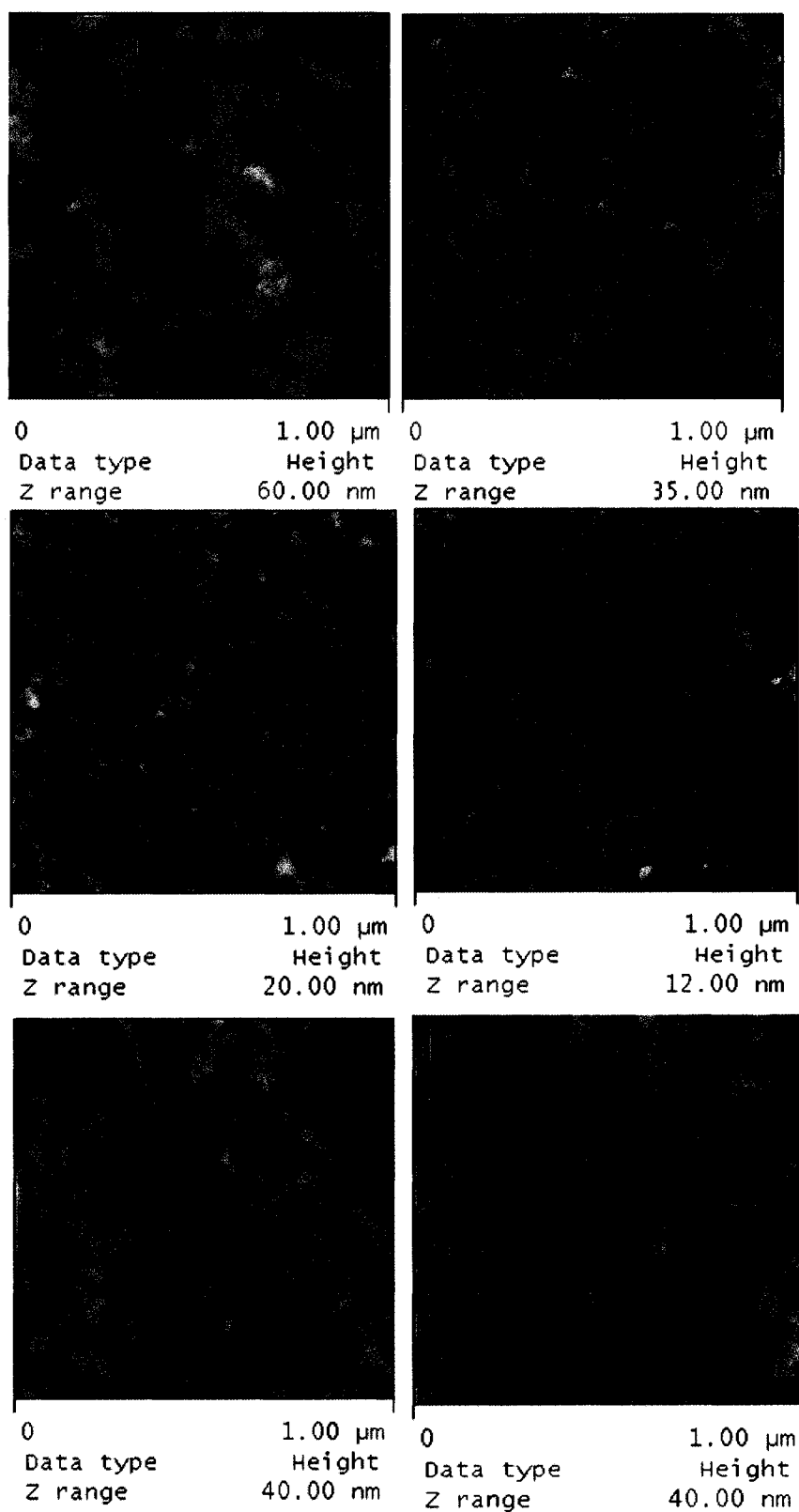


Figure A.1. AFM images of designed peptide multilayer films (i).

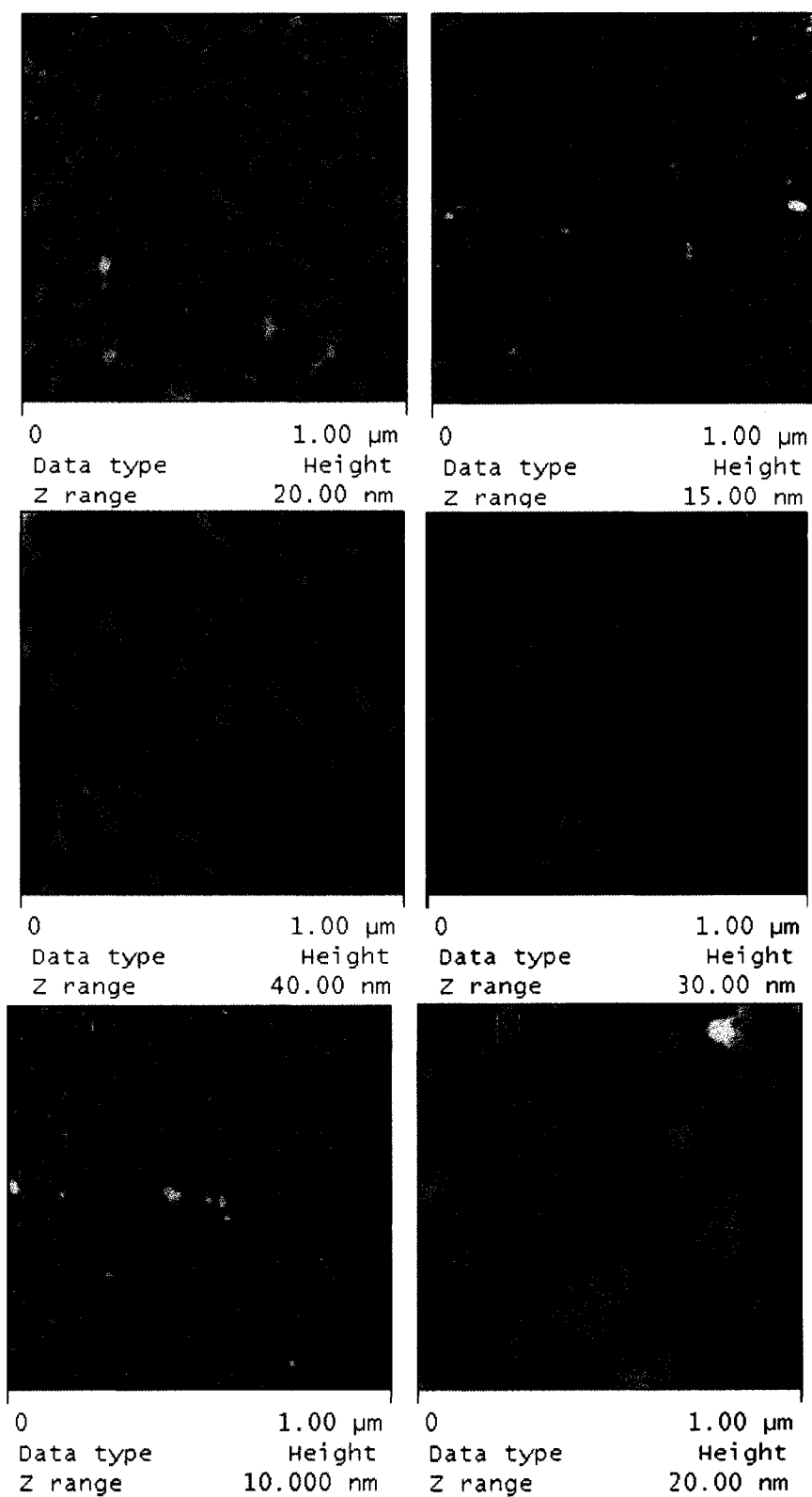


Figure A.2. AFM images of designed peptide multilayer films (ii).

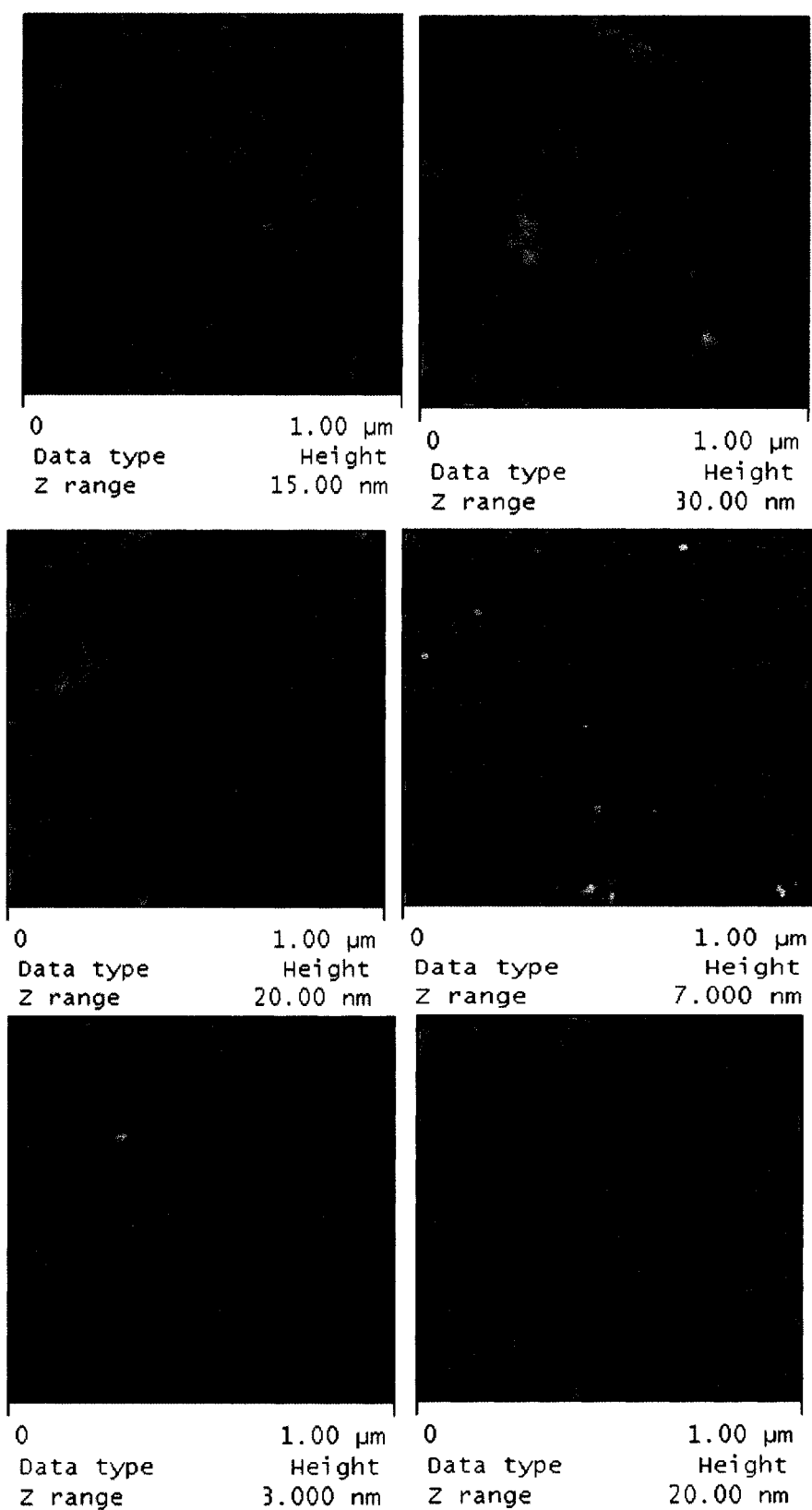


Figure A.3. AFM images of designed polypeptide multilayer films (iii).

APPENDIX B

BLOOD CHEMISTRY DATA FOR MICE INJECTED WITH PEPTIDE
FORMULATIONS

Table B.1. Blood chemistry data for control mice before injections.

	C-M-H-1	C-M-H-2	C-M-L-1	C-M-L-1(2)	C-M-L-2
ALB	3.3	3.3	-	2.7	3.5
ALP	141	184	-	145	157
ALT	22	28	-	26	32
AMY	566	488	-	727	527
TBIL	0.3	0.3	-	0.3	0.3
BUN	28	22	-	36	31
CA	9.7	9.4	-	9.7	10.4
PHOS	9.3	8.7	-	8.8	9.8
CRE	0.2	0.2	-	0.2	0.2
GLU	160	147	-	141	131
NA	162	157	-	163	164
K	6.2	7.8	-	8.5	-
TP	6	5.8	-	5.5	6.2
GLOB	2.7	2.4	-	2.8	2.7
	C-F-H-1	C-F-H-1(2)	C-F-H-2	C-F-L-1	C-F-L-2
ALB	-	3.8	4	3.6	3.1
ALP	-	179	180	159	123
ALT	-	32	48	35	45
AMY	-	645	595	576	521
TBIL	-	0.3	0.3	0.3	0.3
BUN	-	31	18	30	22
CA	-	9.6	10	9.4	8.9
PHOS	-	5.5	10	6.3	3.9
CRE	-	0.2	0.2	0.2	0.2
GLU	-	122	119	144	285
NA	-	161	159	153	147
K	-	6.1	-	6.9	4.5
TP	-	6	6	5.5	4.8
GLOB	-	2.3	2	1.9	1.7

Table B.2. Blood chemistry data for control mice after formulation injections.

1- bleed	C-M-H-1	C-M-H-2	C-M-L-1	C-M-L-1(2)	C-M-L-2
ALB	3.6	3.2	3.4	3	3.3
ALP	136	138	150	134	168
ALT	42	30	80	37	34
AMY	606	531	525	583	530
TBIL	0.3	0.4	0.4	0.4	0.4
BUN	28	28	24	24	24
CA	10.8	9.6	9.7	9.6	9.8
PHOS	14.4	5.9	9.2	8	5.2
CRE	0.2	0.2	0.2	0.2	0.2
GLU	122	138	209	140	166
NA	169	152	160	160	156
K	8.5	6.8	8.1	7.4	6.2
TP	6.4	5.7	5.3	5.9	5.9
GLOB	2.9	2.5	2	2.9	2.6
	C-F-H-1	C-F-H-1(2)	C-F-H-2	C-F-L-1	C-F-L-2
ALB	4.1	3.8	3.7	3.8	4
ALP	194	146	170	155	161
ALT	34	39	73	42	57
AMY	625	643	610	595	608
TBIL	0.4	0.4	0.4	0.4	0.4
BUN	18	24	35	21	24
CA	10.2	10.2	10.5	10.3	9.9
PHOS	6.5	9.6	8.1	5.1	5.6
CRE	0.2	0.2	0.3	0.3	0.2
GLU	155	146	197	160	139
NA	158	163	155	152	151
K	6.3	7.7	6.2	5.2	4.9
TP	6	5.7	5.4	6	5.9
GLOB	1.9	1.9	1.7	2.1	1.9

Table B.3. Blood chemistry data for F1 group mice before injections.

0-bleed	F1-M-H-1	F1-M-H-2	F1-M-L-1	F1-M-L-2	F1-M-L-2(2)
ALB	3.1	2.9	2.3	-	3.4
ALP	164	217	94	-	137
ALT	20	64	42	-	16
AMY	788	629	1281	-	715
TBIL	0.3	0.6	0.4	-	0.6
BUN	25	25	26	-	25
CA	9.9	9.2	9.6	-	9.9
PHOS	10.4	8.7	7.5	-	6.5
CRE	0.2	0.2	0.2	-	0.2
GLU	128	194	199	-	148
NA	154	146	143	-	152
K	8	7.3	6.6	-	6.1
TP	5.6	5.4	4.7	-	6.1
GLOB	2.6	2.4	2.4	-	2.7
	F1-F-H-1	F1-F-H-2	F1-F-L-1	F1-F-L-2	
ALB	3.5	3.9	3.6	3.7	
ALP	208	178	178	204	
ALT	34	57	28	33	
AMY	792	654	608	618	
TBIL	0.3	0.3	0.6	0.5	
BUN	18	19	16	15	
CA	9.5	10.3	9.9	9.7	
PHOS	5.7	10.9	6.4	4.8	
CRE	0.2	0.2	0.2	0.2	
GLU	157	139	137	139	
NA	153	161	156	147	
K	5.8	8.2	6.4	5.8	
TP	5.5	6.2	5.5	5.9	
GLOB	2.1	2.3	2	2.2	

Table B.4. Blood chemistry data for F1 group mice after formulation injections.

	F1-M-H-1	F1-M-H-2	F1-M-L-1	F1-M-L-2	F1-M-L-2(2)
ALB	3.4	3.2	3.3	2.9	3.5
ALP	132	162	142	130	126
ALT	28	35	28	32	31
AMY	571	549	581	509	633
TBIL	0.3	0.4	0.4	0.4	0.4
BUN	34	30	26	24	31
CA	10.1	9.3	9.8	9.5	10.3
PHOS	6.8	4.6	4.9	7	8.4
CRE	0.2	0.3	0.2	0.2	0.2
GLU	131	191	174	126	167
NA	164	152	151	154	160
K	7.3	6	7.2	6.9	7.9
TP	5.9	5.7	5.8	5.4	6.1
GLOB	2.5	2.4	2.5	2.5	2.6
	F1-F-H-1	F1-F-H-2	F1-F-L-1	F1-F-L-2	
ALB	3.8	3.7	4	4	
ALP	160	154	170	165	
ALT	37	93	54	45	
AMY	775	721	561	574	
TBIL	0.4	0.4	0.3	0.3	
BUN	21	29	19	24	
CA	9.6	10.5	10.4	10.4	
PHOS	5.2	12	7.4	6.7	
CRE	0.2	0.2	0.2	0.2	
GLU	128	142	176	155	
NA	152	161	154	154	
K	5.9	7.2	7.1	7.7	
TP	5.5	5.5	6.1	6.1	
GLOB	1.7	1.8	2.1	2.1	

Table B.5. Blood chemistry data for F2 group mice before injections.

	F2-M-H-1	F2-M-H-2	F2-M-L-1	F2-M-L-2
ALB	2.6	2.6	2.7	2.7
ALP	115	133	144	146
ALT	306	23	22	24
AMY	432	484	546	516
TBIL	0.3	0.3	0.3	0.3
BUN	25	28	21	21
CA	9.2	9.4	9	9
PHOS	7.8	4.8	6.7	8.2
CRE	0.2	0.2	0.2	0.2
GLU	198	251	190	183
NA	155	151	152	151
K	7.6	5.8	5.8	6
TP	4.9	5	4.8	4.7
GLOB	2.3	2.4	2.1	2.1
	F2-F-H-1	F2-F-H-2	F2-F-L-1	F2-F-L-2
ALB	3.2	3.3	3.7	3.2
ALP	65	95	197	171
ALT	85	86	36	44
AMY	3516	-	636	656
TBIL	-	0.3	0.3	0.3
BUN	22	17	18	16
CA	10	10.3	9.8	9.3
PHOS	7	6.1	6.2	6.1
CRE	0.2	0.2	0.2	0.2
GLU	243	186	152	174
NA	151	154	156	151
K	-	7.2	5.9	4.7
TP	5.2	5.5	5.7	5.1
GLOB	2	2.2	1.9	1.8

Table B.6. Blood chemistry data for F2 group mice after formulation injections.

1- bleed	F2-M-H-1	F2-M-H-2	F2-M-L-1	F2-M-L-2
ALB	3.2	3.3	2.9	-
ALP	149	129	110	-
ALT	30	30	54	-
AMY	511	489	520	-
TBIL	0.4	0.4	0.4	-
BUN	29	29	24	-
CA	9.6	9.6	9.5	-
PHOS	6.1	5.8	7.2	-
CRE	0.2	0.2	0.2	-
GLU	147	164	189	-
NA	156	154	154	-
K	5.7	7.1	5.8	-
TP	5.4	5.7	5.1	-
GLOB	2.3	2.4	2.2	-
	F2-F-H-1	F2-F-H-2	F2-F-L-1	F2-F-L-2
ALB	3.7	3.9	3.9	-
ALP	158	174	167	-
ALT	32	37	30	-
AMY	642	532	506	-
TBIL	0.4	0.3	0.3	-
BUN	20	17	19	-
CA	10.3	10.5	10	-
PHOS	7.2	7	5.7	-
CRE	0.2	0.2	0.2	-
GLU	169	171	159	-
NA	152	152	151	-
K	6.1	7.8	5.3	-
TP	5.6	6	5.6	-
GLOB	1.8	2.1	1.7	-

REFERENCES

1. Feynman, R.P. *Plenty of room at the bottom: Presented at annual meeting of the American Physical Society*; California Institute of Technology: Pasadena, 1959.
2. O'Neil, T. *Movie awards: the ultimate unofficial guide to the Oscars, Golden Globes, Critics, Guild & Indie Honors*; Perigee Books: New York, 2003.
3. Rasmussen, C. *L.A. then and now: Pasadena's Gold Line will travel a history-laden route*; Los Angeles Times: New York, 2003.
4. Goodsell, D.S. *Bionanotechnology*; John Wiley: New Jersey, 2004.
5. Eigler, D.M.; Schweizer, E.K. "Positioning Single Atoms with a Scanning Tunnelling Microscope," *Nature* **1990**, *344*, 524-526.
6. Voet, D.; Voet J.G. *Biochemistry*; John Wiley: New York, 1995.
7. Holter, H.; Møller, K.M. *The Carlsberg laboratory*; The Carlsberg Foundation: Copenhagen, 1976; p. 88
8. Branden, C.; Tooze, J. *Introduction to protein structure*; Garland Inc: New York, 1999.
9. Poland, D.; Scheraga, H.A. *Theory of helix-coil transitions in biopolymers*; Academic Press: New York, 1970; p. 502.
10. Cooper, A.; Eyles, S.J.; Radford, S.E.; Dobson, C.M. "Thermodynamic Consequences of the Removal of a Disulphide Bridge from Hen Lysozyme," *J. Mol. Biol* **1992**, *225*, 939-943.
11. Bodanszky, M.; S Klausner, Y.S.; Ondetti, M.A. *Peptide Synthesis*; John Wiley & Sons: New York, 1976.
12. Creighton, T.E. *Proteins: Structures and Molecular Properties*; Freeman: New York, 1993.
13. Chou, P.Y.; Fasman, G.D. "Conformational Parameters for Amino Acids in Helical, Beta-sheet, and Random Coil Regions Calculated from Proteins," *Biochemistry* **1974**, *13*, 211-222.

14. Decher, G. "Fuzzy Nanoassemblies: Toward Layered Polymeric Multicomposites," *Science* **1997**, *277*, 1232-1237.
15. Tripathy, S.K.; Kumar, J.; Nalwa, H.S. Eds; *Handbook of Polyelectrolytes and their Applications. Vol 1* Polyelectrolyte-based Multilayers, Self-assemblies and Nanostructures; American Scientific Publishers: Stevenson Ranch, CA, 2002.
16. Decher, G.; Schlenoff, J.B. Eds; *Multilayer Thin Films: Sequential Assembly of Nanocomposite Materials*; Wiley-VCH: Weinheim, Germany, 2003.
17. Iler, R.K. "Multilayers of Colloidal Particles," *J. Colloid Interf. Sci.* **1966**, *21*, 569-594.
18. Lvov, Y.; Möhwald, H. Eds; *Protein Architecture: Interfacing Molecular Assemblies and Immobilization Biotechnology*; Marcel Dekker: New York, 2000.
19. Hoogeveen, N.G.; Cohen Stuart, M.A.; Fler, G.J.; Bohmer, M.R. "Formation and Stability of Multilayers of Polyelectrolytes," *Langmuir* **1996**, *12*, 3675-3681.
20. Laschewsky, A.; Mayer, B.; Wischerhoff, E.; Arys, X.; Bertrand, P.; Delcorte, A.; Jonas, A. "A New Route to Thin Polymeric, Non-Centrosymmetric Coatings," *Thin Solid Films* **1996**, *284*, 334-337.
21. Caruso, F.; Donath, E.; Möhwald, H. "Influence of Polyelectrolyte Multilayer Coatings on Förster Resonance Energy Transfer between 6-Carboxyfluorescein and Rhodamine B-Labeled Particles in Aqueous Solution," *J. Phys. Chem. B* **1998**, *102*, 2011-2016.
22. Sukhorukov, G.B.; Donath, E.; Lichtenfeld, H.; Knippel, E.; Knippel, M.; Budde, A.; Möhwald, H. "Layer-by-Layer Self Assembly of Polyelectrolytes on Colloidal Particles," *Colloids Surf. A* **1998**, *137*, 253-266.
23. Sukhorukov, G.B.; Donath, E.; Davis, S.; Lichtenfeld, H.; Caruso, F.; Popov, V.I.; Möhwald, H. "Stepwise Polyelectrolyte Assembly on Particle Surfaces: A Novel Approach to Colloid Design," *Polym. Adv. Technol.* **1998**, *9*, 759-767.
24. Caruso, F.; Möhwald, H. "Preparation and Characterization of Ordered Nanoparticle and Polymer Composite Multilayers on Colloids," *Langmuir* **1999**, *15*, 8276-8281.
25. Caruso, F.; Lichtenfeld, H.; Donath, E.; Möhwald, H. "Investigation of Electrostatic Interactions in Polyelectrolyte Multilayer Films: Binding of Anionic Fluorescent Probes to Layers Assembled onto Colloids," *Macromolecules* **1999**, *32*, 2317-2328.

26. Caruso, F.; Schüler, M.; Kurth, D.G. "Core-shell Nanoparticles and Hollow Shells Containing Metallo-supramolecular Components," *Chem. Mater.* **1999**, *11*, 3394-3399.
27. Donath, E.; Sukhorukov, G.B.; Möhwald, H. "Polyelektrolytkapseln im Submikrometer- und Mikrometerbereich," *Nachr. Chem. Tech. Lab.* **1999**, *47*, 400-404.
28. Joanny, J.-F. "Polyelectrolyte Adsorption and Charge Inversion," *Eur. Phys. J. B* **1999**, *9*, 117-122.
29. Lappan, U.; Buchhammer, H.M.; Lunkwitz, K. "Surface Modification of Poly(tetrafluoroethylene) by Plasma Pretreatment and Adsorption of Polyelectrolytes," *Polymer* **1999**, *40*, 4087-4091.
30. Okuba, T.; Suda, M. "Absorption of Polyelectrolytes on Colloidal Surfaces as Studied by Electrophoretic and Dynamic Light-Scattering Techniques," *J. Colloid Interf. Sci.* **1999**, *213*, 565-571.
31. Okuba, T.; Suda, M. "Alternate Sign Reversal in the Zeta Potential and Synchronous Expansion and Contraction in the Absorbed Multi-layers of Poly(4-vinyl-N-n-butylpyridinium bromide) Cations and Poly(styrene sulfonate) Anions on Colloidal Silica Spheres," *Colloid Polym. Sci.* **1999**, *277*, 813-817.
32. Schwarz, S.; Eichhorn, K.J.; Wischerhoff, E.; Laschewsky, A. "Polyelectrolyte Adsorption onto Planar Surfaces: a Study by Streaming Potential and Ellipsometry Measurements," *Coll. Surf. A* **1999**, *159*, 491-501.
33. Haynie, D.T.; Zhang, L.; Zhao, W.; Rudra, J.S. "Protein-Inspired Multilayer Nanofilms: Science, Technology and Medicine," *Nanomedicine: Nanotechnology, Biology, and Medicine* **2006**, *2(3)*, 150-157.
34. Voigt, A.; Lichtenfeld, H.; Sukhorukov, G.B.; Zastrow, H.; Donath, E.; Baumler, H.; Möhwald, H. "Membrane Filtration for Microencapsulation and Microcapsules Fabrication by Layer-by-Layer Polyelectrolyte Adsorption," *Ind. Eng. Chem. Res.* **1999**, *38*, 4037-4043.
35. Caruso, F. "Hollow Capsule Processing through Colloidal Templating and Self-Assembly," *Chem.-Eur. J.* **2000**, *6*, 413-419.
36. Bertrand, P.; Jonas, A.; Laschewsky, A.; Legras, R. "Ultrathin Polymer Coatings by Complexation of Polyelectrolytes at Interfaces: Suitable Materials, Structure and Properties," *Macromol. Rapid Comm.* **2000**, *21*, 319-348.

37. Chen, W.; McCarthy, T.J. "Layer-by-Layer Deposition: A Tool for Polymer Surface Modification," *Macromolecules* **1997**, *30*, 78-86.
38. Hammond, P.T. "Recent Explorations in Electrostatic Multilayer Thin Film Assembly," *Curr. Opin. Colloid Interf. Sci.* **2000**, *4*, 430-442.
39. Decher, G. In *Multilayer Thin Films: Sequential Assembly of Nanocomposite Materials*; Decher, G. and Schlenoff, J.B. Eds.; Wiley-VCH: Weinheim, Germany, 2003; p. 1
40. Schönhoff, M. "Self-Assembled Polyelectrolyte Multilayers," *Curr. Opin. Colloid Interf. Sci.* **2003**, *8*, 86-95.
41. Hammond, P.T. "Form and Function in Multilayer Assembly: New Applications at the Nanoscale," *Adv. Mater.* **2004**, *16*, 1271-1293.
42. Müller, M.; Meier-Haack, J.; Schwarz, S.; Buchhammer, H.M.; Eichhorn, K.-J.; Janke, A.; Keßler, B.; Nagel, J.; Oelmann, M.; Reihs, T.; Lunkwitz, K. "Polyelectrolyte Multilayers and their Interactions," *J. Adhesion* **2004**, *80*, 521-547.
43. Rudra, J.S.; Dave, K.; and Haynie, D.T. "Antimicrobial Polypeptide Multilayer Nanocoatings," *J. Biomater. Sci. Polym. Edn.* **2006**, *17(11)*, 1301-1315.
44. Rubner, M.F. In *Multilayer Thin Films: Sequential Assembly of Nanocomposite Materials*; Decher, G. and Schlenoff, J.B. Eds.; Wiley-VCH: Weinheim, Germany, 2003; p. 133.
45. Schmitt, J.; Grünewald, T.; Decher, G.; Pershan, P.S.; Kjaer, K.; Lösche, M. "Internal Structure of Layer-by-Layer Adsorbed Polyelectrolyte Films: A Neutron and X-ray Reflectivity Study," *Macromolecules* **1993**, *26*, 7058-7063.
46. Decher, G.; Lvov, Y.; Schmitt, J. "Proof of Multilayer Structural Organization in Self-assembled Polyanion-Polycation Molecular Films," *Thin Solid Films* **1994**, *244*, 772-777.
47. Lvov, Y. In *Protein Architecture: Interfacing Molecular Assemblies and Immobilization Biotechnology*; Lvov, Y.; Möhwald, H. Eds.; Marcel Dekker: New York, 2000; p. 125.
48. Schlenoff, J.B.; Dubas, S.T.; Farhat, T. "Sprayed Polyelectrolyte Multilayers," *Langmuir* **2000**, *16*, 9968-9969.
49. Cho, J.; Char, K.; Hong, J.-D.; Lee, K.-B. "Fabrication of Highly Ordered Multilayer Films Using a Spin Self-Assembly Method," *Adv. Mater.* **2001**, *13*, 1076-1078.

50. Lee, S.-S.; Hong, J.-D.; Kim, C.H.; Kim, K.; Koo, J.P.; Lee, K.-B. "Layer-by-Layer Deposited Multilayer Assemblies of Ionene-Type Polyelectrolytes Based on the Spin-Coating Method," *Macromolecules* **2001**, *34*, 5358-5360.
51. Chiarelli, P.S.; Johal, M.S.; Casson, J.L.; Roberts, J.B.; Robinson, J.M.; Wang, H.-L. "Controlled Fabrication of Polyelectrolyte Multilayer Thin Films Using Spin-Assembly," *Adv. Mater.* **2001**, *13*, 1167-1171.
52. Porcel, C.H.; Izquierdo, A.; Ball, V.; Decher, G.; Voegel, J.-C.; Schaaf, P. "Ultrathin Coatings and (Poly(glutamic acid)/Polyallylamine) Films Deposited by Continuous and Simultaneous Spraying," *Langmuir* **2005**, *21*, 800-802.
53. Izquierdo, A.; Ono, S.S.; Voegel, J.-C.; Schaaf, P.; Decher, G. "Dipping versus Spraying: Exploring the Deposition Conditions for Speeding up Layer-by-Layer Assembly," *Langmuir* **2005**, *21*, 7558-7567.
54. Hiorth, M.; Ingunn, T.; Sverre, A.S. "The Formation and Permeability of Drugs across free Pectin and Chitosan Films Prepared by a Spraying Method," *Eur. J. Pharm. Biopharm.* **2003**, *56*, 175-181.
55. Hubbell, J.A.; Elbert, D.L.; Herbert, C.B. U.S. Patent 6,743,521, 2004.
56. Klitzing, R.v.; Möhwald, H. "Proton Concentration Profile in Ultrathin Polyelectrolyte Films," *Langmuir* **1995**, *11*, 3554-3559.
57. Yoo, D.; Shiratori, S.S.; Rubner, M.F. "Controlling Bilayer Composition and Surface Wettability of Sequentially Adsorbed Multilayers of Weak Polyelectrolytes," *Macromolecules* **1998**, *31*, 4309-4318.
58. Mendelsohn, J.D.; Barrett, C.J.; Chan, V.V.; Pal, A.J.; Mayes, A.M.; Rubner, M.F. "Fabrication of Microporous Thin Films from Polyelectrolyte Multilayers," *Langmuir* **2000**, *16*, 5017-5023
59. Shiratori, S.S.; Rubner, M.F. "pH-Dependent Thickness Behavior of Sequentially Adsorbed Layers of Weak Polyelectrolytes," *Macromolecules* **2000**, *33*, 4213-4219.
60. Xie, A.F.; Granick, S. "Weak versus Strong: A Weak Polyacid Embedded within a Multilayer of Strong Polyelectrolytes," *J. Am. Chem. Soc.* **2001**, *123*, 3175-3176.
61. Kato, N.; Schuetz, P.; Fery, A.; Caruso, F. "Thin Multilayer Films of Weak Polyelectrolytes on Colloid Particles," *Macromolecules* **2002**, *35*, 9780-9787.

62. Rmaile, H.H.; Schlenoff, J.B. "Internal pKa's in Polyelectrolyte Multilayers: Coupling Protons and Salt," *Langmuir* **2002**, *18*, 8263-8265
63. Burke, S.E.; Barrett, C.J. "Acid-Base Equilibria of Weak Polyelectrolytes in Multilayer Thin Films," *Langmuir* **2003**, *19*, 3297-3303.
64. Fler, G.J. and Lyklema, J. In *Adsorption from Solutions at the Solid/Liquid Interface*, Parfitt, G.D. and Rochester, C.H. Eds.; Academic Press: London, 1983; p. 153.
65. Park, S.Y.; Barrett, C.J.; Rubner, M.F.; Mayes, A.M. "Anomalous Adsorption of Polyelectrolyte Layers," *Macromolecules* **2001**, *34*, 3384-3388.
66. Joly, S.; Kane, R.; Radzilowski, L.; Wang, T.; Wu, A.; Cohen, R.E.; Thomas, E.L.; Rubner, M.F. "Multilayer Nanoreactors for Metallic and Semiconducting Particles," *Langmuir* **2000**, *16*, 1354-1359.
67. Boulmedais, F.; Frisch, B.; Etienne, O.; Lavalle, Ph.; Picart, C.; Ogier, J.; Voegel, J.-C.; Schaaf, P.; Egles, C. "Polyelectrolyte Multilayer Films with Pegylated Polypeptides as a new type of Antimicrobial Protection for Biomaterials," *Biomaterials* **2004**, *25*, 2003-2011.
68. Hübsch, E.; Fleith, G.; Fatisson, J.; Labbé, P.; Voegel, J.C.; Schaaf, P.; Ball, V. "Multivalent Ion/Polyelectrolyte Exchange Processes in Exponentially Growing Multilayers," *Langmuir* **2005**, *21*, 3664-3669.
69. Picart, C.; Mutterer, J.; Richert, L.; Luo, Y.; Prestwich, G. D.; Schaaf, P.; Voegel, J.C.; Lavalle, P. "Molecular Basis for the Explanation of the Exponential Growth of Polyelectrolyte Multilayers," *Proc. Natl Acad. Sci. (U.S.A.)* **2002**, *99*, 12531-12535.
70. Elbert, D.L.; Herbert, C.B.; Hubbell, J.A. "Thin Polymer Layers Formed by Polyelectrolyte Multilayer Techniques on Biological Surfaces," *Langmuir* **1999**, *15*, 5355-5362.
71. Richert, L.; Lavalle, Ph.; Vautier, D.; Senger, B.; Stoltz, J.-F.; Schaaf, P.; Voegel, J.-C.; Picart, C. "Cell Interactions with Polyelectrolyte Multilayer Films," *Biomacromolecules* **2002**, *3*, 1170-1178.
72. Halthur, T.J.; Claesson, P.M.; Elofsson, U.M. "Stability of Polypeptide Multilayers As Studied by in Situ Ellipsometry: Effects of Drying and Post-Buildup Changes in Temperature and pH," *J. Am. Chem. Soc.* **2004**, *126*, 17009-17015.

73. Richert, L.; Arntz, Y.; Schaaf, P.; Voegel, J.-C.; Picart, C. "Ph Dependent Growth of Poly(l-lysine)/Poly(l-glutamic) acid Multilayer Films and their Cell Adhesion Properties," *Surf. Sci.* **2004**, *570*, 13-29.
74. Palath, N. MS thesis, Louisiana Tech University, Ruston, LA, 2005.
75. Santoso, S.; Hwang, W.; Hartman, H.; Zhang, S. "Self-Assembly of Surfactant-like Peptides with Variable Glycine tails to form Nanotubes and Nanovesicles," *Nano Letters* **2002**, *2*, 687-691.
76. Vauthey, S.; Santoso, S.; Gong, H.; Watson, N.; Zhang, S. "Molecular Self-assembly of Surfactant-like Peptides to form Nanotubes and Nanovesicles," *Proc. Natl. Acad. Sci. (USA)* **2002**, *99*, 5355-5360.
77. Aggeli, A.; Bell, M.; Carrick, L.M.; Fishwick, C.W.G.; Harding, R.; Mawer, P.J.; Radford, S.E.; Strong, A.E.; Boden, N. "pH as a Trigger of Peptide β -Sheet Self-Assembly and Reversible Switching between Nematic and Isotropic Phases," *J. Am. Chem. Soc.* **2003**, *125*, 9619-9628.
78. Maltzahn, G.v.; Vauthey, S.; Santoso, S.; Zhang, S. "Positively Charged Surfactant-like Peptides Self-assemble into Nanostructures," *Langmuir* **2003**, *19*, 4332-4337.
79. Bellomo, E.G.; Wyrsta, M.D.; Pakstis, L.; Pochan, D.J.; Deming, T.J. "Stimuli-Responsive Polypeptide Vesicles by Conformation-Specific Assembly," *Nat. Mater.* **2004**, *3*, 244-248.
80. Burkoth, T.S.; Benzinger, T.L.S.; Urban, V.; Lynn, D.G.; Meredith, S.C.; Thiyagarajan, P. "Self-Assembly of A β ₍₁₀₋₃₅₎-PEG Block Copolymer Fibrils," *J. Am. Chem. Soc.* **1999**, *121*, 7429-7430.
81. Lloyd-Williams, P.; Albericio, F.; Giralt, E. *Chemical Approaches to the Synthesis of Peptides and Proteins*; CRC press: Boca Raton, FL, 1997.
82. Grant, G.A. *Synthetic Peptides* Ed.; Oxford University Press: New York, 2002.
83. Chan, W.C.; White, P.D. Eds.; *Fmoc Solid Phase Peptide Synthesis: a Practical Approach*; Oxford University Press: New York, 2000.
84. Merrifield, R.B. "Solid Phase Peptide Synthesis," *J. Am. Chem. Soc.* **1963**, *85*, 2149-2154.
85. http://www.sigmaaldrich.com/img/assets/19200/Solid_Phase_Synthesis.pdf

86. Cunico, R.L.; Gooding, K.M.; Wehr, T. *Basic HPLC and CE of Biomolecules*, Bay Bioanalytical Laboratory: Richmond, CA, 1998.
87. Boysen, R.I.; Hearn, M.T.W. *Current Protocols in Protein Science*; John Wiley & Sons, Inc: New York, 2001.
88. Beckman Coulter HPLC User's Guide, August 2001.
89. Yasuaki M. *Technology of Water Pollution Continuous Monitoring in JAPAN* GEC Foundation: Japan, 1997.
90. Rivier, J.; McClintock, R.; Galyean, R.; Anderson, H. "Reversed-phase High-performance Liquid Chromatography: Preparative Purification of Synthetic Peptides," *J. Chrom.* **1984**, *288*, 303-328.
91. Hoeger, C.; Galyean, R.; Boublik, J.; McClintock, R.; Rivier, J. "Preparative Reversed Phase High Performance Liquid Chromatography. II. Effects of Buffer pH on the Purification of Synthetic Peptides," *Biochromatography* **1987**, *2*, 134-142.
92. Mochizuki, D.; March, C.J.; Cosman, D.; Deeley, M.C.; Klinke, R.; Clevenger, W.; Gillis, S.; Baker, P.; Urdal, D. "Expression, Purification and Characterization of Recombinant Murine Granulocyte-macrophage Colony-Stimulating Factor and Bovine Interleukin-2 from Yeast," *Gene* **1987**, *55*, 287-293.
93. Kroeff, E.P.; Owens, R.A.; Campbell, E.L.; Johnson, R.D.; Marks, H.I. "Production Scale Purification of Biosynthetic Human Insulin by Reversed-Phase High Performance Liquid Chromatography," *J. Chrom.* **1989**, *461*, 45-61.
94. Hjerten, S. "Free Zone Electrophoresis," *Chromatogr. Rev.* **1967**, *9*, 122-219.
95. Xu, Y. *The Chemical Educator*; Springer-Verlag: New York, 1996.
96. Florance, J.R.; Konteatis, Z.D.; Macielag, M.J.; Lessor, R.A.; Galdes, A. J. "Capillary Zone Electrophoresis Studies of Motilin Peptides. Effects of Charge, Hydrophobicity, Secondary Structure and Length," *Chromatogr.* **1991**, *559*, 391-399.
97. Grossman, P.D.; Wilson, K.J.; Petrie, G.; Lauer, H.H. "Effect of Buffer pH and Peptide Composition on the Selectivity of Peptide Separations by Capillary Zone Electrophoresis," *Anal. Biochem.* **1988**, *173*(2), 265-270.
98. McCormick, R.M. "Capillary Zone Electrophoretic Separation of Peptides and Proteins Using Low pH Buffers in Modified Silica Capillaries," *Anal. Chem.* **1988**, *60*(21), 2322-2328.

99. Young, P.M.; Astephen, N.E.; Wheat, T. "Effects of pH and Buffer Composition on Peptide Separations by High Performance Liquid Chromatography and Capillary Electrophoresis," *LC-GC* **1992**, *10(1)*, 26-32.
100. Chen, N.; Wang, L.; Zhang, Y. "Electrophoretic Selectivity as a Function of Operating Parameters in Free-Solution Capillary Electrophoretic Separation of Dipeptides: Capillary Electrophoretic Techniques," *J. Liq. Chromatogr.* **1993**, *16(17)*, 3609-3622.
101. Cifuentes, A.; and Poppe, H. "Effect of pH and ionic strength of running buffer on peptide behavior in capillary electrophoresis: Theoretical calculation and experimental evaluation," *Electrophoresis* **1995**, *16(1)*, 516-524.
102. Clore, G. H.; Grogenborn, A.M. "Structures of Larger Proteins, Protein-Ligand and Protein-DNA Complexes by Multi-Dimensional Heteronuclear NMR," *Prot. Sci.* **1994**, *3*, 372-390.
103. Campbell, A. P.; Sykes, B.D. "The Two-Dimensional Transferred Nuclear Overhauser Effect: Theory and Practice," *Annu. Rev. Biophys. Biomol. Structure* **1993**, *22*, 99-122.
104. Lane, A.N.; Lefèvre, J. F., "Nuclear Magnetic Resonance Measurements of Slow Conformational Dynamics in Macromolecules," *Methods Enzymol.* **1994**, *239*, 596-619.
105. London, R.E. "Interpreting Protein Dynamics with Nuclear Magnetic Resonance Relaxation Measurements," *Methods Enzymol.* **1989**, *176*, 358-375.
106. Peng, J.W.; Wagener, G. "Investigation of protein motions via relaxation measurements," *Methods Enzymol.* **1994**, *239*, 563-596.
107. Rodriguez, L.; De Paul, S. M.; Barrett, C. J.; Reven, L. G.; Spiess, H. W. "Fast MAS and Double Quantum ¹H Solid-State NMR Spectroscopy of Polyelectrolyte Multilayers," *Adv. Mater.*, **2000**, *12*, 1934-1938.
108. Smith, R.; Reven, L.; Barrett, C. J. "¹³C Solid-State NMR Study of Polyelectrolyte Multilayers," *Macromolecules*, **2003**, *36*, 1876-1881.
109. McCormick, M.; Smith, R.; Graf, R.; Barrett, C.; Reven, L.; Spiess, H. W. "NMR Studies of the Effect of Adsorbed Water on Polyelectrolyte Multilayer Films in the Solid State," *Macromolecules*, **2003**, *36*, 3616-3625.
110. Smith, R.; McCormick, M.; Barrett, C. J.; Reven, L.; Spiess, H. W. "NMR Studies of PAH/PSS Polyelectrolyte Multilayers Adsorbed onto Silica," *Macromolecules*, **2004**, *37*, 4830-4838.

111. Barber, M.; Bordoli, R.S.; Sedgewick, R.D.; Tyler, A.N. "Fast Atom Bombardment of Solids as an Ion Source in Mass Spectrometry," *Nature* **1981**, *293*, 270-275.
112. Whitehouse, C.M.; Dreyer, R.N.; Yamashita, M.; Fenn, J.B. "Electrospray Interface for Liquid Chromatographs and Mass Spectrometers," *Anal. Chem.* **1985**, *57*, 675-679.
113. Karas, M.; Hillenkamp, F. "Laser Desorption Ionization of Proteins with Molecular Mass Exceeding 10000 Daltons," *Anal. Chem.* **1988**, *60*, 2299-2301.
114. Falick, A.M.; Maltby, D.A. "Derivatization of Hydrophilic Peptides for Liquid Secondary Ion Mass Spectrometry at the Picomole Level," *Anal. Biochem.* **1989**, *182*, 165-169.
115. Sauerbrey, G. "Use of Quartz Crystal Vibrator for Weighting Thin Films on a Microbalance," *Z Phys.* **1959**, *155*, 206-222.
116. Haynie, D.T.; Balkundi, S.; Palath, N.; Chakravarthula, K.; Dave, K. "Polypeptide Multilayer Films: Role of Molecular Structure and Charge," *Langmuir* **2004**, *20*, 4540-4547.
117. Li, B.; Haynie, D.T. "Multilayer Biomimetics: Reversible Covalent Stabilization of a Nanostructured Biofilm," *Biomacromolecules* **2004**, *5*, 1667-1670.
118. Zhi, Z.-l.; Haynie, D.T. "Direct Evidence of Controlled Structure Reorganization in a Nanoorganized Polypeptide Multilayer Thin Film," *Macromolecules* **2004**, *37*, 8668-8675.
119. Zheng, B.; Haynie, D.T.; Zhong, H.; Sabnis, K.; Surpuriya, V.; Pargaonkar, N.; Sharma, G.; Vistakula, K. "Design of Peptides for Thin Films, Coatings and Microcapsules for Applications in Biotechnology," *J. Biomater. Sci. Polym. Edn* **2005**, *16*, 285-299.
120. Zhang, L.; Li, B.; Zhi, Z.-l.; Haynie, D.T. "Perturbation of Nanoscale Structure of Polypeptide Multilayer Thin Films," *Langmuir* **2005**, *21*, 5439-5445.
121. Li, B.; Haynie, D.T.; Palath, N.; Janisch, D. "Nano-Scale Biomimetics: Fabrication and Optimization of Stability of Peptide-Based Thin Films," *J. Nanotech. Nanosci.* **2005**, *5*, 1-8.
122. Li, B.; Rozas, J.; Haynie, D.T. "Structural Stability of Polypeptide Nanofilms under Extreme Conditions," *Biotechnol. Progr.* **2006**, *22(1)*, 111-117.

123. Picart, C.; Lavalle, Ph.; Hubert, P.; Cuisinier, F.J.G.; Decher, G.; Schaaf, P.; Voegel, J.-C. "Buildup Mechanism for Poly(L-lysine)/Hyaluronic Acid Films onto a Solid Surface," *Langmuir* **2001**, *17*, 7414-7424.
124. Lavalle, Ph.; Gergely, C.; Cuisinier, F.J.G.; Decher, G.; Schaaf, P.; Voegel, J.C.; Picart, C. "Comparison of the Structure of Polyelectrolyte Multilayer Films Exhibiting a Linear and an Exponential Growth Regime: An in Situ Atomic Force Microscopy Study," *Macromolecules* **2002**, *35*, 4458-4465.
125. Zhong, Y.; Li, B.; Haynie, D.T. "Fine Tuning of Physical Properties of Designed Polypeptide Multilayer Films by Control of pH," *Biotechnol. Progr.* **2006**, *22(1)*, 126-132.
126. http://www.cryst.bbk.ac.uk/PPS2/course/section8/ss-960531_21.html
127. Müller, M.; Kessler, B.; Lunkwitz, K. "Induced Orientation of α -Helical Polypeptides in Polyelectrolyte Multilayers," *J. Phys. Chem. B* **2003**, *107*, 8189-8197.
128. Jirgensens, B. *Optical Activity of Proteins and other Macromolecules*; Springer Verlag: New York, 1973.
129. Cooper, T.M.; Campbell, A.L.; Crane, R.L. "Formation of Polypeptide-Dye Multilayers by an Electrostatic Self-Assembly Technique," *Langmuir* **1995**, *11*, 2713-2718.
130. Sreerama, N.; Venyaminov, S. Yu.; Woody, R.W. "Estimation of Protein Secondary Structure from Circular Dichroism Spectra: Inclusion of Denatured Proteins with Native Proteins in the Analysis," *Anal. Biochem.* **2000**, *287*, 243-251.
131. Fasman, G.D.; Hoving, H.; Timasheff, S.N. "Circular Dichroism of Polypeptide and Protein Conformations. Film Studies," *Biochemistry* **1970**, *17*, 3316-3324.
132. Yang, J.J.; Buck, M.; Pitkeathly, M.; Kotik, M.; Haynie, D.T.; Dobson, C.M.; Radford, S.E. "Conformational Properties of Four Peptides Spanning the Sequence of Hen Lysozyme," *J. Mol. Biol.* **1995**, *252*, 483-491.
133. Haynie, D.T.; Zhang, L.; Zhao, W. *Prepr. Am. Chem. Soc. Polym. Sci. Eng. Div.* 230th annual meeting of the American Chemical Society: Washington DC, 2005.
134. Halthur, T.J.; Elofsson, U.M. "Multilayers of Charged Polypeptides as Studied by *In situ* Ellipsometry and Quartz Crystal Microbalance with Dissipation," *Langmuir* **2004**, *20*, 1739-1745.
135. Balkundi, S. MS thesis, Louisiana Tech University, Ruston, LA, 2004.

136. Birdi, K.S. Vu, D.T. In Birdi, K.S. *Handbook of Surface and Colloid Chemistry*, Eds.; CRC Press: Boca Raton, 2003; p. 653.
137. Blackford, B.L.; Jericho, M.H.; Mulhern, P.J. "A Review of Scanning Tunneling Microscope and Atomic Force Microscope Imaging of Large Biological Structures: Problems and Prospects," *Scanning Microsc.* **1991**, *5*, 907-918.
138. Rees, W. A.; Keller, R.W.; Vesenka, J.P.; Yang, G.; Bustamante, C. "Evidence of DNA bending in transcription complexes imaged by scanning force microscopy," *Science* **1993**, *260*, 1646-1649.
139. Hansma, H.G.; Sinsheimer, R.L.; Groppe, J.; Bruice, T.C.; Elings, V.; Gurley, G.; Bezanilla, M.; Mastrangelo, I.A.; Hough, P.V.; Hansma, P.K. "Recent Advances in Atomic Force Microscopy of DNA," *Scanning* **1993**, *15*, 296-299.
140. Ohnishi, S.; Hara, M.; Furuno, T.; Okada, T.; Sasabe, H. "Direct Visualization of Polypeptide Shell of Ferritin Molecule by Atomic Force Microscopy," *Biophys. J.* **1993**, *65*, 573-577.
141. Breen, J.J.; Flynn, G.W. "Scanning Tunneling Microscopy Studies of the Synthetic Polypeptide Poly(γ -benzyl L-glutamate)," *J. Phys. Chem.*, **1992**, *96*, 6825-6829.
142. de-Grooth, B.G.; Putman, C.A. "High-Resolution Imaging of Chromosome-related Structures by Atomic Force Microscopy," *J. Microsc.* **1992**, *168*, 239-247.
143. Gergely, C.; Bahi, S.; Szalontai, B.; Flores, H.; Schaaf, P.; Voegel, J.-C.; Cuisinier, F.J.G. "Human Serum Albumin Self-Assembly on Weak Polyelectrolyte Multilayer Films Structurally Modified by pH Changes," *Langmuir* **2004**, *20*, 5575-5582.
144. Chluba, J.; Voegel, J.-C.; Decher, G.; Erbacher, P.; Schaaf, P.; Ogier, J. "Peptide Hormone Covalently Bound to Polyelectrolytes and Embedded into Multilayer Architectures Conserving Full Biological Activity," *Biomacromolecules* **2001**, *2*, 800-805.
145. Hoogeveen, N.G.; Cohen Stuart, M.A.; Fleer, G.J.; Bohmer, M.R. "Formation and Stability of Multilayers of Polyelectrolytes," *Langmuir* **1996**, *12*, 3675-3681.
146. Messina, R.; Holm, C.; Kremer, K. "Polyelectrolyte Multilayering in Spherical Geometry," *Langmuir* **2003**, *19*, 4473-4482.
147. Messina, R.; Holm, C.; Kremer, K. "Polyelectrolyte Adsorption and Multilayering on Charged Colloidal Particles," *J. Polym. Sci. B* **2004**, *42*, 3557-3570.

148. Messina R. "Polyelectrolyte Multilayering on a Charged Planar Surface," *Macromolecules* **2004**, *37*, 621-629.
149. Lowack, K.; Helm, C.A. "Polyelectrolyte Monolayers at the Mica/Air Interface: Mechanically Induced Rearrangements and Monolayer Annealing," *Macromolecules* **1995**, *28*, 2912-2921.
150. Dubas, S.T.; Schlenoff, J.B. "Factors Controlling the Growth of Polyelectrolyte Multilayers," *Macromolecules* **1999**, *32*, 8153-8160.
151. Panchagnula, V.; Jeon J.; Rusling, J.F.; Dobrynin, A.V. "Molecular Dynamics Simulations of Layer-by-layer Assembly of Polyelectrolytes at Charged Surfaces. Effects of Chain Degree of Polymerization and Fraction of Charged Monomers," *Langmuir* **2005**, *21*, 1118-1125.
152. Haynie, D.T.; Zhang, L.; Rudra, J.S.; Zhao, W.; Zhong, Y.; Palath, N.; "Polypeptide Multilayer Films," *Biomacromolecules* **2005**, *6*, 2895-2913.
153. Thurman, R.B.; Gerba, C.P. "The Molecular Mechanism of Copper and Silver Ion Disinfection of Bacteria and Viruses," *CRC Crit. Rev. Environ. Control* **1989**, *18*, 295-315.
154. Guggenbichler, J.P.; Boeswald, M.; Lugauer, S.; Krall, T. "A New Technology of Microdispersed Silver in Polyurethane Induces Antimicrobial Activity in Central Venous Catheters," *Infection* **1999**, *27*, S16-S23.
155. Donelli, G.; Francolini, I. "Efficacy of Antiadhesive, Antibiotic and Antiseptic Coatings in Preventing Catheter-related Infections: Review," *J. Chemother.* **2001**, *13*, 595-606.
156. Pai, M.P.; Pendland, S.L.; Danziger, L.H. "Antimicrobial-Coated/Bonded and Impregnated Intravascular Catheters," *Ann. Pharmacother.* **2001**, *35*, 1255-1263.
157. Takai, K.; Ohtsuka, T.; Senda, Y.; Nakao, M.; Yamamoto, K.; Matsuoka-Junji, J.; Hirai, Y. "Antibacterial Properties of Antimicrobial-finished Textile Products," *Microbiol. Immunol.* **2002**, *46*, 75-81.
158. Labuza, T.P.; Breene, W.M. "Application of Active Packaging for Improvement of Shelf-life and Nutritional Quality of Fresh and Extended Shelf-life Foods," *J. Food. Process. Preserv.* **1988**, *13*, 1-69.
159. Floros, J.D.; Dock, L.L.; Han, J.H. "Active Packaging Technologies and Applications," *Food Cosmet. & Drug. Packag.* **1997**, *20*, 10-17
160. Han, J.H. "Antimicrobial Food Packaging," *Food. Technol.* **2002**, *54*, 56-65.

161. Krochta, J.M. In *Protein-Based films and coatings*; Gennadios, A. Ed.; CRC Press: Boca Raton, FL, 2002; p. 1.
162. Hunt, R.G.; Sellers, V.R.; Franklin, W.E.; Nelson, J.M.; Rathje, W.L.; Hughes, W.W.; Wilson, D.C. *The Garbage Project*; Franklin Associates: Tucson, 1990.
163. Krochta J.M.; De Mulder-Johnston, C. "Edible Biodegradable Polymer Films: Challenge and Opportunities," *Food Technol.* **197**, *51*, 61-74.
164. Appendini, P.; Hotchkiss, J.H. "Review of Antimicrobial Food Packaging , Innovative Food Science & Emerging Technologies," *Innov. Food Sci. Emerg. Technol.* **2002**, *3*, 113-126.
165. Gennadios, A. *Protein-based films and coatings*. Ed.; CRC Press: Boca Raton, FL, 2002.
166. Horbett, T. A.; Brash, J. L. In *Proteins at Interfaces, Physicochemical and Biochemical Studies*, Brash, J. L., Horbett, T. A., Eds.; ACS Symposium Series 343; American Chemical Society: Washington, DC, 1987; p 1
167. Tanaka, M.; Ishizaki, S.; Suzuki, T.; Takai, R. "Water Vapor Permeability of Edible Films Prepared from Fish Water Soluble Proteins as Affected by Lipid Type," *J. Tokyo Univ. Fisheries* **2001**, *87*, 31-37.
168. Etienne, O.; Picart, C.; Taddei, C.; Haikel, Y.; Dimarcq, J.L.; Schaaf, P.; Voegel, J.C.; Ogier, J.A.; Engles, C. "Multilayer Polyelectrolyte Films Functionalized by Insertion of Defensin: a New Approach to Protection of Implants from Bacterial Colonization," *Antimicrob. Agents. and Chemother.* **2004**, *48*, 3662-3669.
169. Lee, D.; Cohen, R.E.; Rubner, M.F. "Antibacterial Properties of Ag Nanoparticle Loaded Multilayers and Formation of Magnetically Directed Antibacterial Microparticles," *Langmuir* **2005**, *21*, 9651-9659.
170. Yang, Y.; Hamaguchi, K. "Hydrolysis of 4-methylumbelliferyl N-acetylchitotetraoside Catalyzed by Hen Lysozyme," *J. Biochem. (Tokyo)* **1980**, *87*, 1003-1014.
171. Sothornvit, R.; Krotcha, J.M. "Water Vapor Permeability and Solubility of Films from Hydrolyzed Whey Protein," *J. Food Sci.* **2000**, *65*, 700-703.
172. Gekko, K.; Timasheff, S.N. "Thermodynamic and Kinetic Examination of Protein Stabilization by Glycerol," *Biochemistry*, **1981**, *20*, 4667-4676.

173. Branen, J.K.; Davidson, P.M. "Enhancement of Nisin, Lysozyme, and Monolaurin Antimicrobial Activities by Ethylenediaminetetraacetic Acid and Lactoferrin," *Intl. J. Food Microbiol.* **2004**, *90*, 63-74
174. Shugar, D. "The Measurement of Lysozyme Activity and the Ultra-violet Inactivation of Lysozyme," *Biochim. Biophys. Acta* **1952**, *8*, 302-309.
175. Osserman, E. "Crystallization of Human Lysozymes," *Science* **1957**, *155*, 1536-1542.
176. Holler, E.; Rupley, J.; Hess, G. "Productive and Unproductive Lysozyme-Chitosaccharide Complexes. Equilibrium Measurements," *Biochemistry* **1975**, *14*, 1088-1094.
177. Hughey, V.L.; Johnson, E.A. "Antimicrobial Activity of Lysozyme against Bacteria Involved in Food Spoilage and Food-borne Disease," *Appl. Environ. Microbiol.* **1987**, *53*, 2165-2170.
178. Quintavalla, S.; Vincini, L. "Antimicrobial Food Packaging in Meat Industry," *Meat Sci.* **2002**, *62*, 373-380.
179. Mecitoğlu, C.; Yemenicioğlu, A.; Arslanoğlu, A.; Elmaci, S.; Korel, F.; Çetin, A.E. "Incorporation of Partially Purified Hen Egg White Lysozyme into Zein Films for Antimicrobial Food Packaging," *Food Res. Intl.* **2006**, *39*, 12-21.
180. Haynie, D.T.; Zhang, L.; Zhao, W. "Polypeptide Multilayer Films: Experiments, Simulations, Implications," *Polym. Mater. Sci. Eng.* **2005**, *93*, 94-97.
181. Haynie, D.T.; Palath, N.; Liu, Y.; Li, B.; Pargaonkar, N. "Biomimetic Nanostructured Materials: Inherent Reversible Stabilization of Polypeptide Microcapsules," *Langmuir* **2005**, *21*, 1136-1138.
182. Zelikin, A.; Quinn, J.F.; Caruso, F. "Disulfide Cross-Linked Polymer Capsules: En Route to Biodeconstructible Systems," *Biomacromolecules* **2006**, *7*, 27-30.
183. Hubbell, J.A. "Bioactive Biomaterials," *Curr. Opin. Biotechnol.* **1999**, *10*, 123-129.
184. Shakesheff, K.M.; Cannizzaro, S.M.; Langer, R. "Creating biomimetic micro-environments with synthetic polymer-peptide hybrid molecules," *J. Biomat. Sci. Polym. Ed.* **1998**, *9*, 507-518
185. Elbert, D.L.; Hubbell, J.A. "Surface Treatments of Polymers for Biocompatibility," *Annu. Rev. Mater. Sci.* **1996**, *26*, 365-394.

186. Drumheller, P.D.; Herbert, C.B.; Hubbell, J.A. "Bioactive Peptide and Surface Design," *Bioprocess Technol.* **1996**, *23*, 273.
187. Hubbell, J.A. "Biomaterials in Tissue Engineering," *Bio/Technology* **1995**, *13*, 565-576.
188. Ikada, Y. "Surface Modification of Polymers for Medical Applications," *Biomaterials* **1994**, *15*, 725-736.
189. Pierschbacher, M.D.; Polarek, J.W.; Craig, W.S.; Tschopp, J.F.; Sipes, N.J.; Harper, J.R. "Manipulation of Cellular Interactions with Biomaterials toward a Therapeutic Outcome: a Perspective," *J. Cell Biochem.* **1994**, *56*, 150-154.
190. Beckerle, M.C. *Cell Adhesion (Frontiers in Molecular Biology)* Ed.; Oxford University Press: New York, 2002.
191. Li, J.M.; Menconi, M.J.; Wheeler, H.B.; Rohrer, M.J.; Klassen, V.A.; Ansell, J.E.; Appel, M.C. "Precoating Expanded Polytetrafluoroethylene Grafts Alters Production of Endothelial Cell-derived Thrombomodulators," *J. Vasc. Surg.* **1992**, *15*, 1010-1017.
192. Miyata, T.; Conte, M.S.; Trudell, L.A.; Mason, D.; Whittemore, A.D.; Birinyi, L.K. "Delayed Exposure to Pulsatile Shear Stress Improves Retention of Human Saphenous Vein Endothelial Cells on Seeded ePTFE Grafts," *J. Surg. Res.* **1991**, *50*, 485-493.
193. Vohra, R.; Thomson, G.J.; Carr, H.M.; Sharma, H.; Walker, M.G. "Comparison of Different Vascular Prostheses and Matrices in Relation to Endothelial Seeding," *Br. J. Surg.* **1991**, *78*, 417-420.
194. Thomson, G.J.; Vohra, R.K.; Carr, M.H.; Walker, M.G. "Adult Human Endothelial Cell Seeding Using Expanded Polytetrafluoroethylene Vascular Grafts: a Comparison of Four Substrates," *Surgery* **1991**, *109*, 20-27.
195. Kaehler, J.; Zilla, P.; Fasol, R.; Deutsch, M.; Kadletz, M. "Precoating Substrate and Surface Configuration Determine Adherence and Spreading of Seeded Endothelial Cells on Polytetrafluoroethylene Grafts," *J. Vasc. Surg.* **1989**, *9*, 535-541.
196. Seeger, J.M.; Klingman, N. "Improved Endothelial Cell Seeding with Cultured Cells and Fibronectin-coated Grafts," *J. Surg. Res.* **1985**, *38*, 641-647.
197. Sentissi, J.M.; Ramberg, K.; O'Donnell Jr, T.F.; Connolly, R.J.; Callow, A.D. "The Effect of Flow on Vascular Endothelial Cells Grown in Tissue Culture on Polytetrafluoroethylene Grafts," *Surgery* **1986**, *99*, 337-343.

198. Pierschbacher, M.D.; Ruoslahti, E. "Cell Attachment Activity of Fibronectin can be Duplicated by Small Synthetic Fragments of the Molecule," *Nature* **1984**, *309*, 30-33.
199. Ulrich, H.; Claudia, D.; and Horst, K. "RGD Modified Polymers: Biomaterials for Stimulated Cell Adhesion and Beyond," *Biomaterials* **2003**, *24*, 4385-4415.
200. Pfaff, M. In Eble, J.A. *Recognition sites of RGD-dependent integrins Integrin-Ligand Interaction*; Ed.; Springer-Verlag: Heidelberg, 1997; p. 101.
201. Katz, B.Z.; Zamir, E.; Bershadsky, A.; Kam, Z.; Yamada, K.M.; Geiger, B. "Physical State of the Extracellular Matrix Regulates the Structure and Molecular Composition of Cell-matrix Adhesions," *Mol Biol. Cell* **2000**, *11*, 1047-1060.
202. Pelham Jr, R.J.; Wang, Y.L. "Cell Locomotion and Focal Adhesions are Regulated by the Mechanical Properties of the Substrate," *Biol. Bull.* **1998**, *194*, 348-350.
203. Choquet, D.; Felsenfeld, D.P.; Sheetz, M.P. "Extracellular Matrix Rigidity Causes Strengthening of Integrin-cytoskeleton Linkages," *Cell* **1997**, *88*, 39-48.
204. Grinnell, F. "Focal Adhesion Sites and the Removal of Substratum-bound Fibronectin," *J. Cell Biol.* **1986**, *103*, 2697-2706.
205. Gaebel, K.; Feuerstein, I.A. "Platelets Process Adsorbed Protein: A Morphological Study," *Biomaterials* **1991**, *12*, 597-602.
206. Zamir, E.; Geiger, B. "Molecular Complexity and Dynamics of Cell-matrix Adhesions," *J. Cell Sci.* **2001**, *114*, 3583-3590.
207. Castel, S.; Pagan, R.; Mitjans, F.; Piulats, J.; Goodman, S.; Jonczyk, A.; Huber, F.; Vilaro, S.; Reina, M. "RGD Peptides and Monoclonal Antibodies, Antagonists of Alpha(v)-integrin, enter the Cells by Independent Endocytic Pathways," *Lab Invest.* **2001**, *81*, 1615-1626.
208. Memmo, L.M.; McKeown-Longo, P. "The Alphavbeta5 Integrin Functions as an Endocytic Receptor for Vitronectin," *J. Cell Sci.* **1998**, *111*, 425-433.
209. Harrison, D.; Johnson, R.; Tucci, M.; Puckett, A.; Tsao, A.; Hughes, J. Benghuzzi, H. "Interaction of Cells with UHMWPE Impregnated with the Bioactive Peptides RGD, RGE or Poly-L-Lysine," *Biomed. Sci. Instrum.* **1997**, *34*, 41-46.

210. McConachie, A.; Newman, D.; Tucci, M.; Puckett, A.; Tsao, A.; Hughes, J.; Benghuzzi, H. "The Effect on Bioadhesive Polymers either Freely in Solution or Covalently Attached to a Support on Human Macrophages," *Biomed. Sci. Instrum.* **1999**, *35*, 45-50.
211. Healy, K.E.; Tsai, D.; Kim, J.E. "Osteogenic Cell Attachment to Degradable Polymers," *Mater. Res. Soc. Symp. Proc.* **1992**, *252*, 109-114.
212. Johnson, R.; Harrison, D.; Tucci, M.; Tsao, A.; Lemos, M.; Puckett, A.; Hughes, J.L.; Benghuzzi, H. "Fibrous Capsule Formation in Response to Ultrahigh Molecular Weight Polyethylene Treated with Peptides that Influence Adhesion," *Biomed. Sci. Instrum.* **1997**, *34*, 47-52.
213. Kobayashi, H.; Ikada, Y. "Corneal Cell Adhesion and Proliferation on Hydrogel Sheets Bound with Cell-adhesive Proteins," *Curr. Eye. Res.* **1991**, *10*, 899-908.
214. Dettin, M.; Conconi, M.T.; Gambaretto, R.; Pasquato, A.; Folin, M.; Bello, C.D.; Parnigotto, P.P. "Novel Osteoblast-adhesive Peptides for Dental/orthopedic Biomaterials," *J. Biomed. Mater. Res.* **2002**, *60*, 466-471.
215. Ruoslahti, E. "RGD and Other Recognition Sequences for Integrins," *Annu. Rev. Cell Dev. Biol.* **1996**, *12*, 697-715.
216. Yamada, K.M.; Kennedy, D.W. "Dualistic Nature of Adhesive Protein Function: Fibronectin and its Biologically Active Peptide Fragments can Autoinhibit Fibronectin Function," *J. Cell Biol.* **1984**, *99*, 29-36.
217. Gardner, J.M.; Hynes, R.O. "Interaction of Fibronectin with its Receptor on Platelets," *Cell* **1985**, *42*, 439-448.
218. Suzuki, S.; Oldberg, A.; Hayman, E.G.; Pierschbacher, M.D.; Ruoslahti, E. "Complete Amino Acid Sequence of Human Vitronectin Deduced from cDNA. Similarity of Cell Attachment Sites in Vitronectin and Fibronectin," *EMBO J.* **1985**, *4*, 2519-2524.
219. Gartner, T.K.; Bennett, J.S. "The Tetrapeptide Analogue of the Cell Attachment Site of Fibronectin is an Inhibitor of Platelet Aggregation and Fibrinogen Binding," *J. Biol. Chem.* **1985**, *260*, 11891-11899.
220. Plow, E.F.; Pierschbacher, M.D.; Ruoslahti, E.; Marguerie, G.A.; Ginsberg, M.H. "The Effect of Arg-Gly-Asp-containing Peptides on Fibrinogen and von Willebrand Factor Binding to Platelets," *Proc. Natl. Acad. Sci.* **1985**, *82*, 8057-8061.

221. Yamada, K.M.; Kennedy, D.W. "Peptide Inhibitors of Fibronectin, Laminin, and other Adhesion Molecules: Unique and Shared Features," *J. Cell Physiol.* **1987**, *130*, 21-28.
222. Pierschbacher, M.D.; Ruoslahti, E. "Variants of the Cell Recognition Site of Fibronectin that Retain Attachment-promoting Activity," *Proc. Natl. Acad. Sci.* **1984**, *81*, 5985-5988.
223. Pierschbacher, M.D.; Ruoslahti, E. "Influence of Stereochemistry of the Sequence Arg-Gly-Asp-Xxx on Binding Specificity in Cell Adhesion," *J. Biol. Chem.* **1987**, *262*, 17294-17298.
224. D'Souza, S.E.; Ginsberg, M.H.; Burke, T.A.; Plow, E.F. "The Ligand Binding Site of the Platelet Integrin Receptor GPIIb-IIIa is Proximal to the Second Calcium Binding Domain of its Alpha Subunit," *J. Biol. Chem.* **1990**, *265*, 3440-3446.
225. D'Souza, S.E.; Haas, T.A.; Piotrowicz, R.S.; Byers-Ward, V.; McGrath, D.E.; Soule, H.R.; Cierniewski, C.; Plow, E.F.; Smith, J.W. "Ligand and Cation Binding are Dual Functions of a Discrete Segment of the Integrin beta 3 Subunit: Cation Displacement is Involved in Ligand Binding," *Cell* **1994**, *79*, 659-667.
226. Marchi-Artzner, V.; Lorz, B.; Gosse, C.; Jullien, L.; Merkel, R.; Kessler, H.; Sackmann, E. "Adhesion of Arg-Gly-Asp (RGD) Peptide Vesicles onto an Integrin Surface: Visualization of the Segregation of RGD Ligands into the Adhesion Plaques by Fluorescence," *Langmuir* **2003**, *19*, 835-841.
227. Hautanen, A.; Gailit, J.; Mann, D.M.; Ruoslahti, E. "Effects of Modifications of the RGD Sequence and its Context on Recognition by the Fibronectin Receptor," *J. Biol. Chem.* **1989**, *264*, 1437-1442.
228. Dal Pozzo, A.; Fagnoni, M.; Bergonzi, R.; Vanini, L.; de Castiglione, R.; Aglio, C.; Colli, S. "Synthesis and Anti-aggregatory Activity of Linear Retro-inverso RGD Peptides," *J. Peptide Res.* **2000**, *55*, 447-454.
229. Kim, J.; Hong, S.Y.; Park, H.S.; Kim, D.S.; Lee, W. "Structure and Function of RGD Peptides Derived from Disintegrin Proteins," *Mol. Cells* **2005**, *19*, 205-211.
230. Yamamoto, M.; Fisher, J.E.; Gentile, M.; Seedor, J.G.; Leu, C.-T.; Rodan, S.B. Rodan G.A. "The Integrin Ligand Echistatin Prevents Bone Loss in Ovariectomized Mice and Rats," *Endocrinology* **1998**, *139*, 1411-1419.
231. Pettersson, E.; Lünig, B.; Mickos, H.; Heinegård, D. "Synthesis, NMR and Function of an O-phosphorylated Peptide, Comprising the RGD-adhesion Sequence of Osteopontin," *Acta Chem. Scand.* **1991**, *45*, 604-608.

232. Geiger, T.; Clarke, S. "Deamidation, Isomerization, and Racemization at Asparaginy and Aspartyl Residues in Peptides. Succinimide-linked Reactions that Contribute to Protein Degradation," *J. Biol. Chem.* **1987**, *262*, 785-794.
233. Olenych, S.G.; Moussallem, M.D.; Salloum, D.S.; Schlenoff, J.B.; Keller, T.C.S. "Fibronectin and Cell Attachment to Cell and Protein Resistant Polyelectrolyte Surfaces," *Biomacromolecules* **2005**, *6*, 3252-3258.
234. Mendelsohn, J.D.; Yang, S.Y.; Hiller, J.; Hochbaum, A.I.; Rubner, M.F. "Rational Design of Cytophilic and Cytophobic Polyelectrolyte Multilayer Thin Films," *Biomacromolecules* **2003**, *4*, 96-106.
235. Yang, S.Y.; Mendelsohn, J.D.; Rubner, M.F. "New Class of Ultrathin, Highly Cell-Adhesion-Resistant Polyelectrolyte Multilayers with Micropatterning Capabilities," *Biomacromolecules* **2003**, *4*, 987-994.
236. Boura, C.; Menu, P.; Payan, E.; Picart, C.; Voegel, J.C.; Muller, S.; Stoltz, J.F. "Endothelial Cells Grown on Thin Polyelectrolyte Multilayered Films: An Evaluation of a New Versatile Surface Modification," *Biomaterials* **2003**, *24*, 3521-3530.
237. Kreke, M.R.; Badami, A.S.; Brady, J.B.; Akers, R.M.; Goldstein, A.S. "Modulation of Protein Adsorption and Cell Adhesion by Poly(allylamine hydrochloride) Heparin Films," *Biomaterials* **2005**, *26*, 2975-2981.
238. Jessel, N.; Atalar, F.; Lavalle, P.; Mutterer, J.; Decher, G.; Schaaf, P.; Voegel, J.C.; Ogier, J. "Bioactive Coatings Based on a Polyelectrolyte Multilayer Architecture Functionalized by Embedded Proteins," *Adv. Mater.* **2003**, *15*, 692-695.
239. Hahn, S.K.; Hoffman, A.S. "Characterization of Biocompatible Polyelectrolyte Complex Multilayer of Hyaluronic acid and Poly-L-lysine," *Biotechnol. Bioprocess Eng.* **2004**, *9*, 179-183.
240. Hwang, J.J.; Jelacic, S.; Samuel, N.T.; Maier, R.V.; Campbell, C.T.; Castner, D.G.; Hoffman, A.S.; Stayton, P.S. "Monocyte Activation on Polyelectrolyte Multilayers," *J. Biomater. Sci., Polym. Ed.* **2005**, *16*, 237-251.
241. Gheith, M.K.; Sinani, V.A.; Wicksted, J.P.; Matts, R.L.; Kotov, N.A. "Single-Walled Carbon Nanotube Polyelectrolyte Multilayers and Freestanding Films as a Biocompatible Platform for Neuroprosthetic Implants," *Adv. Mater.* **2005**, *17*, 2663-2670.
242. Kommireddi, D.S.; Sriram, S.M.; Lvov, Y.M.; Mills, D.K. "Stem Cell Attachment to Layer-by-layer Assembled TiO₂ Nanoparticle Thin Films," *Biomaterials* **2006**, *27(24)*, 4296-4303.

243. Berg, M.C.; Yang, S.Y.; Hammond, P.T.; Rubner, M.F. "Controlling Mammalian Cell Interactions on Patterned Polyelectrolyte Multilayer Surfaces," *Langmuir* **2004**, *20*, 1362-1368.
244. Mohammed, J.S.; DeCoster, M.A.; McShane, M.J. "Micropatterning of nanoengineered surfaces to study neuronal cell attachment in vitro," *Biomacromolecules* **2004**, *5*, 1745-1755.
245. Reyes, D.R.; Perruccio, E.M.; Becerra, S.P.; Locascio, L.E.; Gaitan, M. "Micropatterning Neuronal Cells on Polyelectrolyte Multilayers," *Langmuir* **2004**, *20*, 8805-8811.
246. Zheng, H.; Berg, M.C.; Rubner, M.F.; Hammond, P.T. "Controlling Cell Attachment Selectively onto Biological Polymer-colloid Templates Using Polymer-on-polymer Stamping," *Langmuir* **2004**, *20*, 7215-7222.
247. Zhu, H.; Ji, J.; Shen, J. "Biomacromolecules Electrostatic Self-assembly on 3-dimensional Tissue Engineering Scaffold," *Biomacromolecules* **2004**, *5*, 1933-1939.
248. Liu, X.; Smith, L.; Wei, G.; Won, Y.; Ma, P.X. "Surface Engineering of Nano-Fibrous Poly(L-Lactic Acid) Scaffolds via Self-Assembly Technique for Bone Tissue Engineering," *J. Biomed. Nanotechnol.* **2005**, *1*, 54-60.
249. Lee, J.; Shanbhag, S.; Kotov, N.A. "Inverted Colloidal Crystals as Three-dimensional Microenvironments for Cellular Co-cultures," *J. Mater. Chem.* **2006**, *16*, 3558-3564.
250. Sinani, V.A.; Koktysh, D.S.; Yun, B.G.; Matts, R.L.; Pappas, T.C.; Motamedi, M.; Thomas, S.N.; Kotov, N.A. "Collagen Coating Promotes Biocompatibility of Semiconductor Nanoparticles in Stratified Lbl Films," *Nano Lett.* **2003**, *3*, 1177-1182.
251. Richert, L.; Boulmedais, F.; Lavalle, P.; Mutterer, J.; Ferreux, E.; Decher, G.; Schaaf, P.; Voegel, J.C.; Picart, C. "Improvement of Stability and Cell Adhesion Properties of Polyelectrolyte Multilayer Films by Chemical Cross-linking," *Biomacromolecules* **2004**, *5*, 284-294.
252. Schneider, A.; Francius, G.; Obeid, R.; Schwinte, P.; Hemmerle, J.; Frisch, B.; Schaaf, P.; Voegel, J.C.; Senger, B.; Picart, C. "Polyelectrolyte Multilayers with a Tunable Young's Modulus: Influence of Film Stiffness on Cell Adhesion," *Langmuir* **2006**, *22*, 1193-1200.

253. Haynie, D.T.; Zhang, L.; Zhao, W.; Smith, J.M. "Quantal Self-assembly of Polymer Layers in Polypeptide Multilayer Nanofilms," *Biomacromolecules* **2006**, *7*, 2264-2268.
254. Benesch, J.; Askendal, A.; Tengvall, P. "The Determination of Thickness and Surface Mass Density of Mesothick Immunoprecipitate Layers by Null Ellipsometry and Protein (125)iodine Labeling," *J. Colloid Interface Sci.* **2002**, *249*, 84-90.
255. Vörös, J. "The Density and Refractive Index of Adsorbing Protein Layers," *Biophys. J.* **2004**, *87*, 553-561.
256. Lutz, S.; Essler, F.; Panzner, S. In *Controlled Release Society 29th Annual Meeting*, Seoul, Korea, 2002; p. 271.
257. Peyratout, C.; Möhwald, H.; Dähne, L. "Preparation of Photosensitive Dye Aggregates and Fluorescent Nanocrystals in Microreaction Containers," *Adv. Mater.* **2003**, *15*, 1722-1726.
258. Förster, S.; Plantenberg, T. "From Self-organizing Polymers to Nanohybrid and Biomaterials," *Angew. Chem.* **2002**, *114*, 712-739.
259. Manna, A.; Imae, T.; Aoi, K.; Okada, M.; Yogo, T. "Synthesis of Dendrimer-Passivated Noble Metal Nanoparticles in a Polar Medium: Comparison of Size between Silver and Gold Particles," *Chem. Mater.* **2001**, *13*, 1674-1681.
260. Sunder, A.; Krämer, M.; Hanselmann, R.; Mühaupt, R.; Frey, H. "Molecular Nanocapsules based on Amphiphilic Hyperbranched Polyglycerols," *Angew. Chem.* **1999**, *111*, 3758-3761.
261. Donath, E.; Sukhorukov, G.B.; Caruso, F.; Davis, S.A.; Möhwald, H. "Novel Hollow Polymer Shells by Colloid-templated Assembly of Polyelectrolytes," *Angew. Chem. Int. Ed.* **1998**, *37*, 2201-2205.
262. Lvov, Y.; Antipov, A.; Mamedov, A.; Möhwald, H.; Sukhorukov, G. B. "Urease Encapsulation in Nanoorganized Microshells," *Nano Lett.* **2001**, *1*, 125-128.
263. Renken, A.; Hunkeler, D. "Microencapsulation: A Review of Polymers and Technologies with a Focus on Bioartificial Organs," *Polimery* **1998**, *43*, 530-539.
264. Zhi, Z-l.; Haynie, D.T. "High-capacity functional protein encapsulation in nanoengineered polypeptide microcapsules," *Chem. Commun.* **2006**, 147-149.